

STRATIGRAPHY AND PALEOENVIRONMENTAL INTERPRETATION
OF THE BANGKOK CLAY FORMATION USING OSTRACOD
ASSEMBLAGES, SAMUT SAKHON PROVINCE, CENTRAL THAILAND



A Thesis Submitted in Partial Fulfillment of the Requirements for
the Degree of Master of Engineering in Civil, Transportation
and Geo-resources Engineering
Suranaree University of Technology
Academic Year 2022

ลำดับชั้นหินและการแปลความหมายสภาพแวดล้อมบรรพกาล ของ
หมวดหินดินเคลย์กรุงเทพฯจากกลุ่มออสตราคอด บริเวณจังหวัด
สมุทรสาคร ภาคกลางประเทศไทย



นางสาวลลิตา วีราชัย

วิทยานิพนธ์นี้เป็นส่วนหนึ่งของการศึกษาตามหลักสูตรปริญญาวิศวกรรมศาสตรมหาบัณฑิต
สาขาวิชาวิศวกรรมโยธา ขนส่ง และทรัพยากรธรณี
มหาวิทยาลัยเทคโนโลยีสุรนารี
ปีการศึกษา 2565

STRATIGRAPHY AND PALEOENVIRONMENTAL INTERPRETATION OF THE
BANGKOK CLAY FORMATION USING OSTRACOD ASSEMBLAGES, SAMUT
SAKHON PROVINCE, CENTRAL THAILAND

Suranaree University of Technology has approved this thesis submitted in
partial fulfillment of the requirements for a Master's Degree.

Thesis Examining Committee



(Asst. Prof. Dr. Chatchalerm Ketwetsuriya)
Chairperson



(Asst. Prof. Dr. Anisong Chitnarin)
Member (Thesis Advisor)



(Asst. Prof. Dr. Prachya Tepnarong)
Member



(Assoc. Prof. Dr. Chatchai Jothityangkoon)
Vice Rector for Academic Affairs and
Quality Assurance



(Assoc. Prof. Dr. Pornsiri Jongkol)
Dean of Institute of Engineering

ลลิตา วีราชัย : ลำดับชั้นหินและการแปลความหมายสภาพแวดล้อมบรรพกาลของหมวดหินดินเคลย์กรุงเทพฯจากกลุ่มออสตราคอด บริเวณจังหวัดสมุทรสาคร ภาคกลางประเทศไทย (STRATIGRAPHY AND PALEOENVIRONMENTAL INTERPRETATION OF THE BANGKOK CLAY FORMATION USING OSTRACOD ASSEMBLAGES, SAMUTSAKHON PROVINCE, CENTRAL THAILAND) อาจารย์ที่ปรึกษา : ผู้ช่วยศาสตราจารย์ ดร. อานิสงส์ จิตนารินทร์, 167หน้า.

คำสำคัญ: ออสตราคอด/จุลบรรพชีวิน/การลำดับชั้นหิน/ตะกอนสมัยโฮโลซีน

การศึกษาครั้งนี้มีวัตถุประสงค์เพื่อแปลความหมายสภาพแวดล้อมการทับถมตะกอนยุคควอเทอร์นารีตอนปลาย โดยศึกษาการลำดับชั้นหิน ศักยภาพเคมีด้วยเทคนิควิเคราะห์การเลี้ยวเบนของรังสีเอ็กซ์ (X-Ray Diffraction analysis; XRD) และการทดสอบความเค็มของตะกอน และการศึกษา กลุ่มออสตราคอดจากตะกอน 139 ตัวอย่าง ที่ได้จาก 5 หลุมเจาะ ในอำเภอกระทุ่มแบน อำเภอบ้านแพ้ว อำเภอชัยมงคล และอำเภอเมือง และจากหลุมขุดค้นเรืออับปางพนมสุรินทร์ อำเภอพันท้ายนรสิงห์ จังหวัดสมุทรสาคร ภาคกลางของประเทศไทย ซึ่งเป็นตะกอนในหมวดหินดินเคลย์กรุงเทพฯ การวิจัยประกอบด้วย การทบทวนวรรณกรรมวิจัยและการทดสอบในห้องปฏิบัติการ ตะกอนที่ศึกษาแบ่งออกเป็น 5 หน่วยตะกอน ได้แก่ หน่วยที่ 1 ตะกอนดินเหนียวปนทรายแป้ง และทราย สีเทาจากหน่วยที่ 2 ตะกอนดินเหนียวปนทรายแป้งสีแดง หน่วยที่ 3 ตะกอนดินเหนียวปนทรายแป้งสีเหลืองอมน้ำตาล หน่วยที่ 4 ตะกอนดินเหนียวปนทรายแป้งสีเทาเข้ม และหน่วยที่ 5 ดินชั้นบน จากด้านล่างขึ้นด้านบนสามารถจำแนกเป็น 2 ชุดลักษณะ ได้แก่ ชุดลักษณะ I ที่ลุ่มราบน้ำขึ้นน้ำลงและร่องน้ำขึ้นน้ำลง (Tidal flat and tidal channel) และชุดลักษณะ II ดินดอนสามเหลี่ยมลึก (Prodelta) ร่องค์ประกอบหลักของทุกหน่วยตะกอนประกอบด้วย ควอตซ์ แคลไซต์ เคโอลิไนต์ มัสโคไวท์ มอนต์มอริลโลไนต์ ไมโครโคลน อัลไบต์ และยิปซัม แต่พบอาราโกไนต์ และแอไซด์เฉพาะในหน่วยตะกอนที่ 4 ค่าความเค็มของตะกอนหน่วยที่ 1 2 และ 3 มีค่าต่ำกว่าร้อยละ 1.7 ค่าความเค็มของหน่วยตะกอนที่ 4 มีค่าสูงถึงร้อยละ 6.1 และมีค่าเฉลี่ยประมาณร้อยละ 2.9 ทั้งนี้สามารถใช้ค่าความเค็มเป็นเกณฑ์ระหว่างชุดลักษณะ I และชุดลักษณะ II

ผลการศึกษาพบออสตราคอดจำนวน 2,189 ตัวอย่าง สามารถจำแนกได้ 15 ชนิด อยู่ใน 10 สกุล และ 7 วงศ์ ประกอบด้วยสกุล *Neocyprideis* *Sinocytheridea* *Propontocypris* *Hemicytheridea* *Keijella* *Neomonoceratina* *Agelaiocypris* *Lankacythere* *Cytherella* และ *Stigmatocythere* โดยมักพบออสตราคอดในตะกอนเนื้อโคลน แต่พบได้น้อยกว่าในตะกอนเนื้อทรายแป้งและทรายละเอียด ตัวอย่างที่พบมีจำนวนฝามากกว่าคาราเพซ แสดงถึงการพัดพาตะกอน

ระยะใกล้ก่อนการสะสมตัว โดยฝามีสภาพดีแสดงลักษณะการประดับตกแต่งอย่างสมบูรณ์ จึงแปล
ความสภาพแวดล้อมการทับถมตะกอนที่ ศึกษาจากซากดึกดำบรรพ์ออสตราคอด ว่าเป็น
สภาพแวดล้อมในทะเลตื้น โดยเปลือกออสตราคอดถูกพัดพาโดยกระแสน้ำขึ้นน้ำลงไปยังร่องน้ำขึ้นน้ำ
ลง (ชุดลักษณะ I) และเป็นการทับถมในตะกอนดินเคลย์เนื้อละเอียดส่วนลึกของสามเหลี่ยมปากแม่น้ำ
ที่จมน้ำตลอดเวลา และมีปริมาณตะกอนมาก (ชุดลักษณะ II)



สาขาวิชา เทคโนโลยีธรณี

ปีการศึกษา 2565

ลายมือชื่อนักศึกษา ฉลิตา วีรัชช

ลายมือชื่ออาจารย์ที่ปรึกษา [Signature]

LALITA WEERACHAI : STRATIGRAPHY AND PALEOENVIRONMENTAL INTERPRETATION OF THE BANGKOK CLAY FORMATION USING OSTRACOD ASSEMBLAGES, SAMUT SAKHON PROVINCE, CENTRAL THAILAND. THESIS ADVISOR : ASST. PROF. ANISONG CHITNARIN, Ph. D., 167 PP.

Keyword: Ostracoda/ Micropaleontology/ Lithostratigraphy/ Holocene sediment

The purpose of this study is to interpret depositional environment of Late Quaternary sediments by lithostratigraphy, geochemistry using X-Ray Diffraction (XRD) and salinity test, and ostracod assemblages from 139 sedimentary samples obtained from a drilled cores from Samut Sakhon Province, central Thailand. The sediments are parts of the Bangkok Clay Formation. The research includes a literature review of relevant studies and comprehensive laboratory works. Therefore, five sedimentary units namely Light grey well sorted silty clay and fine grain sand (GSCS), Red and yellowish brown silty clay (RYSC), Yellowish white silty clay (YWSC), Dark grey well sorted silty clay (DGSC), and Topsoil, in ascending order. These units can be classified into two sedimentary facies: Facies I (Tidal flat and tidal channel) representing the tidal channel and intertidal zone; Facies II (Prodelta) representing marine environment of prodelta deposit. The major mineral composition of these five sedimentary units are composed of quartz, feldspar, kaolinite, muscovite, montmorillonite, microcline, albite, and gypsum. However, aragonite and halite are found exclusively in unit 4. The salinity level of units 1, 2, and 3 are below 1.7%, while the salinity of unit 4 is as high as 6.1%, with an average of approximately 2.9%. Salinity level can be used as criteria between Facies I and Facies II.

2,189 ostracod specimens were recovered, which could be classified into 15 species, belonging to 10 genera and 7 families. The ostracod genera, include Neocyprideis, Sinocytheridea, Propontocypris, Hemicytheridea, Keijella, Neomonoceratina, Aglaiocypris, Lankacythere, Cytherella, and Stigmatocythere. These ostracods are often found in clay sediments but less frequently in silt and fine sand sediments. The discovered specimens have more valves than carapaces, indicating a shortly transportation before burial. The valves are well-preserved, showing

complete ornamentation, suggesting a shallow marine environment. The ostracod shells were transported by tidal currents, with some settling in tidal channels (Facies I), while others were buried in clayey sediments of prodelta, submerged continuously, and with a large amount of sediment (Facies II).



School of Geotechnology
Academic Year 2022

Student's Signature Lalita Weerachai
Advisor's Signature [Signature]

ACKNOWLEDGEMENT

I wish to acknowledge the funding supported by Suranaree University of Technology (SUT).

I would like to express my sincere thanks to Asst. Prof. Dr. Anisong Chitnarin for her valuable guidance and efficient supervision. I appreciate her strong support, encouragement, suggestions and comments during the research period. I also would like to express my gratitude to Asst. Prof. Dr. Chatchalerm Ketwetsuriya (Kasetsart University) and Dr. Wipanu Rugmai (Nakhon Ratchasima Rajabhat University) for their support on my research works.

Grateful thanks are given to all the committee members and staff of Geomechanics Research Unit, Institute of Engineering who supported my work. Finally, I would like to thank beloved parents for their love, support and encouragement.

Lalita Weerachai



มหาวิทยาลัยเทคโนโลยีสุรนารี

TABLE OF CONTENTS

| | Page |
|---|-----------|
| ABSTRACT (THAI)..... | I |
| ABSTRACT (ENGLISH)..... | III |
| ACKNOWLEDGEMENTS..... | V |
| TABLE OF CONTENTS..... | VI |
| LIST OF FIGURES..... | IX |
| LIST OF TABLES..... | XIV |
| CHAPTER | |
| I INTRODUCTION..... | 1 |
| 1.1 Background and rationale..... | 1 |
| 1.2 Research objectives..... | 4 |
| 1.3 Scope and limitations..... | 4 |
| 1.4 Thesis contents..... | 4 |
| II LITERATURE REVIEW..... | 6 |
| 2.1 Geology of Samut Sakhon Province, Central Thailand..... | 6 |
| 2.2 Stratigraphic study and sea-level change in the Gulf of Thailand..... | 10 |
| 2.2.1 Stratigraphy of the Late Quaternary sediment in Central Plain of Thailand..... | 10 |
| 2.2.2 Sea level change in the Late Quaternary, Central Thailand..... | 19 |
| 2.3 Study of taxonomy and paleoenvironmental interpretation from ostracods in the Late Quaternary in Thailand..... | 26 |
| 2.4 Collecting and processing of ostracods..... | 29 |
| 2.5 Ostracod shell morphology..... | 30 |
| III METHODOLOGY..... | 37 |

TABLE OF CONTENTS (Continued)

| | Page |
|--|-----------|
| 3.1 Literature review and study..... | 37 |
| 3.2 Field investigation and sampling | 37 |
| 3.3 Laboratory work..... | 43 |
| 3.3.1 Stratigraphic study | 43 |
| 3.3.2 Ostracod study | 45 |
| 3.3.3 Salinity analysis..... | 45 |
| 3.3.4 XRD analysis | 46 |
| 3.4 Data analysis and interpretation..... | 48 |
| 3.4.1 Stratigraphic study | 48 |
| 3.4.2 Ostracod study | 48 |
| 3.4.3 Salinity analysis..... | 48 |
| 3.4.4 XRD analysis | 48 |
| 3.5 Thesis writing and presentation | 49 |
| IV LITHOSTRATIGRAPHY AND GEOCHEMISTRY | 50 |
| 4.1 Stratigraphy of the Late Quaternary sediment in studied section | 50 |
| 4.1.1 Stratigraphy of Borehole KU1 | 53 |
| 4.1.2 Stratigraphy of Borehole KU2 | 53 |
| 4.1.3 Stratigraphy of Borehole KU3 | 54 |
| 4.1.4 Stratigraphy of Borehole KU4 | 54 |
| 4.1.5 Stratigraphy of Borehole KU5 | 55 |
| 4.1.6 Stratigraphy of Phanom Surin shipwreck site..... | 55 |
| 4.2 Geochemistry of the Bangkok Clay from the study area | 56 |
| 4.2.1 Salinity test..... | 56 |
| 4.2.2 XRD analysis | 59 |
| V SYSTEMATIC PALEONTOLOGY..... | 67 |

TABLE OF CONTENTS (Continued)

| | Page |
|--|-----------|
| 5.1 Systematic paleontology..... | 67 |
| 5.2 Distribution of ostracods | 84 |
| 5.2.1 Distribution of ostracods along the Borehole KU1 | 84 |
| 5.2.2 Distribution of ostracods along the Borehole KU2 | 85 |
| 5.2.3 Distribution of ostracods along the Borehole KU3 | 88 |
| 5.2.4 Distribution of ostracods along the Borehole KU4 | 90 |
| 5.2.5 Distribution of ostracods along the Borehole KU5 | 92 |
| 5.2.6 Distribution of ostracods along the Phanom Surin shipwreck site | 93 |
| VI DISCUSSIONS AND CONCLUSION..... | 96 |
| 6.1 Discussions | 96 |
| 6.1.1 Palaeoenvironmental interpretation by lithostratigraphic and geochemical data | 96 |
| 6.1.2 Palaeoenvironmental interpretation by ostracod assemblages | 102 |
| 6.2 Conclusion..... | 104 |
| 6.3 Recommendations for future studies..... | 106 |
| REFERENCES | 107 |
| APPENDIX A | 120 |
| APPENDIX B | 156 |
| BIOGRAPHY | 162 |

LIST OF FIGURES

| Figure | Page |
|--|------|
| 1.1 Geologic map of Quaternary deposits in the Lower Central Plain of Thailand (Sinsakul, 2000)..... | 2 |
| 2.1 Geologic map of Samut Sakhon Province (DMR, 2016)..... | 7 |
| 2.2 Schematic model of the Lower Central Plain during maximum Holocene transgression (Sinsakul, 2000)..... | 12 |
| 2.3 Geomorphology and sediment distribution of the Chao Phraya delta plain and the adjacent region (Tanabe et al., 2003)..... | 14 |
| 2.4 Sedimentary columns from borehole Sites 1 to 3 and from Pit 1 (Tanabe et al., 2003)..... | 15 |
| 2.5 The evolution of the Chao Phraya delta, paleo-shoreline at 8–7 cal kyr BP (Tanabe et al., 2003)..... | 16 |
| 2.6 Lithostratigraphy of the whale excavation (Chitnarin et al., 2023)..... | 18 |
| 2.7 Holocene sampled sections, with the inferred position of the six timelines (Negri, 2009)..... | 22 |
| 2.8 Sequence of maps showing the bathymetric reconstruction of Thai paleo-gulf (Negri, 2009)..... | 23 |
| 2.9 Stratigraphic correlation among Bangkok Clay sampled sections from N (left) to S (right); correlation lines separate different depositional environments (Negri, 2009)..... | 24 |
| 2.10 Stratigraphic correlation among Bangkok Clay sampled sections from W (left) to E (right); correlation lines separate different depositional environments (Negri, 2009)..... | 25 |
| 2.11 An illustration of the relationship between ostracod population age structures and their interpretation within the fossil record (Boomer et al., 2003)..... | 28 |

LIST OF FIGURES (Continued)

| Figure | Page |
|---|------|
| 2.12 Illustration of valve and limb morphology of the <u>Cyprididae</u> (Martens and Horne, 2009)..... | 31 |
| 2.13 The internal features of a <u>Neocyprideis agilis</u> right valve..... | 32 |
| 2.14 Typical muscle scar pattern of <u>Stigmatocythere bona</u> | 33 |
| 2.15 Schematic drawings of central muscle scars (internal view, arrow points to anterior). 1: <u>Stigmatocythere bona</u> Chen in Hou et al., 1982. 2: <u>Neomonoceratina rhomboidea</u> (Brady, 1968). 3: <u>Sinocytheridea impressa</u> (Brady, 1869). 4: <u>Keijella multisulcus</u> Whatley & Zhao, 1988. 5: <u>Hemicytheridea reticulata</u> Kingma, 1948. 6: <u>Propontocypris bengalensis</u> Maddocks, 1969..... | 33 |
| 2.16 The external features of a <u>Neocyprideis agilis</u> right valve..... | 34 |
| 2.17 Hinge terminology (Jain, 2020)..... | 35 |
| 2.18 Hinge types (Jain, 2020)..... | 36 |
| 3.1 Methodology..... | 39 |
| 3.2 Location of the exploration drill points for collecting samples..... | 40 |
| 3.3 The drilling site from Borehole KU1 (photo by Chatchalerm Ketwetsuriya)..... | 41 |
| 3.4 The drilling site from Borehole KU2 (photo by Chatchalerm Ketwetsuriya)..... | 42 |
| 3.5 The drilling site from Borehole KU3 (photo by Chatchalerm Ketwetsuriya)..... | 43 |
| 3.6 The drilling site from Borehole KU4 (photo by Chatchalerm Ketwetsuriya)..... | 44 |
| 3.7 The drilling site from Borehole KU5 (photo by Chatchalerm Ketwetsuriya)..... | 44 |
| 3.8 The Phanom Surin shipwreck excavation, Samut Sakhon Province, Gulf of Thailand. Photograph Bangkok Post (Fine Arts Department, 2014)..... | 45 |
| 3.9 Ostracod laboratory process..... | 46 |
| 3.10 EC/TDS/Salinity/Resistivity meter; HANNA HI-5521 (Facility Building 7, Suranaree University of Technology)..... | 47 |
| 3.11 Powder sample preparation..... | 47 |

LIST OF FIGURES (Continued)

| Figure | Page |
|--------|--|
| 3.12 | X-ray Diffractometry (XRD) BRUKER, D2 Phaser (Facility Building 10, Suranaree University of Technology).....48 |
| 4.1 | Stratigraphic columns of the study area from Boreholes KU1-KU5, and the Phanom Surin shipwreck site.....51 |
| 4.2 | Lithostratigraphy of Boreholes KU1 and KU5, showing sedimentary units.....52 |
| 4.3 | Salinity levels of 5 boreholes with lithostratigraphic column of Borehole KU5 (representing a composite column) from Samut Sakhon Province.....57 |
| 4.4 | X-ray Diffractogram of sediment at 18.75-meter depth (Borehole KU1).....61 |
| 4.5 | X-ray Diffractogram of sediment at 2.25-meter depth (Borehole KU1).....62 |
| 4.6 | X-ray Diffractogram of sediment at 8.25-meter depth (Borehole KU2).....62 |
| 4.7 | X-ray Diffractogram of sediment at 18.75-meter depth (Borehole KU1).....63 |
| 4.8 | X-ray Diffractogram of sediment at 6.25-meter depth (Borehole KU3).....63 |
| 4.9 | X-ray Diffractogram of sediment at 1.00-meter depth (Borehole KU4).....64 |
| 4.10 | X-ray Diffractogram of sediment at 19.75-meter depth (Borehole KU4).....64 |
| 4.11 | X-ray Diffractogram of sediment at 13.00-meter depth (Borehole KU5).....65 |
| 4.12 | X-ray Diffractogram of sediment at 21.25-meter depth (Borehole KU5).....65 |
| 4.13 | X-ray Diffractogram of sediment at 24.25-meter depth (Borehole KU5).....66 |
| 4.14 | X-ray Diffractogram of sediment at 28.25-meter depth (Borehole KU5).....66 |
| 5.1 | Late Holocene ostracods from Samut Sakhon Province: A-F, <u>Neocyprideis agilis</u> (Guan, 1978); G-H, elongate and rounded sieve pores of <u>N. agilis</u> . See description of the specimen in text. Scale bars are 200 μ m, except for G-H.....69 |

LIST OF FIGURES (Continued)

| Figure | Page |
|--------|---|
| 5.2 | Late Holocene ostracods from Samut Sakhon Province: A-G, <u>Sinocytheridea impressa</u> (Brady, 1869); H-J, <u>Hemicytheridea reticulata</u> Kingma, 1948; K-L, <u>Hemicytheridea cancellata</u> (Brady, 1868). See description of the specimen in text. Scale bars are 100 μm71 |
| 5.3 | Late Holocene ostracods from Samut Sakhon Province: A-F, <u>Keijella multisulcus</u> Whatley & Zhao, 1988; G-K, <u>Keijella gonia</u> Zhao & Whatley, 1989. See description of the specimen in text. Scale bars are 200 μm73 |
| 5.4 | Late Holocene ostracods from Samut Sakhon Province: A-E, <u>Neomonoceratina iniqua</u> (Brady, 1868); F-J, <u>Neomonoceratina rhomboidea</u> (Brady, 1968); K, <u>Neomonoceratina mediterranea malayensis</u> Zhao & Whatley, 1988; L, <u>Neomonoceratina mediterranea mediterranea</u> (Ruggieri, 1953). See description of the specimen in text. Scale bars are 100 μm76 |
| 5.5 | Late Holocene ostracods from Samut Sakhon Province: A-H, <u>Proponocypris bengalensis</u> Maddocks, 1969; I, <u>Aglaiocypris pellucida</u> Mostafawi, 2003. See description of the specimen in text. Scale bars are 100 μm80 |
| 5.6 | Late Holocene ostracods from Samut Sakhon Province: A-D, <u>Lankacythere coralloides</u> (Brady, 1886); E, <u>Cytherella</u> sp.; F-I, <u>Stigmatocythere bona</u> Chen in Hou et al., 1982. See description of the specimen in text. Scale bars are 100 μm82 |
| 5.7 | Occurrence of ostracod species from Borehole KU1.....86 |
| 5.8 | Number of valve and carapace of ostracods from Borehole KU1.....86 |
| 5.9 | Occurrence of ostracod species from Borehole KU2.....87 |
| 5.10 | Number of valve and carapace of ostracods from Borehole KU2.....87 |
| 5.11 | Occurrence of ostracod species from Borehole KU3.....89 |

LIST OF FIGURES (Continued)

| Figure | Page |
|--|------|
| 5.12 Number of valve and carapace of ostracods from Borehole KU3..... | 90 |
| 5.13 Occurrence of ostracod species from Borehole KU4..... | 91 |
| 5.14 Number of valve and carapace of ostracods from Borehole KU4..... | 91 |
| 5.15 Occurrence of ostracod species from Borehole KU5..... | 92 |
| 5.16 Number of valve and carapace of ostracods from Borehole KU5..... | 93 |
| 5.17 Distribution of ostracod from Phanom Surin shipwreck site..... | 95 |
| 5.18 Number of valve and carapace of ostracods from Phanom Surin shipwreck site..... | 95 |
| 6.1 Lithostratigraphy, distribution and abundance of ostracods, and salinity level of Borehole KU5..... | 97 |
| 6.2 Salinity level of the sediments and the abundance of ostracods in each borehole..... | 99 |

LIST OF TABLES

| Table | Page |
|--|------|
| 2.1 Comparison of Holocene sea-level changes from previous studies in Thailand and Southeast Asian countries (Choowong, 2002)..... | 20 |



CHAPTER I

INTRODUCTION

The Quaternary geology of the Lower Central Plain in Thailand remains poorly understood due to the accumulation of unconsolidated sediments and limited access to subsurface data. This study focused to address this knowledge gap, by providing a detailed lithostratigraphy of Late Quaternary Bangkok Clay, geochemical analysis, and fossil ostracods interpretation found in Samut Sakhon Province to reconstruct the depositional environment of the Late Quaternary sediments.

1.1 Background and Rationale

The Central Plain of Thailand is divided into upper and lower parts, with the area of Nakhon Sawan Province as a joint (Alekseev and Takaya, 1967; Dheeradilok, 1995; Sinsakul, 2000). The Quaternary geology of the Lower Central Plain has been neglected and is poorly understood because of the thick accumulation of unconsolidated sediments and inaccessibility of subsurface data (Sinsakul, 2000). The Quaternary deposits of the Lower Central Plain represent a complex sequence of alluvial, fluvial and deltaic sediments, the geologic map of Quaternary deposits in the Lower Central Plain is shown in Figure 1.1.

About 2,000 meters of Pleistocene and Holocene sediments were deposited in the basin (Nutalaya and Rau, 1984). The deltaic and shallow marine Holocene sediments forming the delta plain are called the Bangkok Soft Clay (Rau and Nutalaya, 1983), Bangkok Marine Clay (deltaic sediments) (Somboon, 1988), and Holocene Unit (marine clay) (Songtham et al., 2000), and the Late Pleistocene sediment are called the Bangkok Stiff Clay (Rau and Nutalaya, 1983). Additionally, Moh et al. (1969) has been divided the Bangkok clay into three units; weathered clay, soft clay, and stiff clay.

Several studies have focused on various aspects of the Quaternary geology in the Gulf of Thailand and surrounding areas. Dheeradilok (1992) examined the depositional environments, economic significance, and tectonics of Quaternary

geological formations in Thailand. In a subsequent study, Dheeradilok (1995) investigated the coastal morphology and deposition patterns during the Quaternary period in Thailand. Sinsakul (2000) conducted a study focusing on the Late Quaternary geology of the Lower Central Plain, providing the sequence of sediments, including alluvial, fluvial, and deltaic deposits, that accumulated in the basin. Sinsakul (2002) further contributed to the understanding of Quaternary geology in Thailand. Tanabe et al. (2003) conducted a study on the stratigraphy and Holocene evolution of the mud-dominated Chao Phraya delta, providing the sedimentary processes and environmental changes in the region.

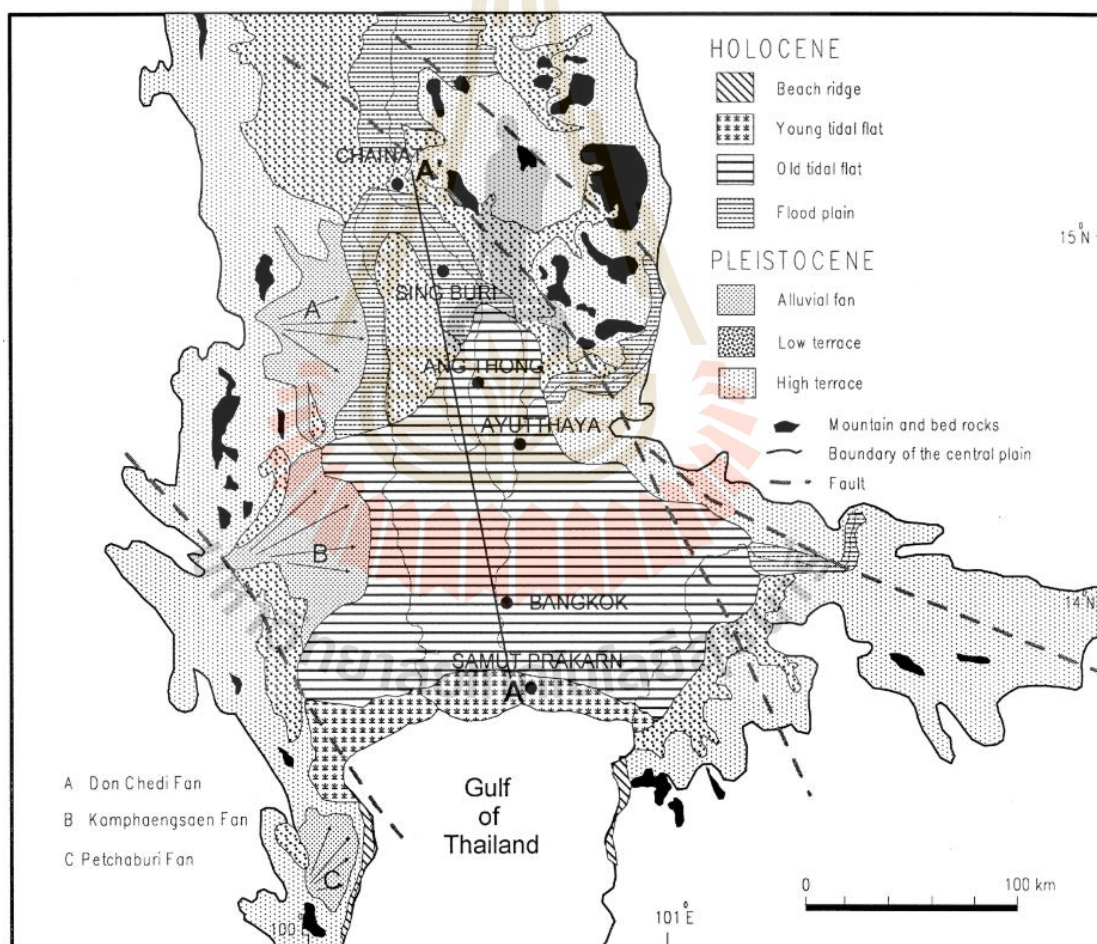


Figure 1.1 Geologic map of Quaternary deposits in the Lower Central Plain of Thailand (Sinsakul, 2000)

To complement the reconstruction of paleoenvironments, the study of paleontology is also invaluable. This study focuses on ostracod study, as they are

useful indicators of past environmental conditions. Ostracods or seed shrimps are microscopic crustaceans whose bodies are covered with calcareous bivalved shell, living in common to almost all aquatic and semi-terrestrial habitats (Ruiz et al., 2005; Holmes and Chivas, 2002). They have lived on the Earth since the Ordovician, and are abundant on both living and fossil species. Many studies on morphology and shell composition revealed that ostracods have a great potential for ecological monitoring and paleoenvironmental analyses in highly variable environments and for modern pollution studies to sea-level change, basin evolution, plate tectonics and paleoceanography (Rosenfeld and Vesper, 1977; Ruiz et al., 2000; Lytle and Wahl, 2005; Yasuhara et al., 2005; Lamb et al., 2006; Yasuhara and Seto, 2006; Yasuhara et al., 2012a).

Several studies have focused on the distribution and ecological characteristics of ostracods in different environments within the Gulf of Thailand and other coastal areas of Thailand. Montenegro et al. (2004) examined the ostracod fauna in a shallow marine environment at the Mae Klong river mouth in the northwest Gulf of Thailand. Pugliese et al. (2006) conducted environmental monitoring using shallow marine ostracods in the Phetchaburi area of the northwest Gulf of Thailand. Yamada et al. (2014) utilized fossil ostracods to identify sediments associated with tsunamis at the mouth of the Khlong Thom River on the western coast of Thailand. Forel (2021) conducted the first detailed study of ostracods dwelling in the Andaman Sea along the southwestern coast of Thailand. Chitnarin et al. (2023) focused on Holocene ostracods in the Chao Phraya delta, particularly in shallow marine environments at depths less than 20 meters.

The study aims to complement the existing knowledge on the Quaternary geology of the region. Despite the existence of studies on the Quaternary of the Gulf of Thailand, the understanding of the Quaternary geology in the region remains limited. This study addressed a notable gap in the understanding of the Quaternary geology in the Gulf of Thailand by integrating multiple approaches (stratigraphy, geochemistry, and micropaleontology).

1.2 Research objectives

1) To create lithostratigraphic columns of Late Quaternary Bangkok Clay from 5 boreholes and sediment samples collected from Phanom Surin shipwreck site, Samut Sakhon Province, Central Thailand.

2) To conduct geochemical data including XRD and salinity analysis from study areas.

3) To establish taxonomy of fossil ostracods found from the study sites in Samut Sakhon Province.

4) To interpret depositional environment of Late Quaternary sediments based on stratigraphic data, geochemical data and ostracod assemblages from the study areas.

1.3 Scope and Limitations

1) The study are conducted on the sediments from 5 boreholes and the Phanom Surin excavation site in Samut Sakhon Province, Central Thailand.

2) Ostracod preparation is processed following Horne and Siveter (2016).

3) The identification of ostracods in this study is based on their shell morphology.

4) Paleoenvironment is interpreted from lithostratigraphic and geochemical data, and ostracod assemblages recovered from the studied samples.

1.4 Contents of the thesis

This thesis contains 6 chapters, including the introduction (Chapter I) and literature review (Chapter II). In chapter II, there are the literature reviews of geology of Samut Sakhon Province, stratigraphic study and sea-level change in the Gulf of Thailand, study of taxonomy and paleoenvironmental interpretation from ostracods of the Late Quaternary in Thailand, collecting and processing of ostracods, and ostracod shell morphology.

Chapter III provides methodology of the study, containing the literature review of the study, field investigation and sampling. In this chapter, the laboratory work on

stratigraphic study, ostracod study, salinity analysis, and XRD analysis were provided. Moreover, the data analysis and interpretation were also mentioned.

Chapter IV, contains the result of lithostratigraphic and geochemical data. The systematic of ostracods and the distribution of ostracods are reported in Chapter V.

The last chapter of this thesis is chapter VI, contains discussion and conclusion from results of paleoenvironmental interpretation from lithostratigraphy and geochemistry, and ostracod assemblages. Appendices are provided at the end of this thesis.



CHAPTER II

LITERATURE REVIEW

The study of geology and stratigraphy is crucial to understanding of evolution and history in a particular region. This chapter provides an overview of general geology and geology of the study sections in the Gulf of Thailand and Central Thailand. The chapter also presents evidence of sea-level changes in the Gulf of Thailand, which help explain the evolution of the plain in this region. The information presented in this chapter is based on previous studies conducted by various researchers and is essential for understanding the geological context of the study sections in subsequent chapters. This chapter also provides an overview of the existing literature related to the topic of ostracods studied in Thailand.

2.1 Geology of Samut Sakhon Province, Central Thailand

Samut Sakhon Province is characterized by its coastal plain landscape, with an elevation of about 1-2 meters above sea level. The Tha Chin River flows through the central part of the province, meandering from north to south towards the Gulf of Thailand in Mueang Samut Sakhon District. The distance is approximately 70 kilometers (DMR, 2016).

According to Department of Minerals Resource (2016), the geology of Samut Sakhon Province can be classified into six sedimentary units (Figure 2.1):

1) Flood plain clay on tidal flat clay on marine clay on old alluvial sandy clay deposit (Qff/tf/mc/oa): This sediment consists of clayey soil, either brown or light gray in color, with a dense and sticky texture. It is layered on top of a soft, gray clay sediment, which, in turn, is deposited on a clayey soil mixed with sand. The clayey soil with a high density is gray in color and often contains fragments of seashells, indicating a marine environment.

The sediment formation is influenced by the Chao Phraya River and its western branch, with the main influence coming from the Chao Phraya River,

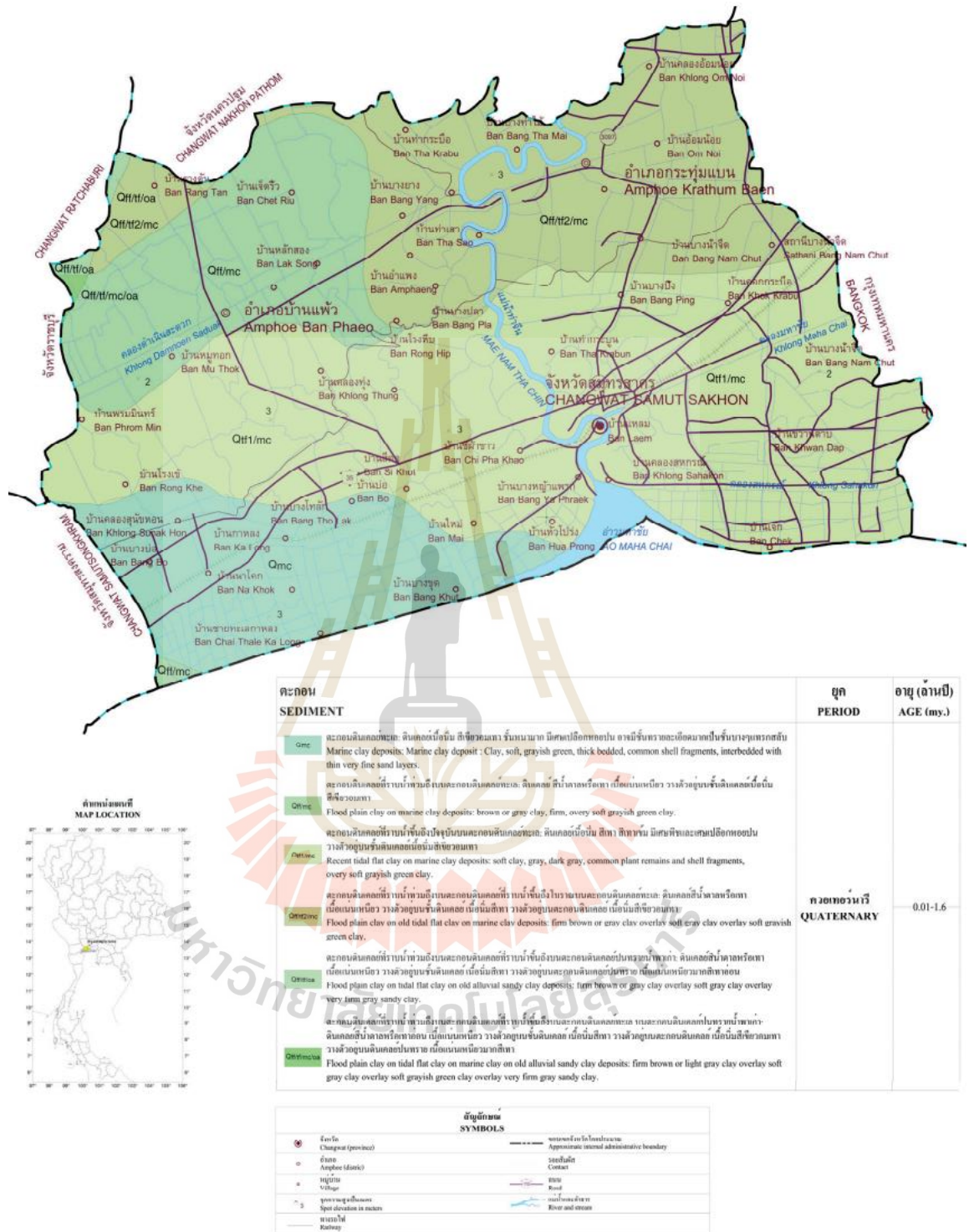


Figure 2.1 Geologic map of Samut Sakhon Province (DMR, 2016)

which transports and accumulates the sediment. The age of this sediment formation ranges from the Holocene period to the present.

2) Flood plain clay on tidal flat clay on old alluvial sandy clay deposit (Qff/ta/oa): This unit consists of clay sediments on the current raised floodplain up to the sea clay. The sedimentary unit of clay on the flooded area extending up to the coastal clay is found in the areas influenced by the current water flow and its surroundings. It is characterized by a wide and extensive plain with very gentle slopes. This sediment is formed by the overflow of water during the monsoon season, and the fine-sized sediment is transported and accumulated continuously and for a long period of time along the coast. The accumulation rate remains constant.

This sedimentary unit is deposited on the clay sediments that extend from the flooded area up to the clay sediments mixed with old river sand. It forms a wide plain that is distributed in narrow areas, particularly in the western part of the province, specifically in Ban Don, Amphoe Ban Phaeo, Samut Sakhon Province. The sediment consists of soft to compact clay soils in light gray, yellowish-gray, and dark gray colors, deposited on the soft gray and greenish-gray clay sediments. Seashell fragments are found, indicating a marine environment, and it is deposited on the clay sediments mixed with sand. The sediment has a very compact and light gray texture. The influence of the Gulf of Thailand is significant in transporting and accumulating sediments in this sedimentary unit. It has an age ranging from the Holocene to the present.

3) Flat clay on marine clay deposit (Qf1/mc): It includes clay sediments on the floodplain, extending up to the ancient sea clay. The clay sediment on the floodplain extends to the clay sediment on the seashore. The sea on the clay sediment mixes with the old sand. The terrain is characterized by wide, flat plains with very gentle slopes. It is a sediment formed by the overflow of the river during the rainy season, and the fine particles of sediment are carried up and accumulated on the shore, forming a continuous and long-lasting accumulation. The accumulation rate remains constant. This type of sediment is deposited on the clay sediment that extends from the floodplain to the clay sediment mixed with sand on the seashore.

The terrain is wide and there is a narrow strip of scattered areas on the western side of the province, near Ban Don, Amphoe Ban Phaeo, Samut Sakhon Province.

4) Flood plain clay on old tidal flat clay on marine clay deposit (Qff/2f2/mc): The clay sediment on the flooded floodplain extends to the ancient clay sediment on the coastal plain. It is found in the fluctuating area of the current river and its surrounding areas. The terrain is characterized by wide and extensive flat plains with very gentle slopes. It is a sediment that is formed by the overflow of the river during the monsoon season. The fine particles of sediment are carried up and accumulated continuously on the shore, forming a long-lasting accumulation. The accumulation rate remains constant.

This sediment covers the clay sediment on the flooded floodplain, extending to the ancient clay sediment on the coastal plain. It is a result of the riverbank erosion during the monsoon season. Due to its fine particle size, it is easily carried and continuously accumulated along the shore. The terrain has a very gentle slope and covers a wide and extensive area. It is primarily located in the northern part of the province, including Ban Don Wua and Amphoe Ban Phaeo, with a smaller portion in Amphoe Krathum Baen. The main influence in the transportation of this sediment comes from the Chao Phraya River, which carries and accumulates the sediment in this clay sediment series.

5) Flood plain clay on marine clay deposit (Qff/mc): The clay sediment on the flooded floodplain extends to the ancient clay sediment on the coastal plain. It is found in the fluctuating area of the current river and its surrounding areas. The terrain is characterized by wide and extensive flat plains with very gentle slopes. It is a sediment that is formed by the overflow of the river during the monsoon season. The fine particles of sediment are carried up and accumulated continuously on the shore, forming a long-lasting accumulation. The accumulation rate remains constant. This sediment covers the clay sediment on the flooded floodplain, extending to the ancient clay sediment on the coastal plain. It is a result of the riverbank erosion during the monsoon season. Due to its fine particle size, it is easily carried and continuously accumulated along the shore. The terrain has a very gentle slope and covers a wide

and extensive area. It is primarily located in the northern part of the province, including Ban Don Wua and Amphoe Ban Phaeo, with a smaller portion in Amphoe Krathum Baen. The main influence in the transportation of this sediment comes from the Chao Phraya River, which carries and accumulates the sediment in this clay sediment series.

6) Marine clay deposit (Qmc): Clay sediment is a type of sediment that originates from the mouth of rivers and deposits in the offshore areas of coastlines. It consists of a mixture of clayey and sandy soil, with a soft and delicate texture. Thin layers of fine sand are often interspersed within the sediment. It is common to find plant debris and scattered shells throughout the sediment. The marine clay layer is formed when the sea level rises and inundates the land during the early Holocene period, approximately 8,000 to 6,000 years ago. This sediment is widely distributed along the southern coast of Thailand, covering the districts of Samut Sakhon. The sediment is characterized by its soft, greenish-gray clayey texture, with a significant thickness. It may also contain layers of fine sand intermittently. The influence of the Gulf of Thailand is responsible for transporting and depositing the sediment in this particular formation, which has an age corresponding to the early Holocene period.

2.2 Stratigraphic study and sea-level change in the Gulf of Thailand

2.2.1 Stratigraphy of the Late Quaternary sediments in Central Plain of Thailand

The Central Plain of Thailand refers to the flat area between mountain ranges in the northern region. It extends from the upper region, starting from the area of Uttaradit-Sukhothai Provinces, following the Yom River, Nan River, and then reaching the area of Nakhon Sawan Province. It further expands into low-lying areas within the influence of Chao Phraya, Tha Chin, Mae Klong, and Bang Pakong river basins, extending down to the coastal areas of Samut Prakan, Samut Sakhon, and Samut Songkhram Provinces. This plain can be classified into the Upper Central Plain and the Lower Central Plain, with the area of Nakhon Sawan serving as a transitional zone (Alekseev and Takaya, 1967; Dheeradilok, 1995; Sinsakul, 2000). The first general outline of Quaternary deposits in Central Thailand was included in a bulletin of the geology and

mineral resources of the country by Brown et al. (1951), and then by Sinsakul (2000) and Sinsakul et al. (2002)

Sinsakul (2000) concluded the evolution of the Chao Phraya Delta based on the stratigraphy, lithology, paleontology and radiocarbon dating. Figure 2.2 illustrates a schematic model of the Lower Central Plain during the peak of the Holocene transgression. According to the model, the sediment in the Late Pleistocene period from the Gulf of Thailand consists of stiff clay, lateritic soil, and weathered rock. In the Holocene period, the sediment comprises intertidal clay and marine clay, which are influenced by river processes.

According to studies of Planchareon (1976), Planchareon and Chuamthaisong (1976), Wongsomsak and Theyapunte (1987), and Sinsakul (2000), it is concluded that a layer of stiff clay, found at a depth of around 15 to 20 meters, representing the uppermost layer of the Late Pleistocene Epoch in Central Plain of Thailand. The composition analysis of this stiff clay layer reveals the presence of iron and manganese elements, along with visible red and brown spots on its surface. The clay has low electrical conductivity, slightly alkaline pH, and low concentration of chloride ions. Kaolinite is identified as the primary clay mineral. The analysis of salt content indicates a minimal presence of salt, particularly beyond the depth of 50 meters, where the influence of saline contamination in the soil is almost negligible. These findings suggest that this stiff clay layer formed on land in floodplain deposits and has undergone weathering processes.

Dheeradilok (1992) suggested that Quaternary depositional processes could be classified according to paleoenvironments into fluvial, coastal, laterite, volcanic and lacustrine deposits. However, the stratigraphic sequences were broadly grouped into two chronostratigraphic units, the Pleistocene and Holocene formations. The Holocene-Pleistocene boundary can be clearly recognized at the coast by an abrupt change in consistency from a soft marine clay to a stiff fluvial sand and clay (Dheeradilok, 1995) as shown in Figure 2.1.

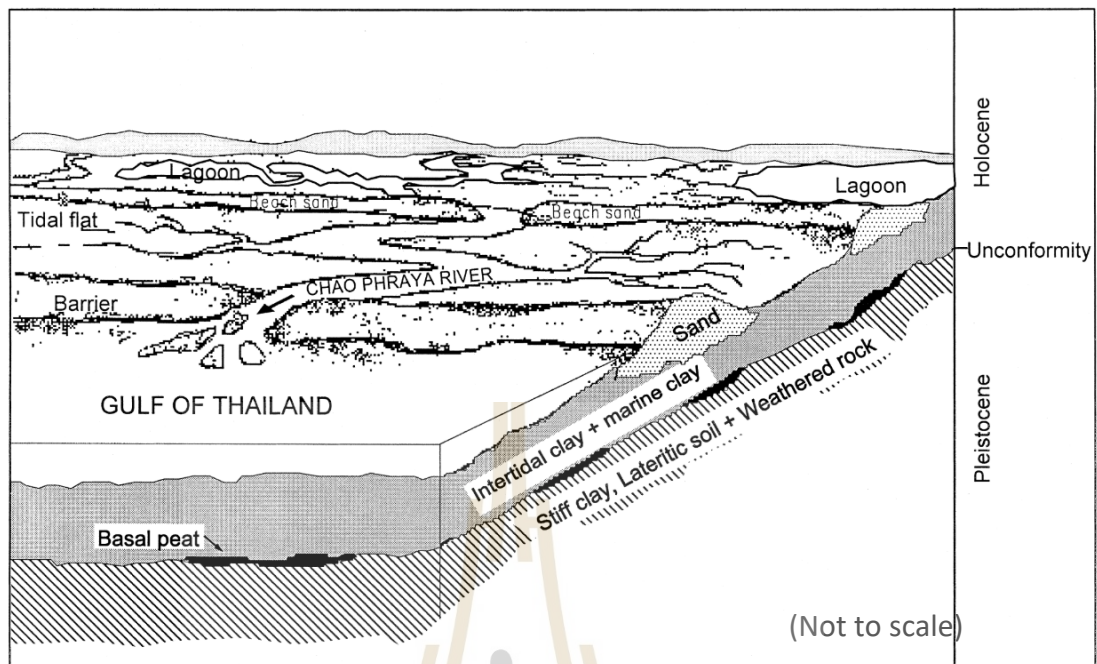


Figure 2.2 Schematic model of the Lower Central Plain during maximum Holocene transgression (Sinsakul, 2000)

Sinsakul et al. (2002) explained that the deposits during the Pleistocene epoch in the Lower Central Plain primarily consist of alluvium and fluvial sediments, characterized by intercalated layers of gravels, sand, silt, and clay. In the upper sequence, stiff clay with orange and red mottles dominates, while some areas may also exhibit laterite and lateritic soil. The Holocene sediments in the Lower Central Plain were strongly impacted by the transgression and regression of the Holocene sea, leading to rapid accumulation of sediment in the deltaic area.

Tanabe et al. (2003) studied the sedimentary succession and depositional environments of the Late Quaternary geology using data obtained from shallow boreholes, open pits and groundwater well samples, and interpreted that the sediments were deposited in fluvial, alluvial, tidal flat and deltaic environments. Figure 2.3 shows their location sites and the distribution of Chao Phraya Delta system and the Mid-Holocene shoreline at maximum transgression based on Somboon and Thiramongkol (1992). The result of the sediment facies as shown in Figure 2.4, the succession are divided into 3 sedimentary units I, II_a, and II_b in ascending order.

Each unit is characterized by lithology, sedimentary structures, texture, contact character, succession character, fossils, and ^{14}C ages. Unit I is the basement strata consisted composes of Late Pleistocene shallow marine and fluvial sediments. The Holocene strata unconformably overlying Unit I are divided into Units II_a and II_b which consist of basal lag and deltaic and shallow marine sediments, respectively.

Figure 2.5 shows the distribution of sediment deposits in the lower central region is influenced by two significant factors. The first factor is the fluvial process, which involves the flow of water and contributes to sediment accumulation in the upper areas of the Chao Phraya River floodplain. This region includes Chai Nat, Sing Buri, and Ang Thong Provinces. The sediment deposits found in this area consist of a mixture of sand, clay, and silt, with varying thicknesses ranging from 1 meter to 18 meters (Wongsomsak and Theyapunte, 1987). The second factor is the tidal process, characterized by the movement of sea water, which results in sediment deposition across the majority of the Chao Phraya River floodplain. These sedimentary deposits mainly consist of marine soft clay or Bangkok Clay.

Boyd et al. (1996) studied the Holocene palaeogeography of the Southeast margin of the Bangkok Plain, and classified the stratigraphic unit into 6 units; bedrock, laterized silty clay, sand and gravel river channel alluvium, fine-grained clay-rich estuarine sediments, freshwater floodplain sediments, and sandy and clay-rich levee sediments. Stratigraphic Units 1 to 3 represent pre-Holocene conditions and provide a basement upon which Holocene sediments were deposited, whereas Stratigraphic Units 4 to 6 represent Holocene conditions.

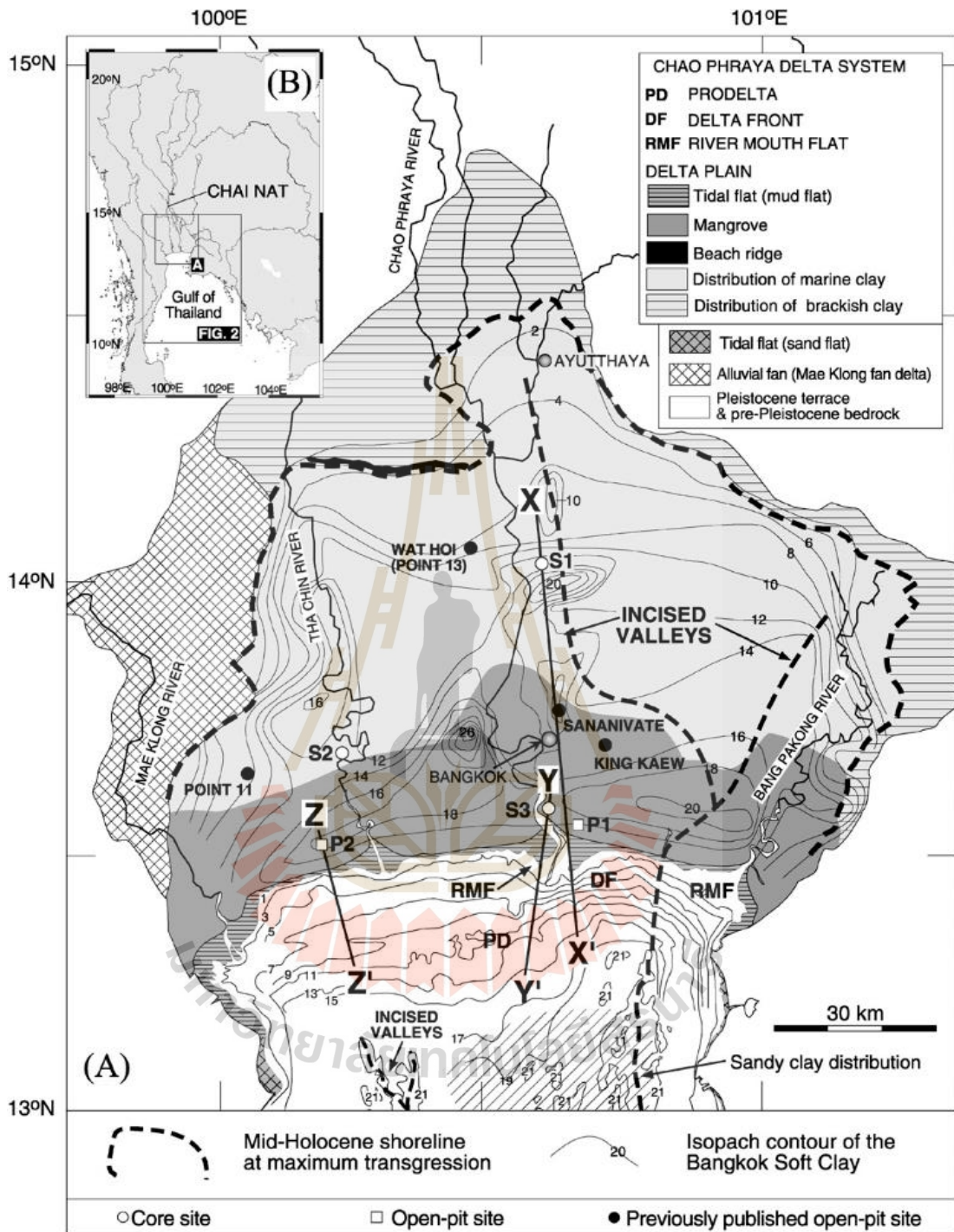


Figure 2.3 Geomorphology and sediment distribution of the Chao Phraya delta plain and the adjacent region (Tanabe et al., 2003)

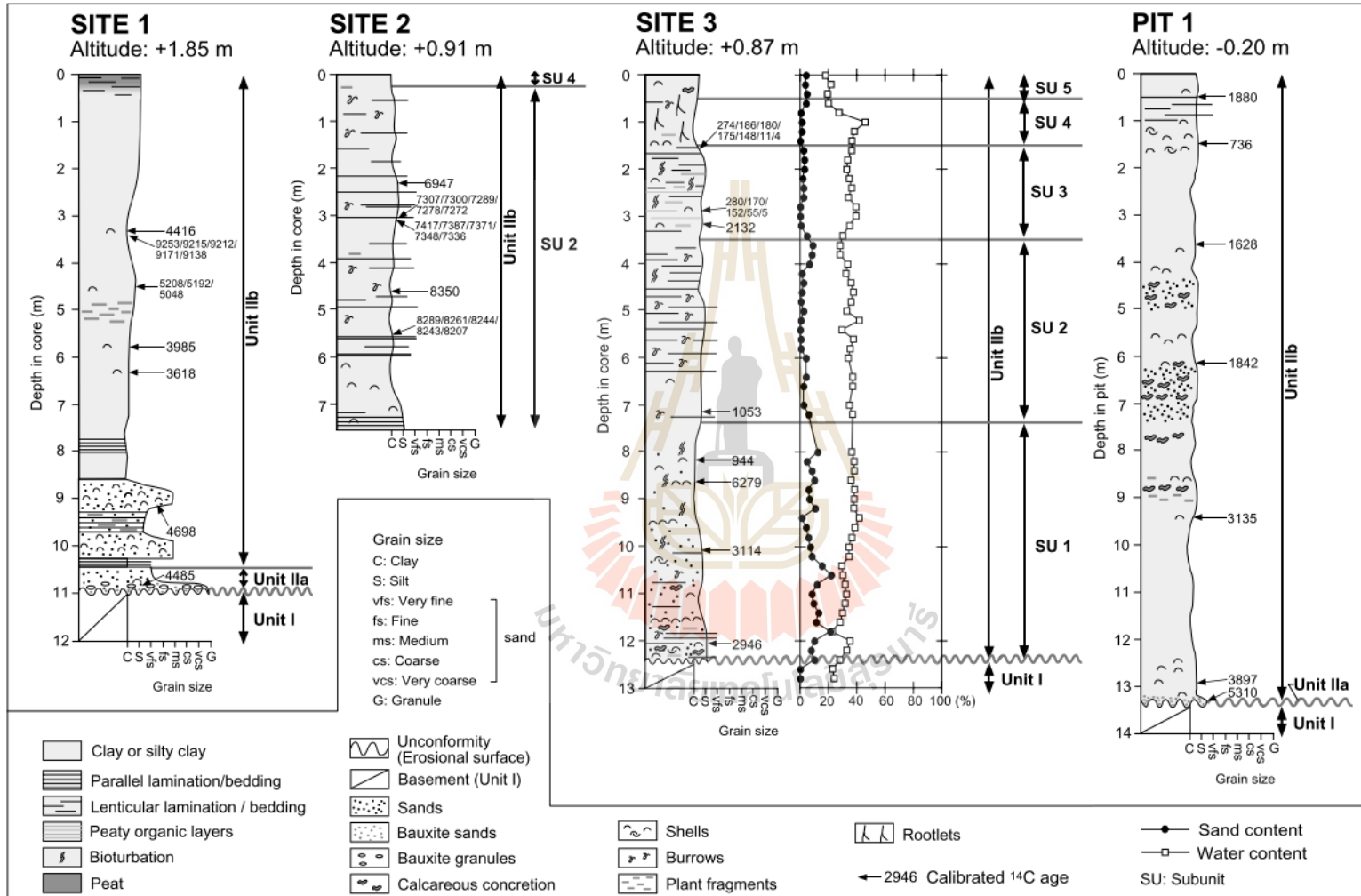


Figure 2.4 Sedimentary columns from borehole sites 1 to 3 and from Pit 1 (Tanabe et al., 2003)

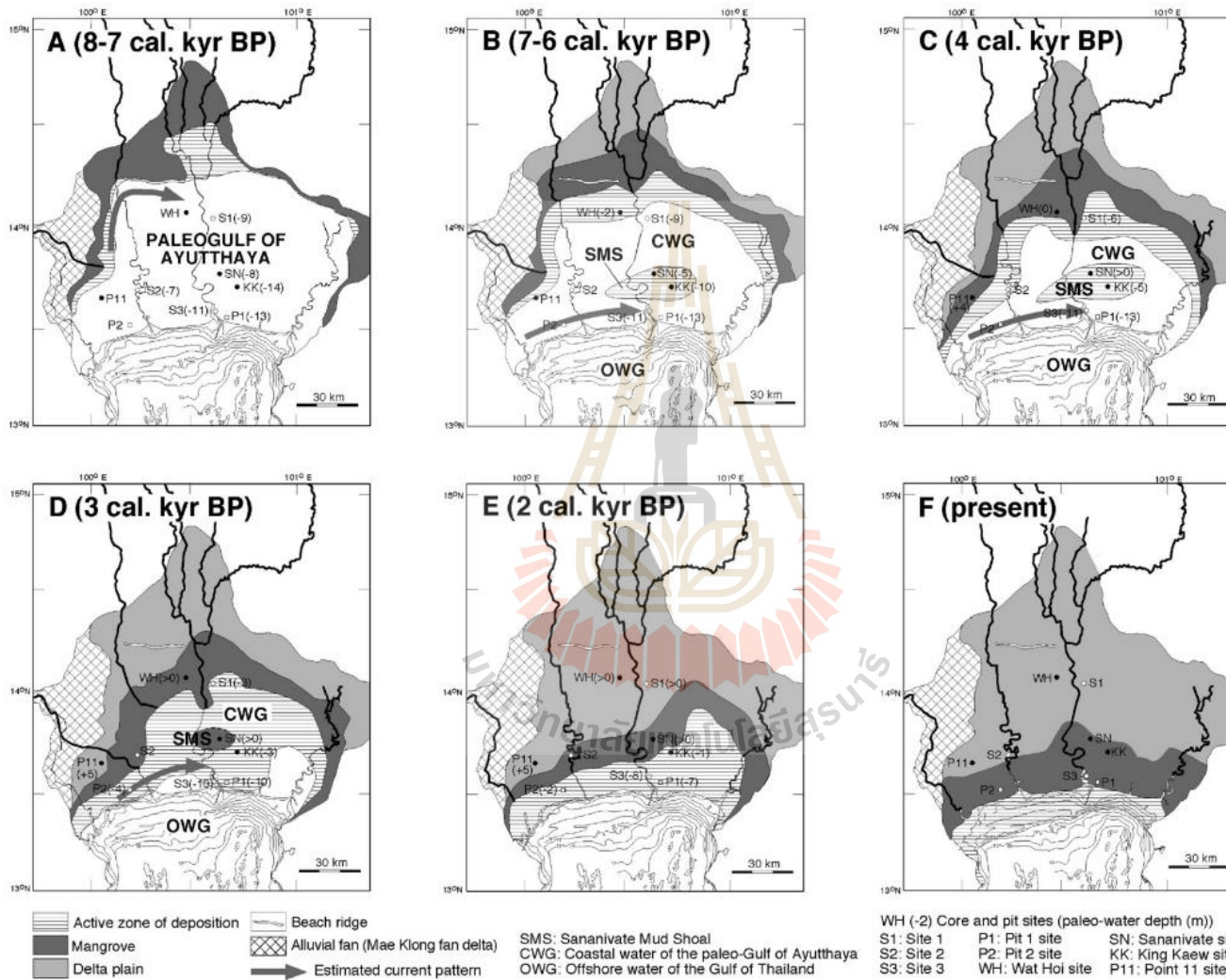


Figure 2.5 The evolution of the Chao Phraya delta, paleo-shoreline at 8–7 cal kyr BP (Tanabe et al., 2003)

The study by Department of Groundwater Resources (2012), described the characteristics of the soil layers in Samut Sakhon Province were determined through the analysis of 37 borehole surveys, covering three districts: Samut Sakhon City, Ban Phaeo, and Krathum Baen. The uppermost layer is composed of Very Soft to Medium Clay, which belongs to the Holocene epoch. It has a thickness ranging from 13 to 17 meters. Below the upper layer, there is a sequence of alternating Medium to Very Stiff Clay and Very Stiff to Hard Clay. These clay layers, originating from the late Pleistocene Epoch, have a considerable thickness of over 20 meters. Interlaced within the clay layers, particularly in the vicinity of the city district, there may be additional layers of medium or dense to very dense sand. These sand layers, also dating back to the late Pleistocene epoch, are present and can be found within the clay layers.

Paleontological and archaeological findings from the Bangkok Clay Formation have revealed significant discoveries, including marine mollusks (Chonglakmani et al., 1983; Robba et al., 1993; Negri, 2009) and the Phanom Surin Shipwreck (Jumprong, 2019; Grote et al., 2021). The Phanom Surin shipwreck site is an archaeological site located off the coast of Samut Sakhon, Thailand. The wreck site is located approximately 8 kilometers inland, the excavation of the Phanom Surin shipwreck has yielded a wide range of artifacts, including ceramics, weaponry, coins, and cargo items. The ceramics discovered at the site indicate that the ship was involved in maritime trade between various regions, including China, Southeast Asia, and the Middle East (Jumprong 2014; 2019).

In 2020, there is the discovery of a whale skeleton, located about 15 kilometers north of the Gulf of Thailand shoreline in Samut Sakhon Province. The whale skeleton is dated to $3,380 \pm 30$ years (Kawira and Saethien 2021; Saethien 2021). Chitnarin et al. (2023) studied lithostratigraphy of the area around the whale excavation consists of four sedimentary units (Figure 2.6): Pleistocene Stiff Clay, Shallow Marine Clay, Old Tidal Flat sediments, and Topsoil. Microfossils such as palynomorphs, foraminifers, and ostracods were studied to interpret paleoenvironment (Chitnarin et al., 2023; Rugmai et al., 2023)

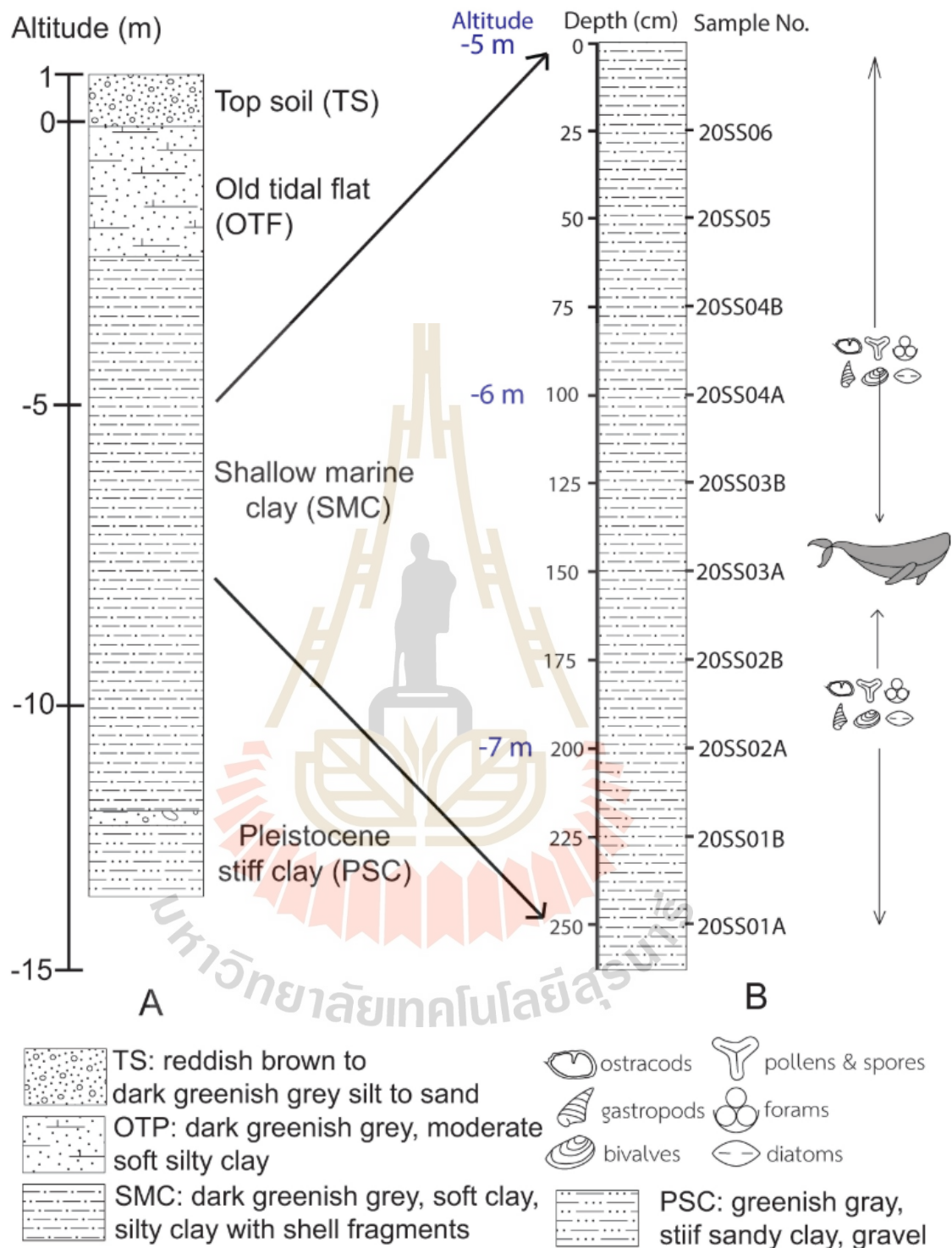


Figure 2.6 Lithostratigraphy of the whale excavation site (Chitnarin et al., 2023)

Additionally, lithostratigraphy in the area of eastern coast of the Gulf of Thailand were studied. Chataro, Choowong and Phantuwoongraj (2022) interpreted the

data from satellite images at Pailin Beach, located in Trat Province. The samples were collected to study lithostratigraphy of this area. The stratigraphic column shows the vertical sequence of the beach ridge sediment, the sediment is composed of fine sand, moderately well to well sorted, and most of the composition is quartz minerals. The result of Optically stimulated luminescence (OSL) dating reveals an age of old beach ridges beginning from $3,230 \pm 250$ years ago to $1,750 \pm 150$ years ago.

2.2.2 Sea level change in the Late Quaternary, Central Thailand

Sinsakul (1992) reviewed the evidence of former sea levels from the morphology and stratigraphy, and discussed with reference to the sea level curve of Thailand. Due to possible errors in ^{14}C dates, tectonic activity, elevation and tidal indicators. He assumed that it will not be possible to draw a good curve of Holocene sea levels in Thailand. In addition, interpretation is made difficult because the coastal areas of these regions have remained tectonically active. Evidence of shoreline erosion has been found in many places.

The geomorphology of sea-level changes to study coastal evolution from the Gulf of Thailand was studied by Choowong (2002), the study discussed an assessment of evidence of sea-level changes in explaining the evolution of the coastal plain from the Gulf of Thailand. Geological indicators are sea notches, sea caves and arches, platforms and beaches with weathered features such as honeycomb structure, former tidal flats and salt marshes, and relict barriers. Biological indicators include palynology, fossil crabs, shell fragments and peats. There are the arguments concerned with the age of the mid-Holocene highstand in Thailand and some adjacent coastal areas in Southeast Asia (Table 2.1).

Choowong et al. (2004) studied Holocene biostratigraphical records in coastal deposits from Sam Roi Yod National Park, Prachuap Khiri Khan. Biological evidences such as palynology, marine molluscs, ooids, corals and reefs, coralline algae, vermetid gastropods, even the diagenetic products of marine carbonates have been used extensively as sea-level indicators (e.g. Van de Plassche, 1986; Pirazzoli, 1991 and 1996). Choowong et al. (2004) confirmed that there are no records and indicators of the Holocene tectonic adjustment. Thus, the interpretation in history of sea-level

changes can be done directly geomorphological features, stratigraphy and biological records.

Table 2.1 Comparison of Holocene sea-level changes from previous studies in Thailand and Southeast Asian countries (Choowong, 2002)

| Researchers | Inferable age of SL changes (Years in BP*) | |
|---|--|-----------------------------------|
| | SL reached highstand | SL started falling to present MSL |
| Thailand | | |
| Chonglakmani et al (1983) | 5,500 ± 50 | ** |
| Thiramongkol (1983b) | 6,000 | 3,670 ± 125 to 2,250 ± 110 |
| Sinsakul et al (1985) and Sinsakul (1992) | 6,000 and 4,500 | 6,000 to 4,700 and 4,500 to 1,500 |
| Somboon and Thiramongkol (1992) | 7,300 to 6,500 | 6,500 to present |
| Southeast Asia | | |
| Hesp et al (1998) (Singapore) | 7,000 to 6,500 | 6,500 to present |
| Tjia (1986) (Malaysia) | 7,000 to 6,000 | 6,000 to present |
| Hoang Ngoc Ky (1988) (Vietnam) | 5,500 to 3,500 | 3,500 to 3,000 |
| Le Van Cu et al (1988) (Vietnam) | 5,000 to 4,500 | 4,500 to 2,300 |

* Uncalibrated ¹⁴C years

**not mentioned

Negri (2009) conducted a study on the Holocene Thai paleo-gulf, focusing on an experimental mapping method that utilized fossil mollusk faunas. The study involved radiometric dating of shell material obtained from the samples. This dating process enabled the establishment of six specific timelines at various depths within each section. These timelines were positioned at approximately 9,000, 8,000, 6,000, 5,500, 5,000, and 4,000 years Before Present (BP), as illustrated in Figure 2.7.

The map showing transgression and regression and the coastline moving during 9,000 – 4,000 years BP in Negri (2009) study in Figure 2.8. In the examination of the available data, an attempt was made to reconstruct the evolution of the Thai paleo-gulf during the Holocene era. The comprehensive analysis involved the assessment of molluscan faunas, radiometric ages, and lithological characteristics. These factors played a crucial role in establishing correlations between stratigraphic logs along both a north-south (N-S) and a west-east (W-E) cross section (Figures 2.9 and 2.10) were utilized.

The studies by Nimnate et al. (2015) and Surakiatchai et al. (2018) provide evidence of sea level regression and paleogeographic in Thailand. Nimnate et al. (2015) focused on the Chumphon coast, while Surakiatchai et al. (2018) conducted their research at Sam Roi Yot National Park. Both studies revealed landforms and dating results indicating sea level regression and historical changes in those specific areas. This evidence contributed to the broader understanding of sea level fluctuations and paleogeographic changes occurring in different coastal regions.

According to Robinson (1974), the Gulf of Thailand can be described as a shallow water estuary with two distinct layers. The surface layer consists of low salinity water that has been diluted by rainfall and freshwater runoff, flowing out of the gulf. In contrast, the deeper layer consists of higher salinity water from the South China Sea, which enters the gulf over a sill located at its mouth. The circulation patterns within the gulf are influenced by various factors such as monsoon winds, heavy precipitation, and tidal currents. As a result, the circulation is complex, with localized areas experiencing divergence, upwelling, downwelling, or convergence of waters. Surface salinities in the Gulf of Thailand generally range between 32‰ and 33‰, except in areas affected by river runoff, upwelling, or intrusion of high salinity water from the South China Sea. Freshwater contributions from rivers are significant in maintaining salinities below 33‰. Menasveta et al. (2019) described the surface salinity levels in the Gulf of Thailand typically range from 30.5 to 33 ppt, but can be higher in areas where water from the South China Sea enters.

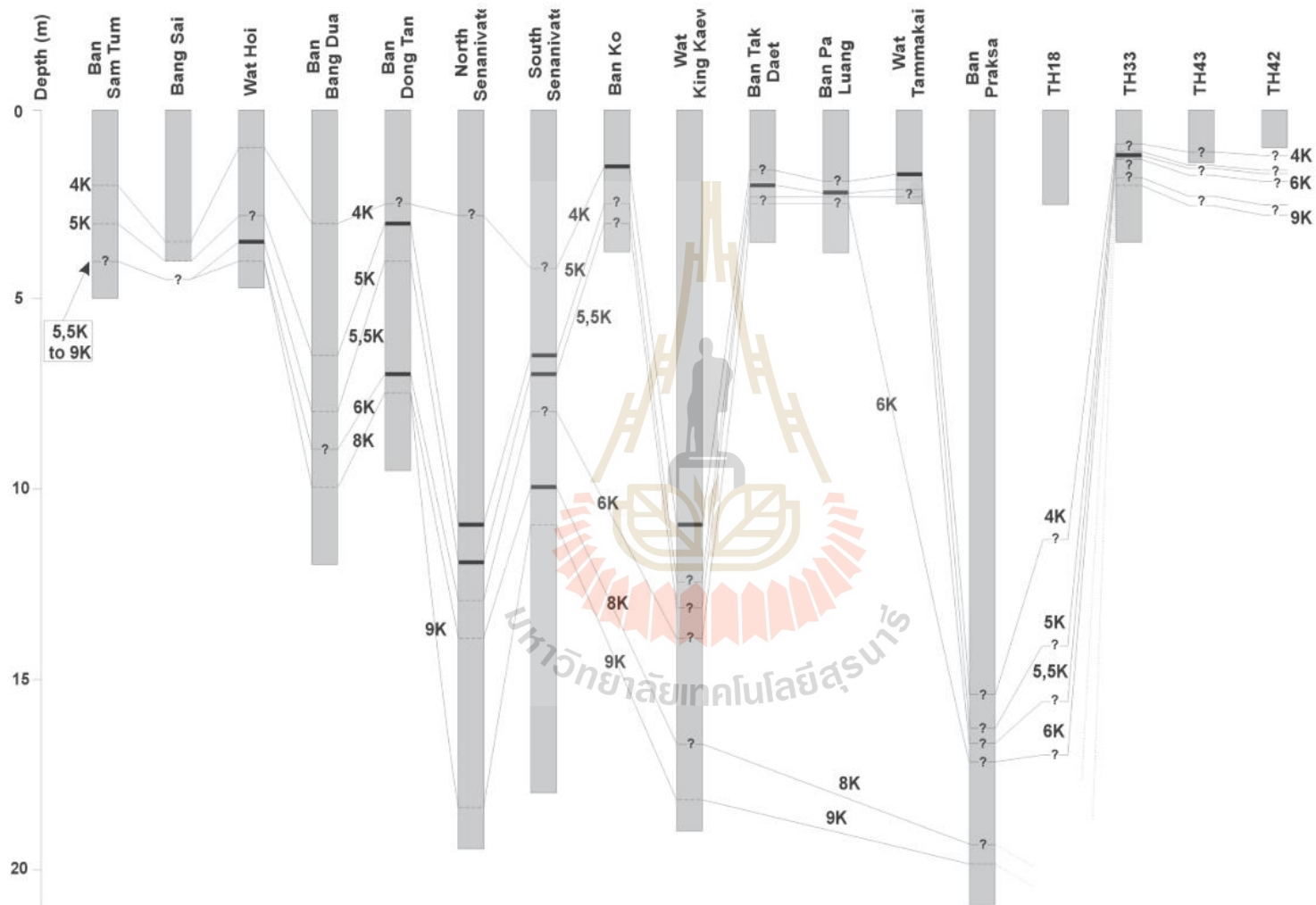


Figure 2.7 Holocene sampled sections, with the inferred position of the six timelines (Negri, 2009)

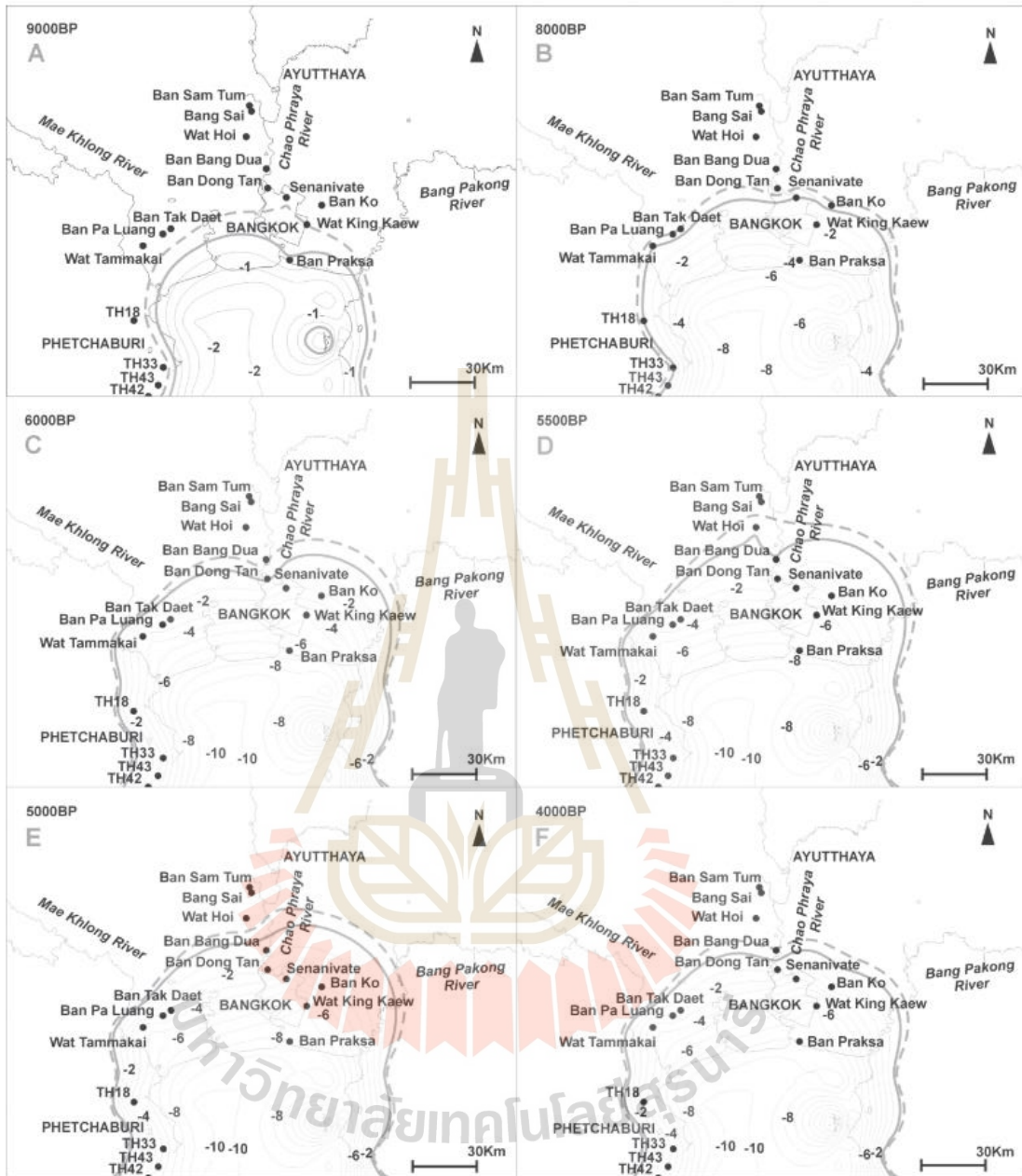


Figure 2.8 Sequence of maps showing the bathymetric reconstruction of Thai paleo-gulf (Negri, 2009)

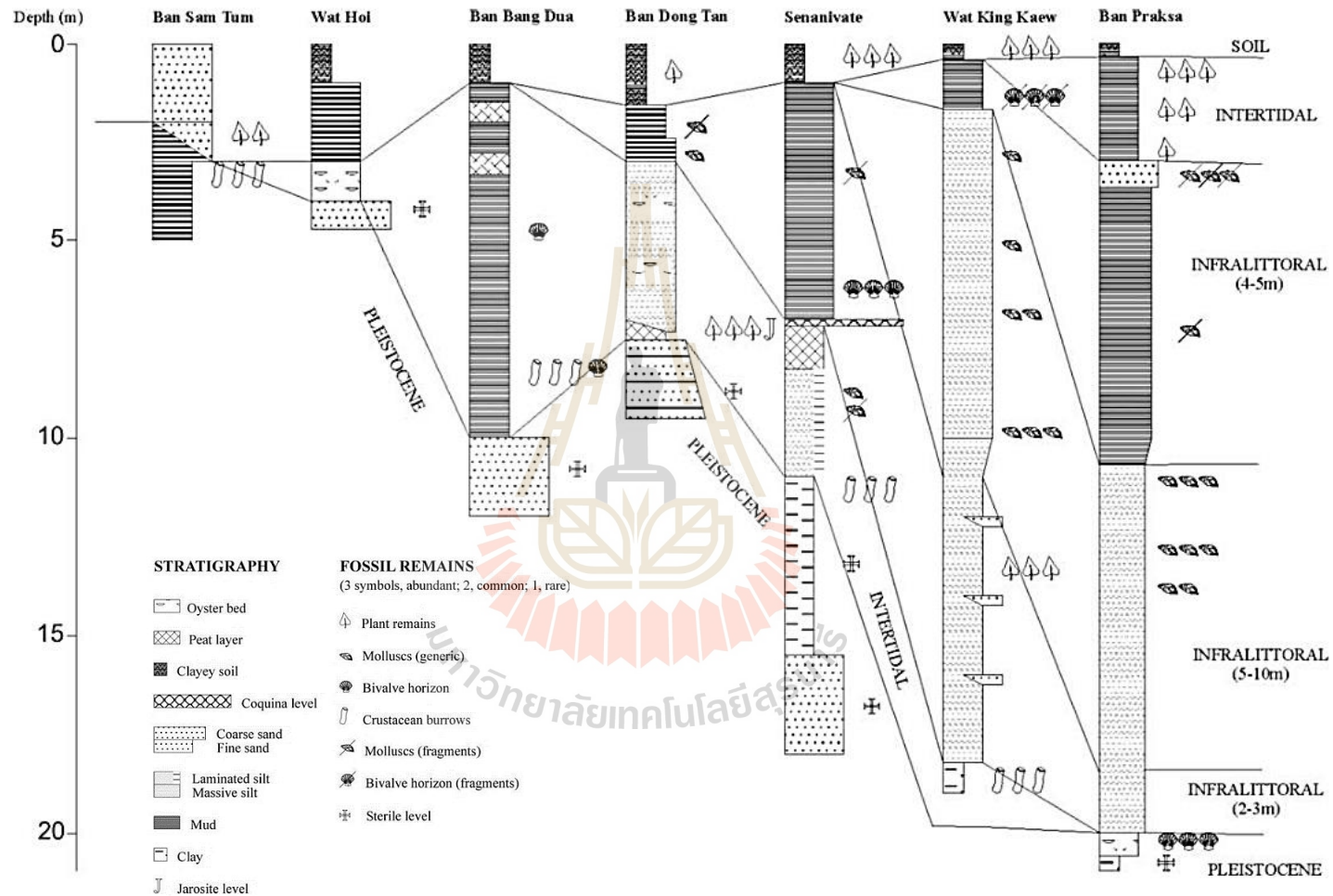


Figure 2.9 Stratigraphic correlation among the Bangkok Clay sections from N (left) to S (right); correlation lines separate different depositional environments (Negri, 2009)

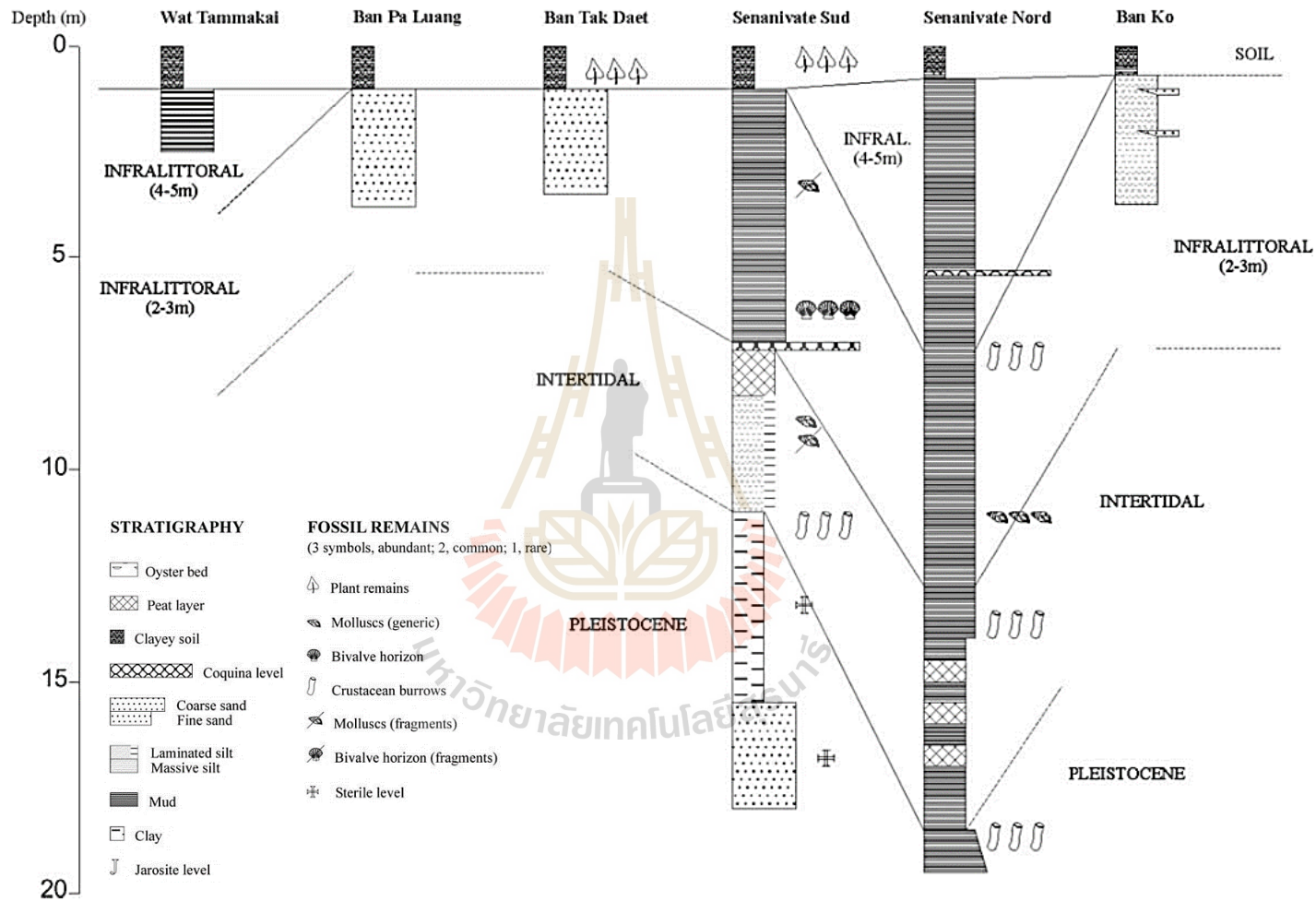


Figure 2.10 Stratigraphic correlation among the Bangkok Clay sections from W (left) to E (right); correlation lines separate different depositional environments (Negri, 2009)

In Central Plains of Thailand and coastal areas are affected by the salt-sprayed from oceanic waters or tidal bores (Kheoruenromne, 2007; Jedrum et al., 2014). The accumulation of calcite in the lower subsoil indicates retarded leaching condition and suggests a possible adverse calcareous effect for deep rooted crops (Kheoruenromne and Suddhiprakarn, 2007).

2.3 Study of ostracod taxonomy and paleoenvironmental interpretation from ostracod assemblage of the Late Quaternary in Thailand

Ostracods are small, well calcified bivalved crustaceans that inhabit a wide range of aquatic environments, including marine and freshwater ecosystems. The first fossil representatives are reported from Cambrian marine sediments (Moore, 1961; Maddocks, 1982). They have been widely used as indicators of environmental change. Changes in salinity, water chemistry, substrate characteristics, temperature, oxygen and nutrient availability and instability of these factors all bring about changes in the composition of the ostracod assemblages (Frenzel and Boomer, 2005). Ostracods can be used for paleoenvironmental reconstruction, ecological monitoring and biodiversity analyses (Rosenfeld and Vesper, 1977; Ruiz et al., 2000; Lytle and Wahl, 2005; Yasuhara et al., 2005; Lamb et al., 2006; Yasuhara and Seto, 2006; Yasuhara et al., 2012a). The use of ostracods in palaeoceanography relies on understanding the specific ecological preferences of different ostracod species. Each species has distinct requirements and is associated with particular water masses (Dingle et al., 1989; Dingle and Lord, 1990; Ayress et al., 1997). The biological attributes, such as the variation in local assemblages, population density, species diversity, age distribution, and genetic variation (Ruiz et al., 2005), are predominantly influenced by the surrounding environmental factors. These factors comprise water salinity, oxygen concentration, substrate characteristics, temperature, productivity, and other related variables (Frenzel and Boomer, 2005).

After the death and decay of organisms, a biocoenosis transforms into a thanatocoenosis. Various processes such as transportation and sorting by currents then act on the skeletal remains, resulting in a taphocoenosis, which is the fossil assemblage

that ultimately gets preserved (Brenchley and Harper, 1998). The development of ostracods, which involves distinct and recognizable stages of molting or growth, helps determine which components of an assemblage are in their original place and which have been moved after death (Figure 2.11). Identifying the post-mortem transported components is less reliable for indicating the ancient environment (Boomer et al., 2003).

There are the existing research on ostracods in both marine (e.g. Montenegro et al., 2004; Nevio et al., 2006; Yamada et al., 2014; Forel, 2021; Chitnarin et al., 2023) and freshwater environments (e.g. Savatnalinton, 2014; 2015; 2017; 2018; 2022; 2023; Savatnalinton and Suttajit, 2016) in Thailand. While ostracods are found in both marine and freshwater environments in Thailand, the previous studies on taxonomy and paleoenvironmental interpretation of ostracods in Late Quaternary sediments in Thailand were reviewed. For instance, Montenegro et al. (2004) conducted a study on ostracods in the Mae Klong river mouth, a shallow marine environment in the North-West Gulf of Thailand. They identified 34 species of ostracods, with 19 considered autochthonous, and observed that the fauna was influenced by the fresh water outflow from the Mae Klong river. Pugliese et al. (2006) investigated the ostracod fauna in Thailand and found 38 species, with 21 considered autochthonous. They noted differences in ostracod composition related to various environmental conditions, such as river inflows in the northern sector and marine conditions in the southern sector.

Yamada et al. (2014) focused on fossil ostracods as a tool for identifying tsunamigenic sediments in the Khlong Thom River area. They identified 96 species of ostracods from sediment samples, highlighting the potential of ostracods in understanding past environmental conditions.

Forel (2021) collected sediments from a shallow embayment near Mu Koh Phetra National Park and identified 35 species of ostracods. The study revealed the presence of ostracods characteristic of specific environmental conditions, such as species tolerating strong river inflows in the northern sector and those associated with marine conditions in the southern sector.

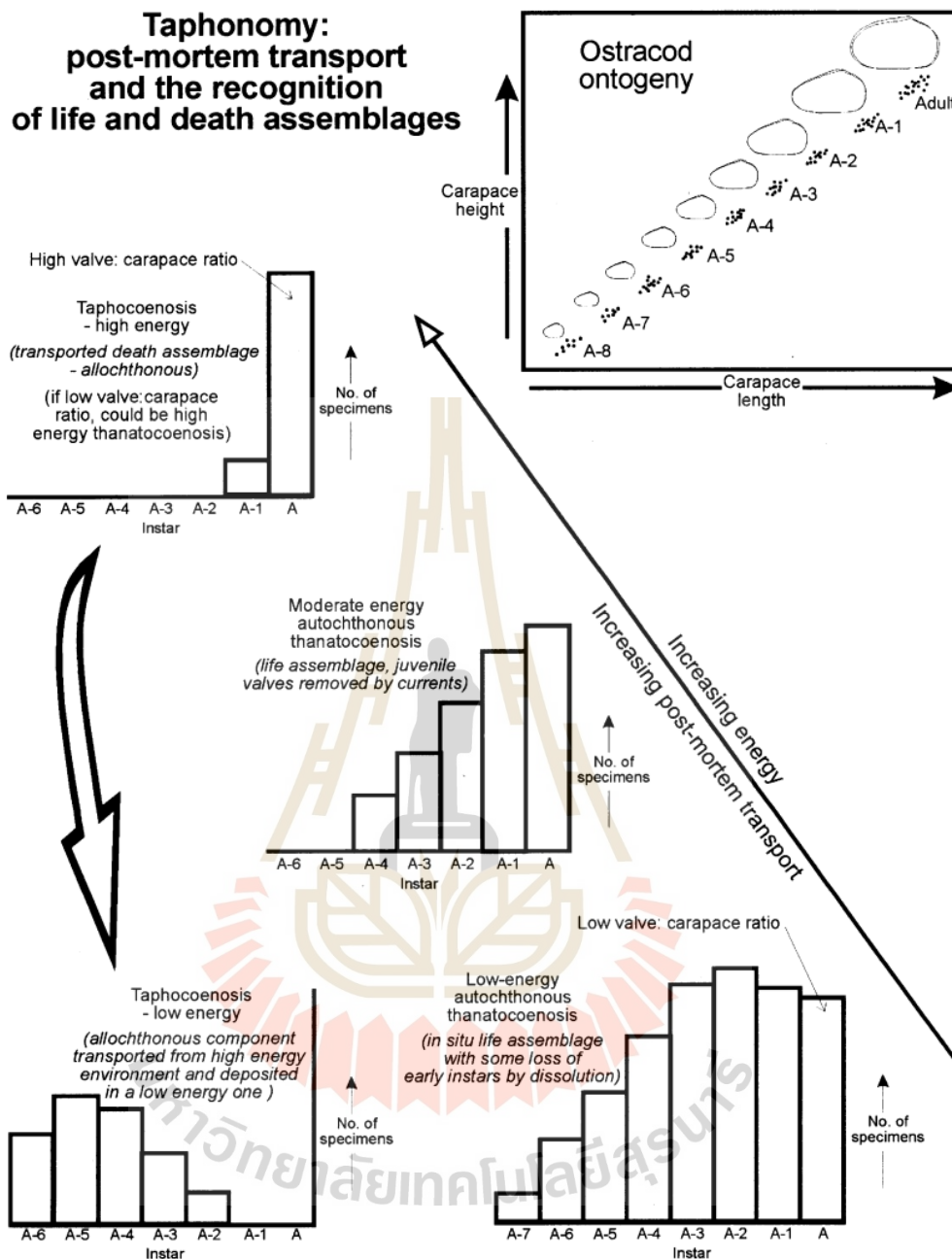


Figure 2.11 An illustration of the relationship between ostracod population age structures and their interpretation within the fossil record (Boomer et al., 2003)

Chitnarin et al. (2023) examined Holocene ostracods in the Chao Phraya delta, specifically focusing on a whale-fall excavation site in Samut Sakhon Province. They identified 13 species of ostracods and provided insights into ostracod assemblages in a shallow marine environment.

2.4 Collecting and processing of ostracods

The techniques used to break down or separate samples into individual components depend on the type of material being studied. The techniques used to break down or separate samples into individual components depend on the type of material being studied.

The techniques used to break down or separate samples into individual components depend on the type of material being studied. For loose sand and silt, a simple washing with water is sufficient. Clays and marls require mild chemical methods using substances that help disperse the particles. In the case of harder rocks, more aggressive chemical agents like hydrogen peroxide are used to dissolve and break down the material (Boomer et al., 2003). Since the sediment sample in this study consists of clay, silt, and fine sand. Chemical methods would be used to disaggregate the sediment sample.

Horne and Siveter (2016) conducted the collecting and processing fossil ostracods. Disaggregation of clays and shales can be achieved with a variety of techniques, in present study more resistant lithologies can be encouraged to break down by gently simmering on a hot plate or by adding chemicals such as Calgon (sodium hexametaphosphate) or 15% w/v hydrogen peroxide (requiring the use of a fume cupboard), in order to remember that the more aggressive the technique, the more likely it is to selectively damage or destroy components of the assemblage.

Disaggregated and originally unconsolidated silts and fine sands may simply be wet-sieved to remove the finest sediment. The residue retained on a 63 or 75 μm mesh will include even small juvenile stages of ostracods, but a 125 μm mesh is usually adequate to obtain a good representation of an assemblage. The resulting residues, containing ostracods and other fossils, are dried and then stored in labelled, lidded containers (e.g., tubes or vials) until required for picking, sorting, and analysis.

Sample picking and sorting is undertaken using a low power binocular microscope with reflected light, a picking tray and a small brush.

2.5 Ostracod shell morphology

In this thesis, it is important to note that the examined ostracod specimens are of a fossilized nature. Consequently, only the resilient components such as the shells or other hard structures have endured the fossilization process, while the soft tissues have not been preserved. Study of fossil ostracod, their most distinctive feature is their calcitic carapace; a hard, bivalved, hinged shell that can entirely cover and protect the non-mineralized body parts and appendages (Figure 2.12). Many ostracods have smooth rounded shells, hence their common name, seed-shrimps, while others are ornamented with pits, striations, spines, ridges, flanges etc. Ostracod carapaces, despite commonly being referred to as 'mussel-shaped' or 'seed-shaped,' exhibit a wide range of shapes and ornamentation (even within families). They can take on forms such as spheroidal, elongated, inflated, or compressed either laterally or vertically (Martens and Horne, 2009). In lateral view, the ostracod carapace is usually ovate, kidney-shaped or bean-shaped with a hinge along the dorsal margin. In some taxa possess a dorsal hinge structure in their valves, characterized by interlocking grooves, bars, teeth, or sockets. The hinge structure serves as a valuable taxonomic characteristic, although it involves a complex nomenclature (Martens and Horne, 2009). Most adult carapaces measure only 0.5–3 mm long though some species can reach up to 30 mm long (Armstrong et al., 2005). Muscles that operate the appendages are attached to the chitinous endoskeleton or the central or dorsal part of the carapace where they form the dorsal muscle-scar pattern. The adductor muscles close the valves and form the central muscle-scar pattern on the valves (Figures 2.13 to 2.15). This adductor muscle scar pattern is another important taxonomic character, particularly useful at superfamily level (Martens and Horne, 2009).

Figure 2.14 illustrates a characteristic muscle scar pattern commonly found in Stigmatocythere bona Chen in Hou et al., 1982. Puckett (2012) described adductor muscle scars serve the purpose of closing the valves, and typically, there are four adductor scars. However, it is not unusual for the first and second scars to be split, while the third and fourth scars may fuse together. These variations in muscle scar

patterns contribute to the diversity observed below the family level, as demonstrated in the specific cases discussed later in this study.

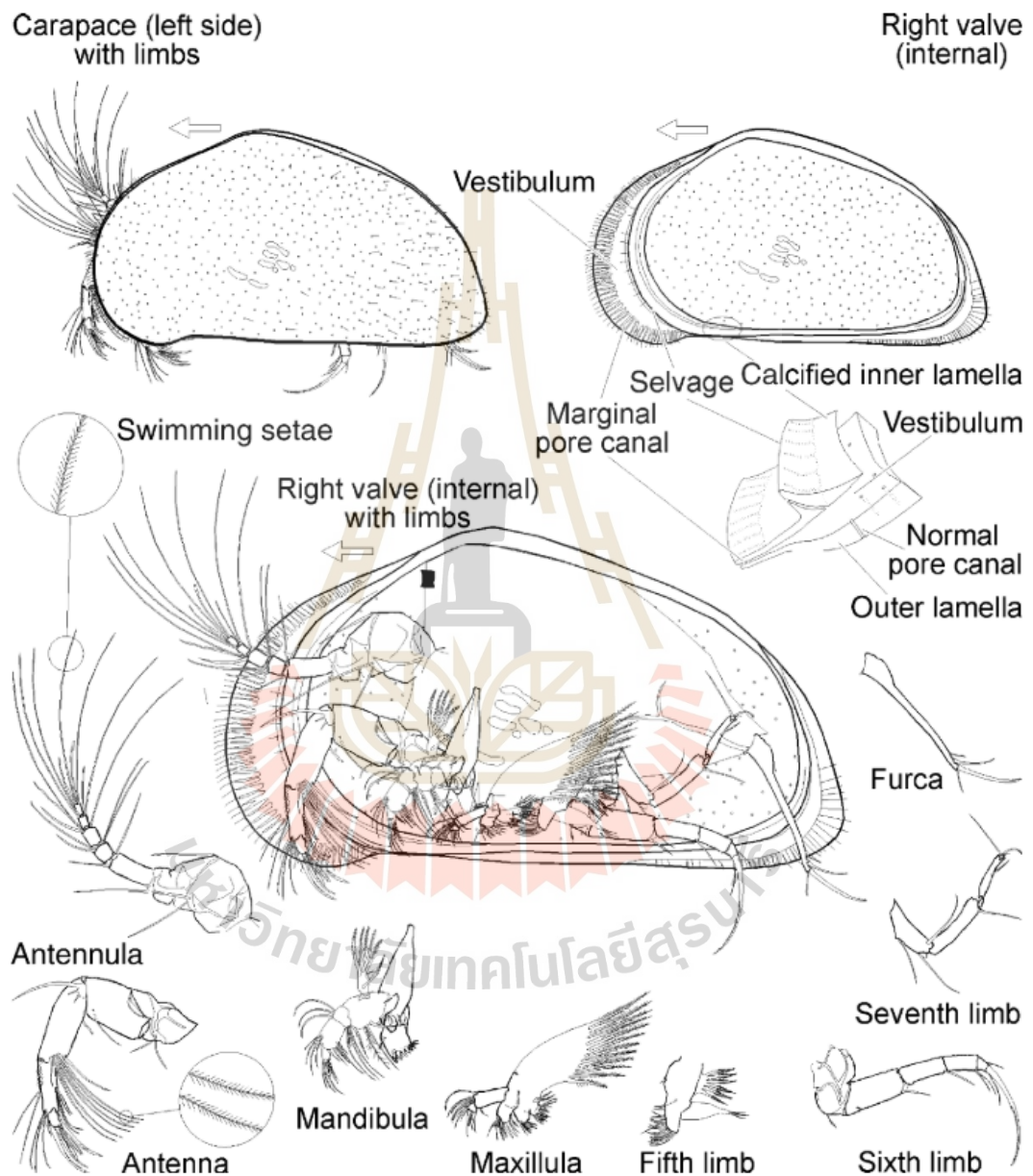


Figure 2.12 Illustrations of valve and limb morphology of the *Cyprididae* (Martens and Horne, 2009)

As stated by Yamada and Keyser (2009), their cellular and histological investigations on cuticle formation of muscle attachment structures revealed that the calcification process of muscle scars occurs later compared to other areas of the protocuticle. Additionally, they observed that the muscle scar pattern tends to be more well-developed in adult individuals. Within a particular species, the muscle scars exhibit remarkable consistency in their patterns, even between the left and right valves.

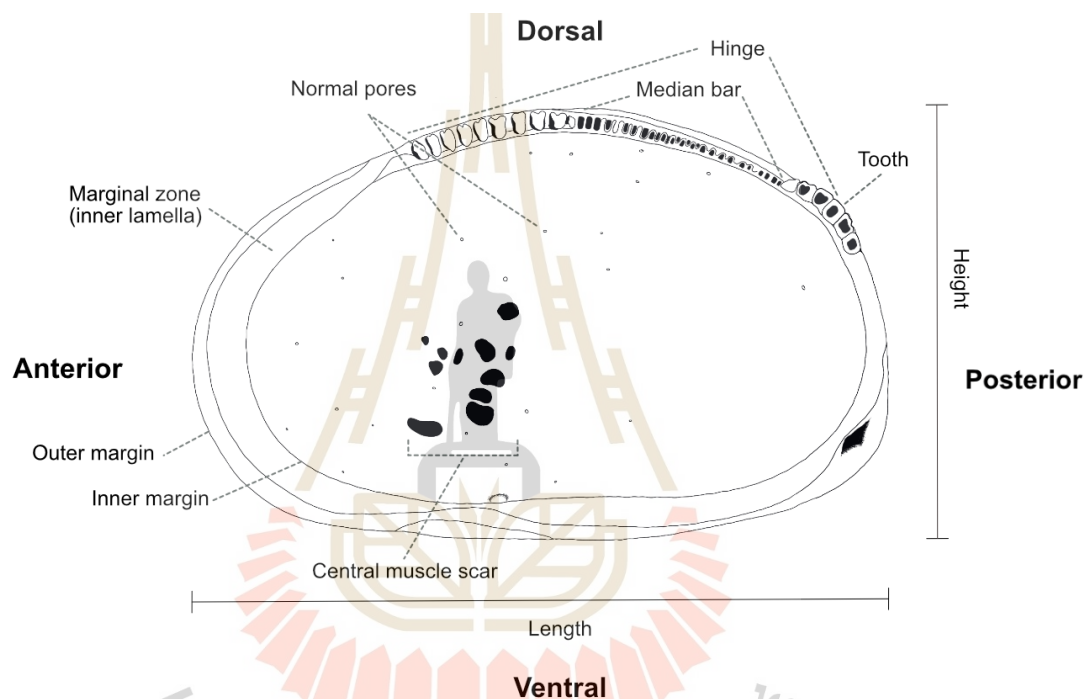


Figure 2.13 The internal features of a *Neocyprideis agilis* (Guan, 1978) right valve (this study)

According to Moore (1961), the general characteristics of ostracod carapaces include a hard-shell layer typically comprised of two distinct parts: the outer lamella and duplicature. The dorsal edge of the carapace can exhibit three different configurations: convex, straight, or concave. The ends of the carapace are commonly rounded, although certain species may possess elongated structures extending from the ends. Additionally, the lateral surface of ostracod valves can be further subdivided into posterior and anterior portions, as well as dorsal and ventral portions (Figure 2.16).



Figure 2.14 Typical muscle scar pattern of *Stigmatocythere bona* Chen in Hou et al., 1982 (this study)

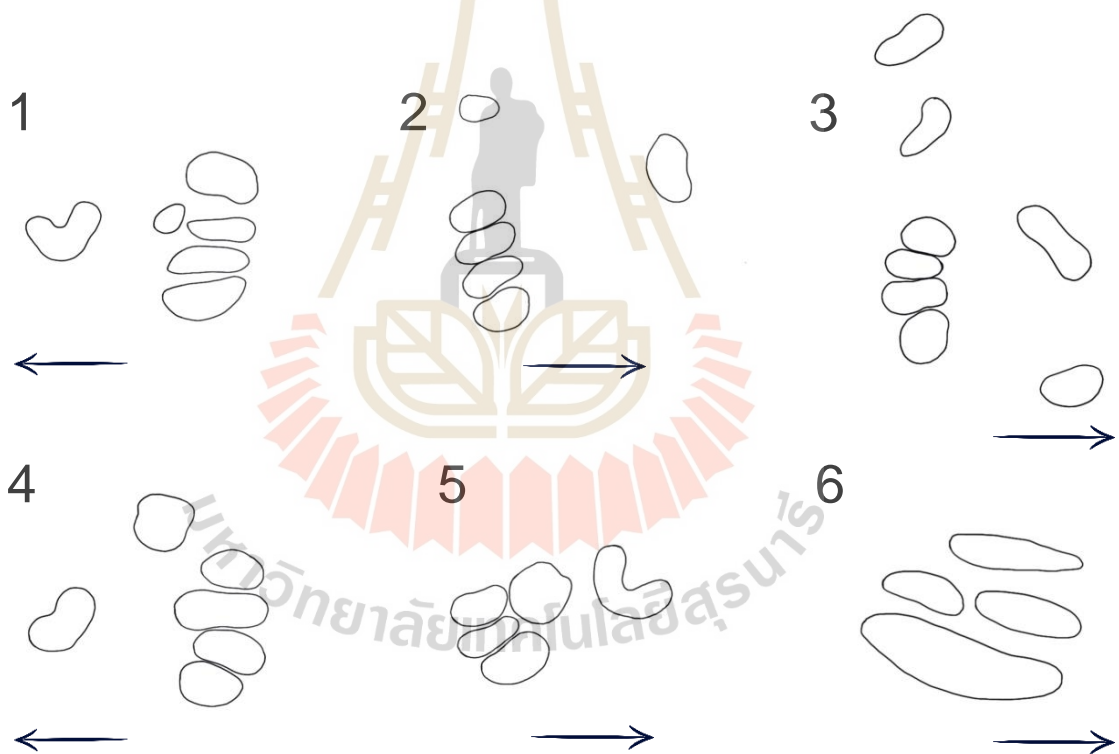


Figure 2.15 Schematic drawings of central muscle scars (internal view, arrow points to anterior): 1. *Stigmatocythere bona* Chen in Hou et al., 1982; 2. *Neomonoceratina rhomboidea* (Brady, 1968); 3. *Sinocytheridea impressa* (Brady, 1869); 4. *Keijella multisulcus* Whatley and Zhao, 1988; 5. *Hemicytheridea reticulata* Kingma, 1948; 6. *Propontocypris bengalensis* Maddocks, 1969 (this study)

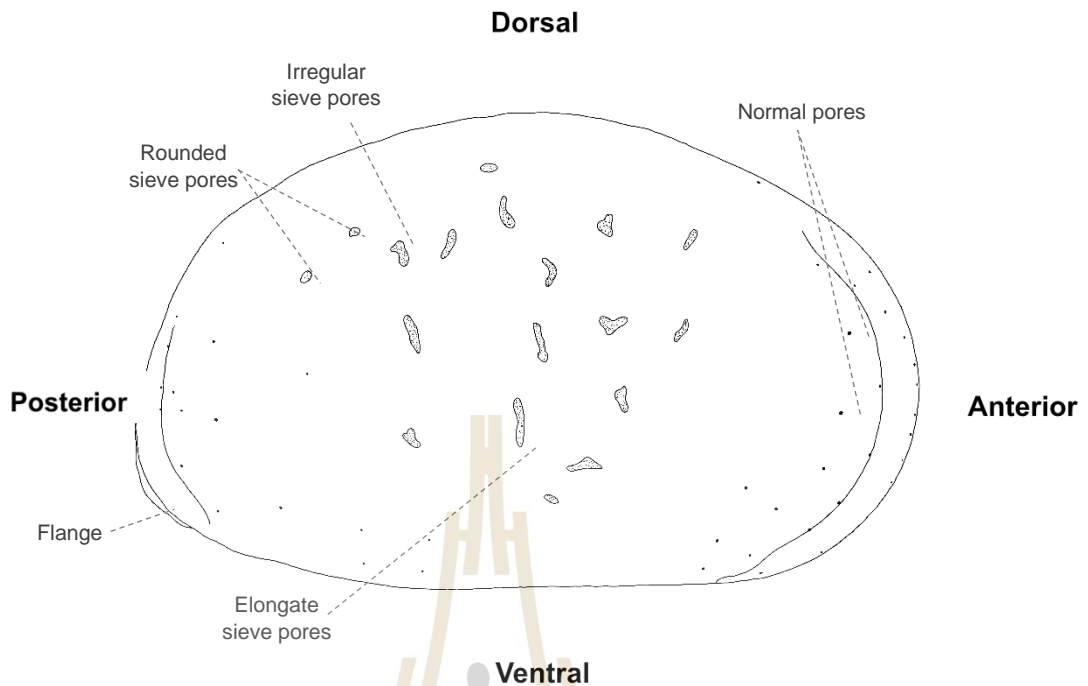


Figure 2.16 The external features of a *Neocyprideis agilis* right valve (this study)

The hinge is an important feature in terms of taxonomy and classification. Four basic types of hinges are recognized following Van Morkhoven (1963): the adont hinge is the simplest, without teeth or sockets, often forms part of a contact groove on the larger valve and a corresponding ridge on the smaller valve; the merodont hinge is composed of a tooth and socket at each end of a groove or ridge structure (complementary negative and positive structures in left and right valves); the entomodont hinge differs from the merodont hinge style by having a coarsely crenulated anterior portion of the median groove/ridge element; the amphidont hinge has a more complex median structure with an anterior tooth and socket. The hinge structure and terminology and hinge types are shown in Figure 2.17 and Figure 2.18.

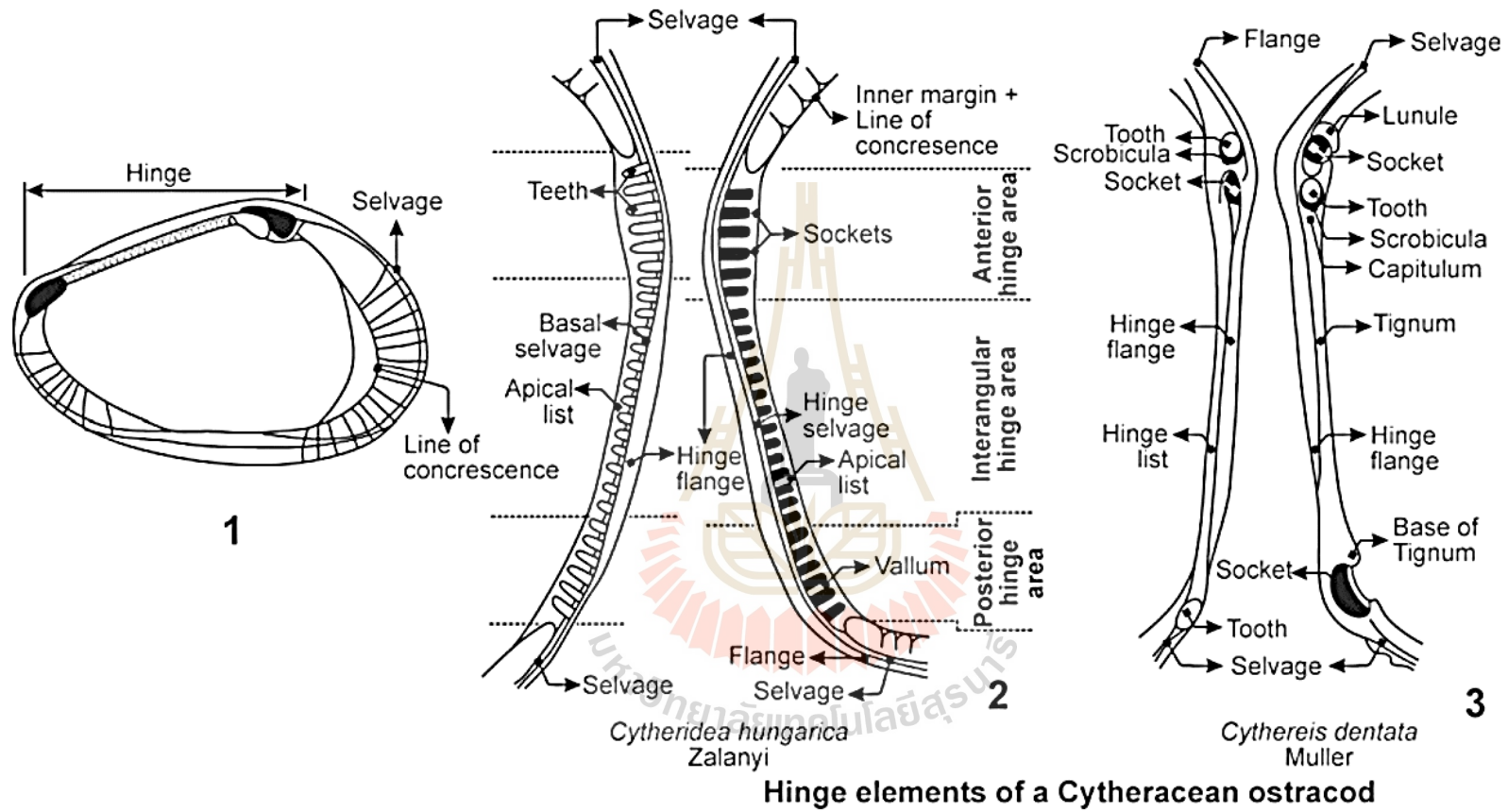


Figure 2.17 Hinge terminology (Jain, 2020)

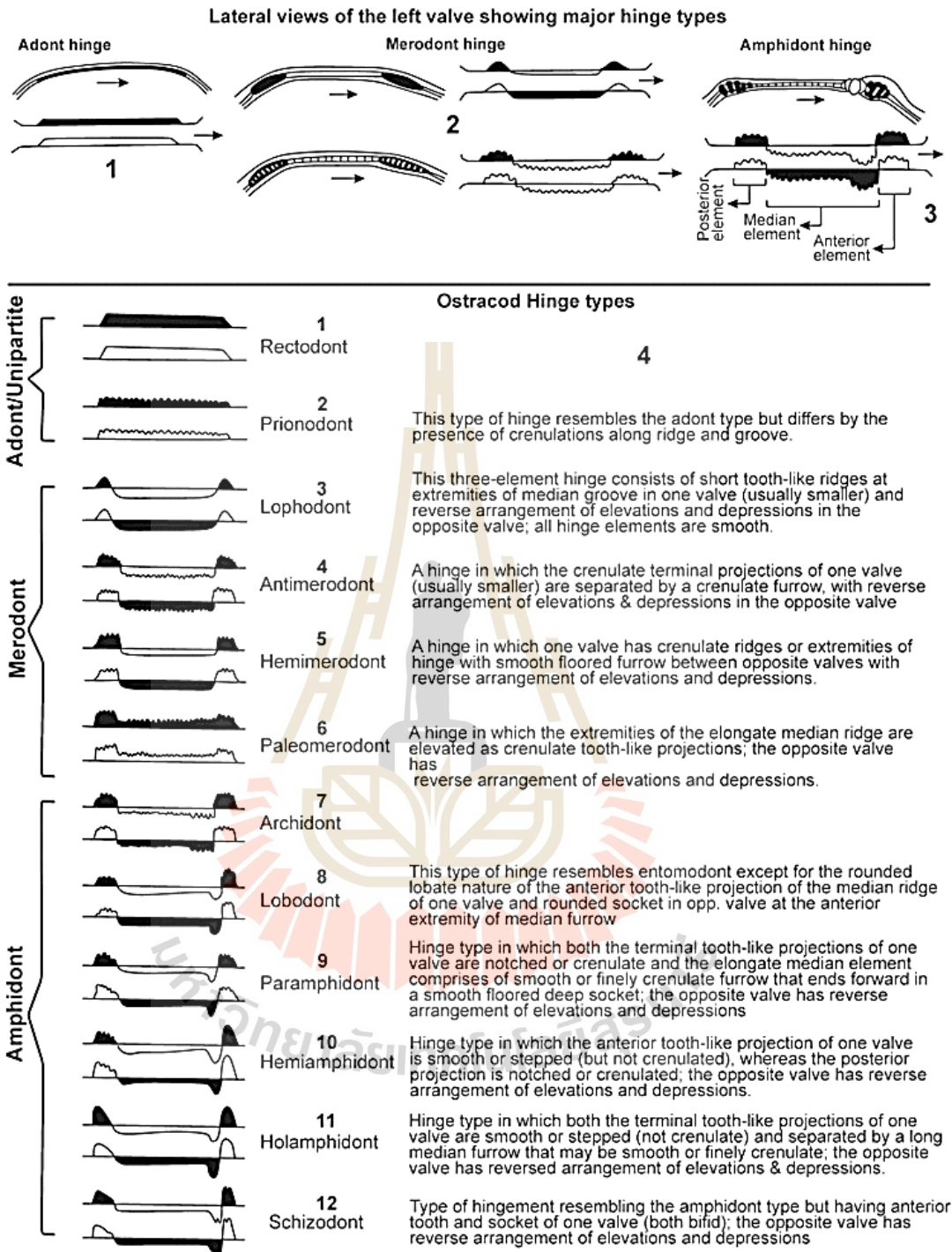


Figure 2.18 Hinge types (Jain, 2020)

CHAPTER III

METHODOLOGY

The study involves literature review, field investigation and sampling, laboratory works, and data analysis and interpretation (Figure 3.1). The field investigation and sampling were conducted in five boreholes and from Phanom Surin shipwreck site (Section 3.2). The laboratory works were divided into four parts - stratigraphic study, ostracod study, and salinity and XRD analysis (Section 3.3). The data analysis and interpretation were conducted in section 3.4. Thesis writing and presentation were provided in section 3.5.

3.1 Literature review and study

Reviews of previous works including stratigraphic study and sea-level change in the Gulf of Thailand, study of taxonomy and paleoenvironmental interpretation from ostracod assemblages, collecting and processing of ostracods, and ostracod shell morphology were achieved. Thesis plan was set up and started as a consequence.

3.2 Field investigation and sampling

Bangkok Clay sediment samples were obtained from two research projects conducted by a research group alliance. Five boreholes were provided by the generous contribution of Kasetsart University, namely Borehole KU1 to Borehole KU5. These boreholes were strategically located across all three districts of Samut Sakhon Province, spanning in a north-south direction. Specifically, one hole was situated in Krathum Ban district (KU1), two holes in Ban Phaeo district (KU2 and KU3), and two holes in Mueang Samut Sakhon district (KU4 and KU5). A total of 99 samples were collected from these boreholes (Assistant Professor Dr. Chatchalerm Ketwetsuriya, personal communication, 2022). Sediment samples from the Phanom Surin shipwreck site were kindly contributed by Nakhon Ratchasima Rajabhat University.

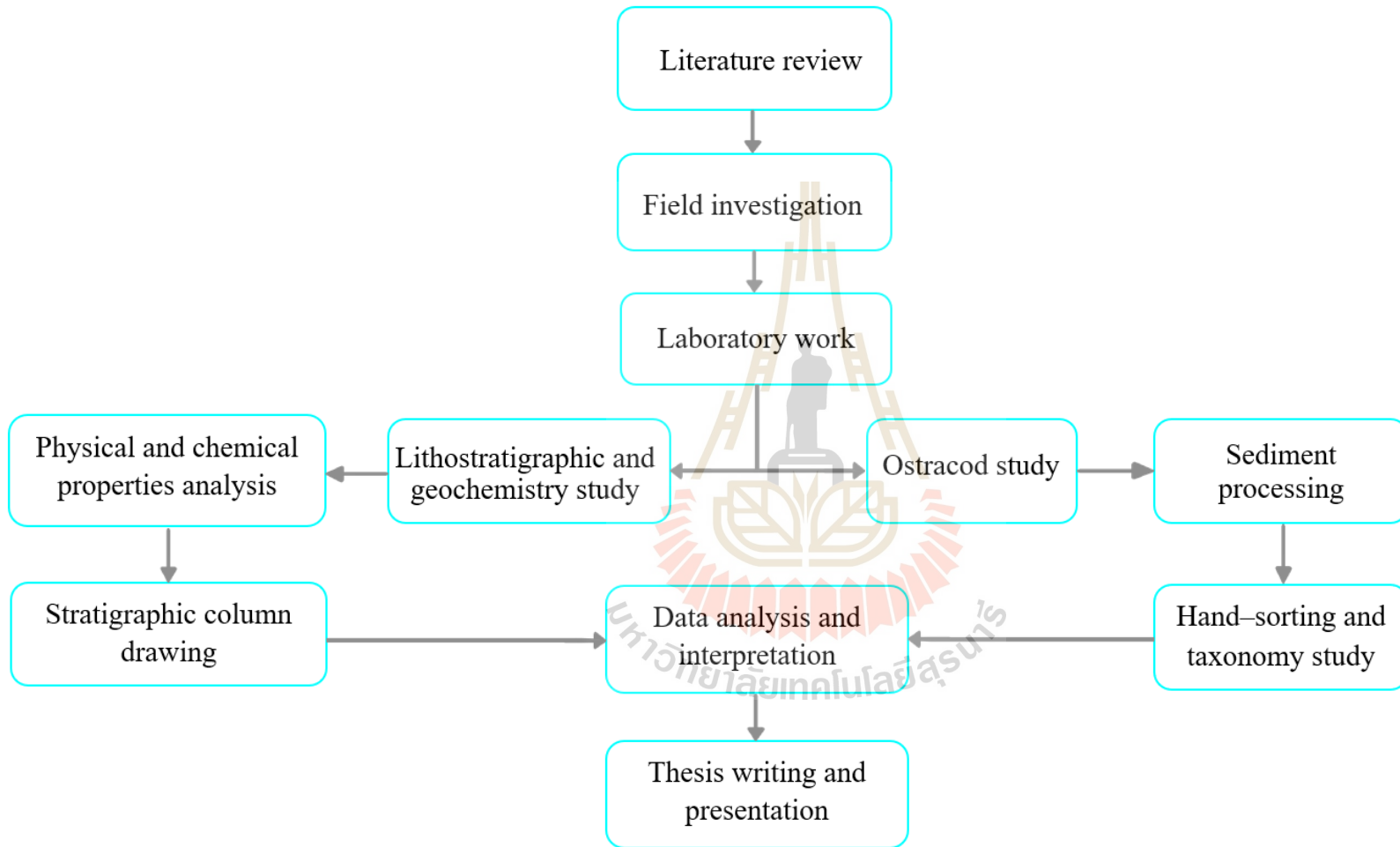


Figure 3.1 Methodology

The total number of samples acquired from this site amounted to 40 (Dr. Wipanu Rugmai, personal communication, 2021). Information of each site is summarized as follow:

1) Borehole KU1, is located in Ban Yang Subdistrict, Kratotum Ban District, Samut Sakhon Province (coordinates $13^{\circ}40'06.9''\text{N}$, $100^{\circ}13'13.6''\text{E}$). Borehole KU1 represents the topmost layer of the stratigraphic sequence in the northern part of Samut Sakhon Province, located approximately 21 kilometers north of the current shoreline, based on the province's geological map. The unit at this borehole is Qff/tf2/mc, which refers to flood plain clay on old tidal flat clay on marine clay deposit (DMR, 2016). The borehole survey was conducted to a depth of 20 meters (Figure 3.3).

2) Borehole KU2 is located in Ban Phaeo Subdistrict, Ban Phaeo District, and drilled to 15 meters deep (coordinates $13^{\circ}36'11.6''\text{N}$, $100^{\circ}11'21.2''\text{E}$). The area is in the central part of the province and is about 15 kilometers away from the current shoreline, based on the map of the geology of this area. The drill site is in the Qtf1/mc unit, which refers to a recent tidal flat clay on a marine clay deposit.

3) Borehole KU3, with a depth of 10 meters, is located in Ampheang Subdistrict, Ban Phaeo District, Samut Sakhon Province (coordinates $13^{\circ}36'10.8''\text{N}$, $100^{\circ}11'21.3''\text{E}$), adjacent to KU2. The purpose of drilling this hole is to study the changes in the eastward direction of the stratigraphic sequence. The drilling survey was conducted to a depth of 10 meters because the drilling machine could not operate further (Figure 3.5). Lithology of sediments in KU3 is similar and can be compared to those in KU2.

4) Borehole KU4 is located in Chai Mongkol Subdistrict, Mueang Samut Sakhon District, Samut Sakhon Province, at coordinates $13^{\circ}32'22.8''\text{N}$, $100^{\circ}11'22.8''\text{E}$. The site is approximately 8 kilometers north of the current shoreline, and drilled to 20 meters with altitude -11 meters. According to the geological map of Samut Sakhon Province (Figure 2.1), the drilling site is in the Qtf1/mc unit, which is recent tidal flat clay on marine clay deposit (Figure 3.6).

5) Borehole KU5 has a depth of 34.5 meters and is located in Chai Mongkhon Subdistrict, Muang Samut Sakhon District, Samut Sakhon Province (coordinates $13^{\circ}32'51.0''\text{N}$, $100^{\circ}11'37.0''\text{E}$). Borehole KU5 is located about 8 kilometers



Figure 3.2 Location of the exploration drill points for collecting samples

north of the current shoreline according to the geologic map of Samut Sakhon Province. This borehole is drilled in the Qtf1/mc unit, the same as Borehole KU 4 (Figure 3.7).



Figure 3.3 The drilling site of Borehole KU1 and examples of sediments range from 5.0 – 12.0 meters depth (photo by Chatchalerm Ketwetsuriya)

6) In the year 2013, a remarkable discovery was made by a landowner: the Phanom Surin shipwreck site, nestled at coordinates $13^{\circ} 33' 24.1''$ N, $100^{\circ} 23' 29.9''$ E. This captivating site, depicted in Figure 3.8, was once a shrimp farming. The location is 8 kilometers away from the present-day shoreline of the Gulf of Thailand. Delving into the depths of this historical treasure, samples were carefully collected from the

Phanom Surin shipwreck site, at a depth of 0.49 meters beneath the surface (Altitude -3 meters). Despite the limited quantity—less than ten grams—of the forty remaining samples, from the palynomorphs study, were used to study ostracod.

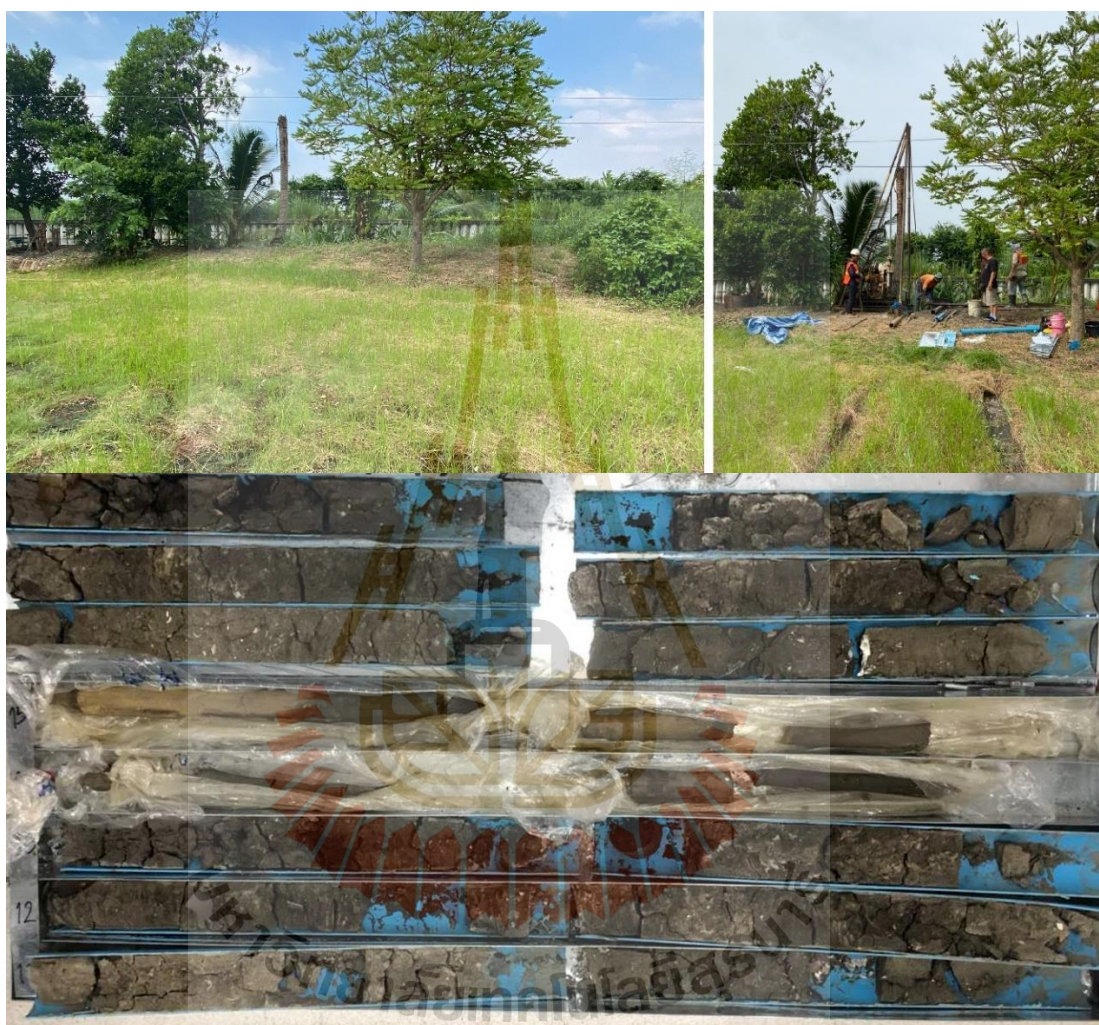


Figure 3.4 The drilling site of Borehole KU2 and examples of sediments, range from 11.0 – 15.0 meters depth (photo by Chatchalerm Ketwetsuriya)



Figure 3.5 The drilling site of Borehole KU3 and examples of sediments, range from 1.0 – 5.0 meters depth (photo by Chatchalerm Ketwetsuriya)

3.3 Laboratory works

The laboratory works are divided into three parts as described below.

3.3.1 Stratigraphic study

The sediments from the core samples were investigated for their physical and chemical properties, including color, particle size, components and reaction with hydrochloric acid. Sedimentary units are classified and the lithostratigraphic columns are established (Chapter 4).



Figure 3.6 The drilling site of Borehole KU4 and examples of sediments, range from 5.0 – 10.0 meters depth (photo by Chatchalerm Ketwetsuriya)



Figure 3.7 The drilling site of Borehole KU5 and examples of sediments, range from 5.0 – 10.0 meters depth (photo by Chatchalerm Ketwetsuriya)



Figure 3.8 The Phanom Surin shipwreck excavation, Samut Sakhon Province, Gulf of Thailand. Photograph Bangkok Post (Fine Arts Department, 2014)

3.3.2 Ostracod study

30 grams of sediment samples (1 sample/meter) were processed by using 15% w/v hydrogen peroxide technique (Horne and Siveter, 2016) for sediment particle separation. Disaggregated and originally unconsolidated clay, silts, and fine sands may simply be wet-sieved to remove the finest sediment. In the present study, the residues retaining on the 0.10- and 0.50-millimeters mesh were collected. The residue from wet-sieved were dried and then stored in labelled. A process of ostracod preparation is shown in Figure 3.9.

Hand – sorting with stereomicroscope and choosing well – preserved samples for photography with the Scanning Electron Microscope (SEM), JEOL Neoscope JCM-5000, at Facility Building 10 (F10), Suranaree University of Technology. The identification of ostracod species follows Moore (1961) and Martens and Horne (2009).

3.3.3 Salinity analysis

The salinity of the sediment samples (1 sample/meter) was measured using the electrical conductivity (EC) method using EC/TDS/Salinity/Resistivity meter;

HANNA HI-5521 (Figure 3.10). The sediment samples from KU1 to KU 5 were available for the salinity test, but sediment samples from Phanom Surin shipwreck site were not sufficient for salinity analysis. A 10-gram of each sample was mixed with 20-ml of distilled water and left to stand for 24 hours to allow equilibration. The electrical conductivity of the resulting supernatant was then measured using a conductivity meter calibrated with standard solutions.



Figure 3.9 Ostracod preparation process

3.3.4 XRD analysis

X-ray diffraction (XRD) analysis was performed on the sediment samples to identify the mineral composition of the samples. The sediments sample from Unit 1, 2, and 4 were selected to represent the mineral composition in each unit. The sediment samples were first dried and ground to a fine powder, then packed into sample holders (Figure 3.11). The BRUKER D2 Phaser was used for the analysis (Figure 3.12). The XRD patterns were obtained over a range of 2θ angles from 5 to 70° and 5

to 60° with a step size of 0.02° . The data were analyzed using the Bruker DiffracPlus EVA software to identify the mineral phases present in the sediment samples.



Figure 3.10 EC/TDS/Salinity/Resistivity meter; HANNA HI-5521 (Facility Building 7, Suranaree University of Technology)



Figure 3.11 Powder sample preparation

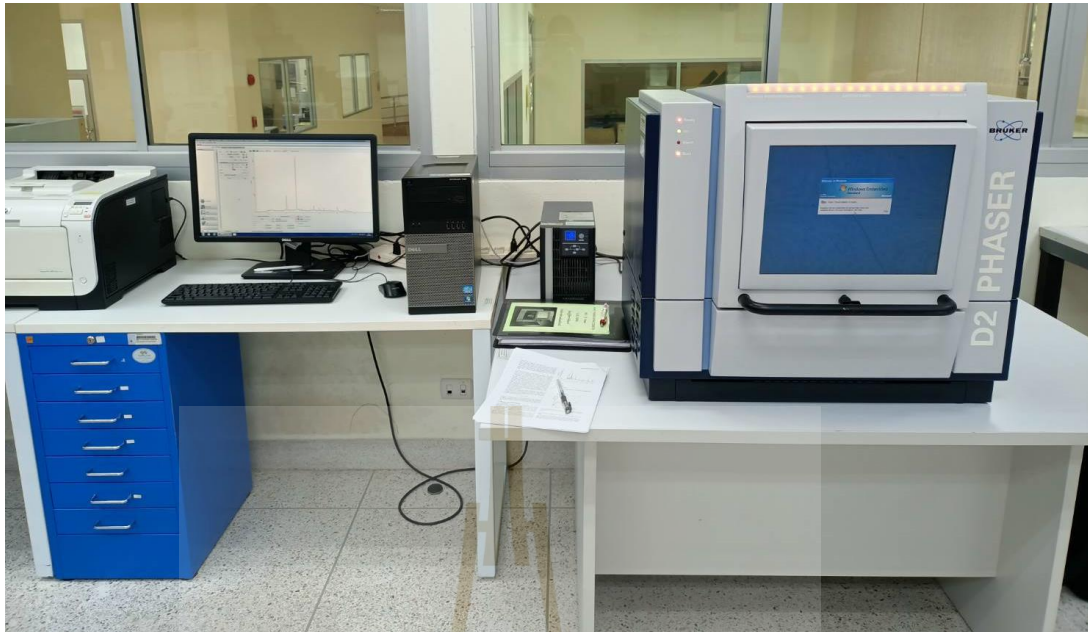


Figure 3.12 X-ray Diffractometry (XRD) BRUKER, D2 Phaser (Facility Building 10, Suranaree University of Technology)

3.4 Data analysis and interpretation

3.4.1 Stratigraphic study

The dried sediment samples were studied for their lithology and geochemistry.

3.4.2 Ostracod study

The depositional environment of study area were interpreted by using ostracod assemblages that resulted from the study of taxonomy base on the morphology of the fauna, and the physical and chemical characteristic of sediment.

3.4.3 Salinity analysis

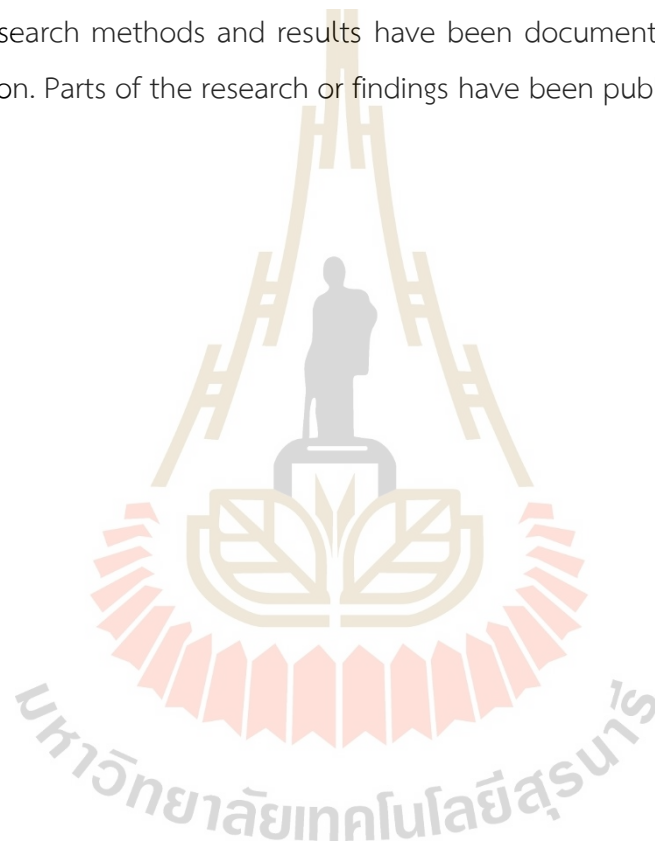
The salinity data were analyzed using descriptive statistics to determine the range and mean of salinity values for each sediment sample. The data analysis was performed to examine the relationships between salinity and other physical and chemical properties of the sediment samples, and the relationship with ostracod assemblages will also be delivered. The salinity values were also compared to historical salinity data for the study area to assess any changes in salinity over time.

3.4.4 XRD analysis

The XRD data were analyzed using the Bruker DiffracPlus EVA software to identify the mineral phases present in the sediment samples. The relative abundances of each mineral phase were determined the peak of the graph. The mineralogical composition of each sample was then compared to historical data for the study area to assess any changes in mineralogical composition over time.

3.5 Thesis writing and presentation

All research methods and results have been documented and carried out in the dissertation. Parts of the research or findings have been published in a conference or a journal.



CHAPTER IV

Lithostratigraphy and Geochemistry

This chapter presents the result of the study, focusing on the Stratigraphy of the Late Quaternary sediments in the studied area (Section 4.1), and also provides geochemical characteristic of the Bangkok Clay Formation (Section 4.2).

4.1 Stratigraphy of the Late Quaternary sediments in the study area

The unconsolidated sediments from bottom to top can be divided into five distinct units, as shown in Figure 4.1. Each unit can be described as follows: Unit 1, Light grey well sorted silty clay and fine grain sand (GSC, S); Unit 2, Red and yellowish-brown silty clay (RYSC); Unit 3, Yellowish white brown silty clay (YWSC); Unit 4, Dark grey well sorted silty clay (DGSC); Unit 5, Topsoil. Sediment characteristics of each borehole were described as follows (Figure 4.2).

From Figure 4.1, the calibrated ages of shell material obtained through AMS (accelerator mass spectrometry) analysis, conducted by Asst. Prof. Dr. Chatchalern Ketwetsuriya (Kasetsart University), provide valuable chronological information for the studied boreholes. In Borehole KU1, the calibrated ages indicate that the shell material found at depths of 1.5-2.0 meters corresponds to a time period ranging from approximately 3,291 to 2,945 calibrated years Before Present (cal BP). Similarly, at depths of 3.0-3.5 meters, the shell material corresponds to a time period ranging from around 3,177 to 2,845 cal BP.

The ages of the shell material retrieved from depths of 6.0-6.5 meters and 7.5-8.0 meters are estimated to be between 3,368-3,055 cal BP and 4,242-3,889 cal BP, respectively. Finally, at depths of 9.5-10.0 meters, the shell material corresponds to a time period ranging from approximately 4,895 to 4,558 cal BP.

In Borehole KU2, the calibrated ages indicate that the shell material found at depths of 8.5-9.0 meters corresponds to a time period ranging from approximately 3,867 to 3,533 cal BP. At depths of 12.0-12.5 meters, the shell material corresponds

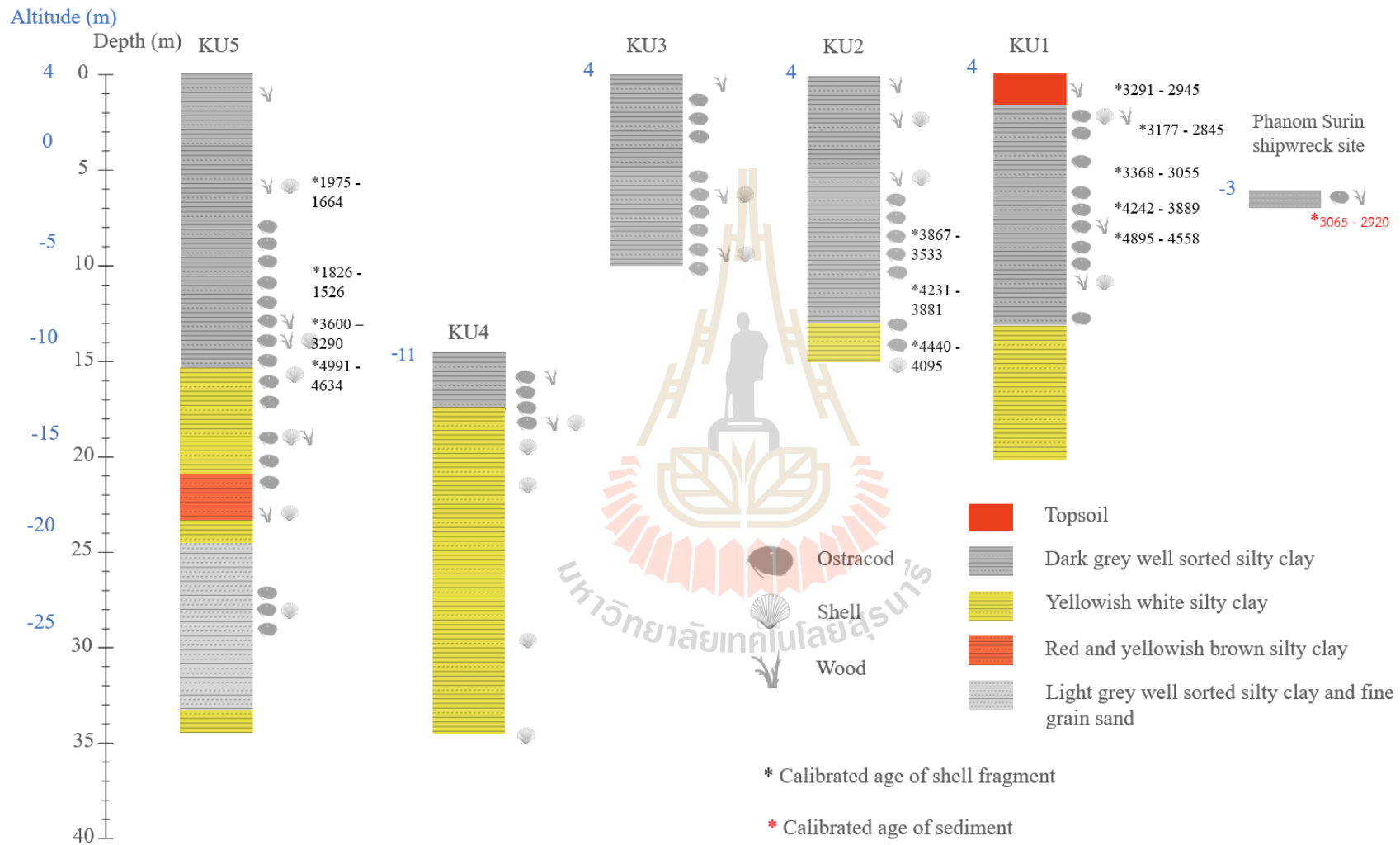


Figure 4.1 Lithostratigraphic columns of the study area from Boreholes KU1-KU5, and the Phanom Surin shipwreck site

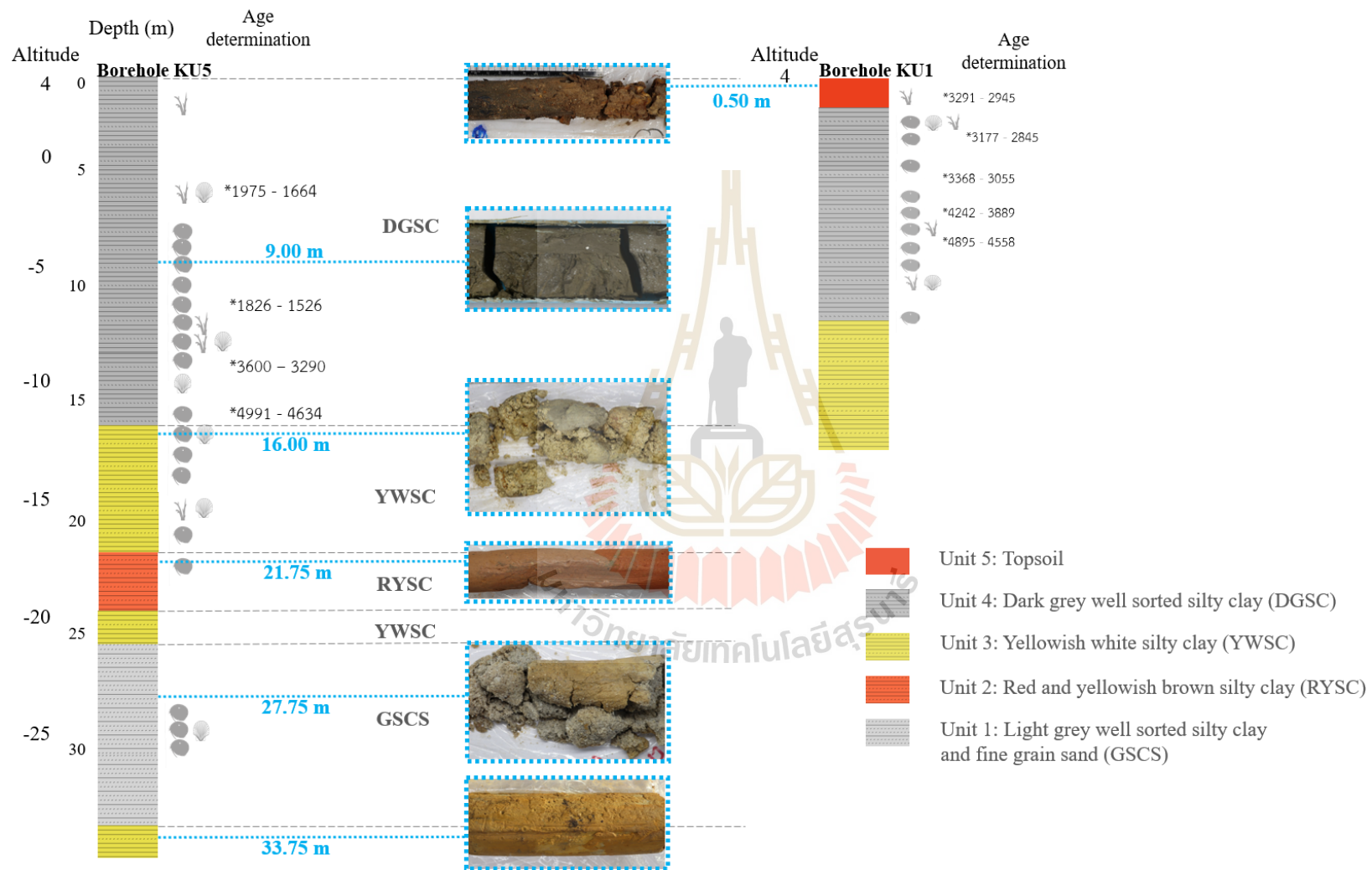


Figure 4.2 Lithostratigraphy of Boreholes KU1 and KU5, showing sedimentary units

to a time period ranging from around 4,231 to 3,881 cal BP. Lastly, at depths of 13.5-14.0 meters, the shell material corresponds to a time period ranging from approximately 4,440 to 4,095 cal BP. For Borehole KU5, the calibrated ages of the shell material retrieved from depths of 5.5-6.0 meters, 10.5-11.0 meters, 12.0-12.5 meters, and 14.5-15.0 meters are estimated to be 1,975-1,664 cal BP, 1,826-1,526 cal BP, 3,600-3,290 cal BP, and 4,991-4,634 cal BP, respectively.

4.1.1 Stratigraphy of Borehole KU1

According to Figure 4.1, from 20.0 to 13.0 meters (Unit 3), the sediment exhibits color variations of yellowish-brown and light grey within the silty clay. These color variations could be attributed to different mineral compositions or changes in environmental conditions during deposition. Between 13.0 and 3.0 meters (Unit 4), the sediment is characterized by dark grey and well-sorted silty clay. This layer indicates a relatively fine-grained sediment with good particle sorting, possibly indicating deposition in a calm or low-energy environment.

From 3.0 to 1.0 meters (Unit 5), the topsoil sediment consists of red and yellowish-brown silty clay. Within this depth range, there is also a distinct layer of reddish brown oxidized silty clay with small fragments. The reddish-brown color suggests the presence of oxidized iron in the sediment. Shells are found along the depth of the core at 3.0 to 2.0 meters and 11.0 to 10.0 meters. The presence of shells suggests the influence of marine environments and indicates the presence of marine organisms during the sediment deposition.

In addition to shells, remains of organic matter are found together on the upper half of the core. This indicates the input of organic materials into the sediment, possibly from marine organisms or terrestrial sources.

4.1.2 Stratigraphy of Borehole KU2

From 15.0 to 14.0 meters (Unit 3), the sediment is light grey and well-sorted clay and there is a presence of brown silt. Shells found along the depth of the core at 10.0 to 9.0 meters and 3.0 to 2.0 meters. From 14.0 to 0 meters (Unit 4), the sediment consists of calcareous dark grey, well-sorted clay. At 14.0 meters, there is a transition in sediment composition between the two sediment units (Figure 4.1). Remains of organic matter such as wood debris found on the upper half core indicates

the input of terrestrial material. This input of terrestrial material suggests that at fluvial or estuarine processes might have transported the organic matter from land into the marine depositional environment (Dalrymple and Choi, 2007).

4.1.3 Stratigraphy of Borehole KU3

From the depth of 10.0 to 0 meters (Unit 4), the sediment is calcareous dark grey, well-sorted clay. Shells found at the lower half core. The presence of shells in the sediment indicates the influence of a marine environment and the existence of marine ecosystems. A relevant study conducted by Ketwetsuriya and Dumrongrojwattana (2021) focused on the investigation of marine microgastropods at a whale-fall excavation site situated close to Borehole KU3. Ketwetsuriya and Dumrongrojwattana (2021) provides the marine ecology and biodiversity associated with this particular location. Remains of organic matter such as wood debris, are found both on the top of the core and in the lower half. The presence of wood debris indicates the input of terrestrial material into the sediment, possibly through fluvial or estuarine processes. This suggests a connection between the marine and terrestrial environments in the area of deposition (Dalrymple and Choi, 2007).

4.1.4 Stratigraphy of Borehole KU4

Continuing up from 20.0 to 3.5 meters (Unit 3), there is another calcareous sediment layer characterized by a mix of yellowish brown and white colors. This layer also consists of well-sorted silty clay. The presence of calcium carbonate in this layer indicates the influence of marine or other carbon-rich environments during deposition.

In Borehole KU4, the sediment layers can be described from the top to a depth of 3.5 to 0 meters (Unit 4), there is a calcareous sediment layer composed of light grey, well-sorted silty clay. This layer indicates the presence of calcium carbonate in the sediment (react with HCl) and suggests a relatively fine-grained composition with good sorting of particles.

The yellowish brown and white colors suggest variations in mineral composition, with different proportions of minerals present in the sediments. The well-sorted nature of the silty clay indicates that the particles are relatively uniform in size, possibly indicating sedimentation in a calm or low-energy environment.

4.1.5 Stratigraphy of Borehole KU5

According to Figure 4.1 and 4.2, between 33.5 and 24.5 meters (Unit 1), the sediment transitions to light-colored medium to coarse-grained sand with pebbles. Some layers within this range are composed of light-colored fine to medium-grained sand with quartz and mica. In certain layers, calcareous fragments are observed, along with yellowish-brown silt and fine to medium-grained sand with mica.

From 23.5 to 21.0 meters (Unit 2), the sediment exhibits a combination of yellowish-brown, red, and white silt, clay, and fine-grained sand. This layer likely indicates variations in mineral composition and possibly changes in depositional environments.

Between 15.5 and 21.0 meters, 23.5 and 24.5 meters, and 33.75 and 34.5 meters (Unit 3), the sediment is characterized by yellowish-white and light grey clay and silt. There are also calcareous fragments observed in the light grey silty clay. The presence of zones of oxidation on the surface of the sediment suggests the influence of oxidation processes in these layers.

From 0 to 15.5 meters (Unit 4), the sediment consists of dark grey clay with brown oxidation on the surface. Additionally, there are calcareous fragments present in the dark grey silty clay. In some layers, shell fragments cannot be seen, suggesting a possible absence of shells in those particular layers.

Borehole KU5 displays a sediment composition that includes dark grey clay with oxidation, calcareous fragments, yellowish-white and light grey clay and silt, yellowish-brown, red, and white silt, clay, and fine-grained sand, and light-colored medium to coarse-grained sand with pebbles. This borehole is the most complete borehole and include four sediment units. The oldest age for unit 4 (DGSC) is 4,991-4,634 cal BP (Figure 4.1 and 4.2).

4.1.6 Stratigraphy of Phanom Surin shipwreck site

These forty sediment samples represented levels below the shipwreck (sediments before sinking), the same level (coeval sedimentation) and above the shipwreck (sealed sediments). The sediment is characterized by dark grey and well-sorted silty clay with fine-grained sediment and good particle sorting. The sediment from this site was classified into unit 4 (DGSC) as shown in Figure 4.1.

4.2 Geochemistry of the Bangkok Clay sediments in this study

4.2.1 Salinity Test

Salinity is an essential parameter that provides insights into the chemical composition of water and can serve as an indicator of environmental conditions. In this section, present the findings of the salinity analysis conducted in the studied section. Salinity measurements were obtained at various depths to examine the vertical distribution of salinity levels and understand any potential variations within the water column.

The result of salinity measurements is reported as percentages (Figure 4.3). Each depth interval was sampled and analyzed to ensure representative data collection throughout the studied section. The salinity values obtained provide valuable information regarding the dissolved salt content in the water samples.

The salinity levels shown in Figure 4.3 are compared according to the sediment units obtained from Borehole KU5. This particular borehole is significant because it reaches the deepest depth and provides the most complete sediment record.

1) Salinity measurement of Borehole KU1

At the shallow depths (0.25 to 3 meters), the salinity levels remain relatively low, ranging from 0.4% to 1.6%. There is a slight increase in salinity from 0.25 to 3 meters, with the highest salinity value recorded at 3 meters (1.6%). From 4 to 5 meters, the salinity drops from 2.9% to 2%, suggesting a slight decrease in salinity. Between 5 and 10 meters, the salinity levels remain relatively stable, ranging from 1.5% to 2.6%.

At depths beyond 10 to 20 meters, the salinity fluctuates from 2.6% to 1.6% at 19 meters. The salinity level of Borehole KU1 suggests a generally low to moderate salinity environment. There are minor fluctuations in salinity within the measured depth range, with no significant overall trend.

2) Salinity measurement of Borehole KU2

The salinity levels show a somewhat fluctuating pattern with increasing depth. From the surface (0.25 meters) to a depth of 2 meters, there is a gradual increase in salinity percentage, with values ranging from 0.1% to 0.7%.

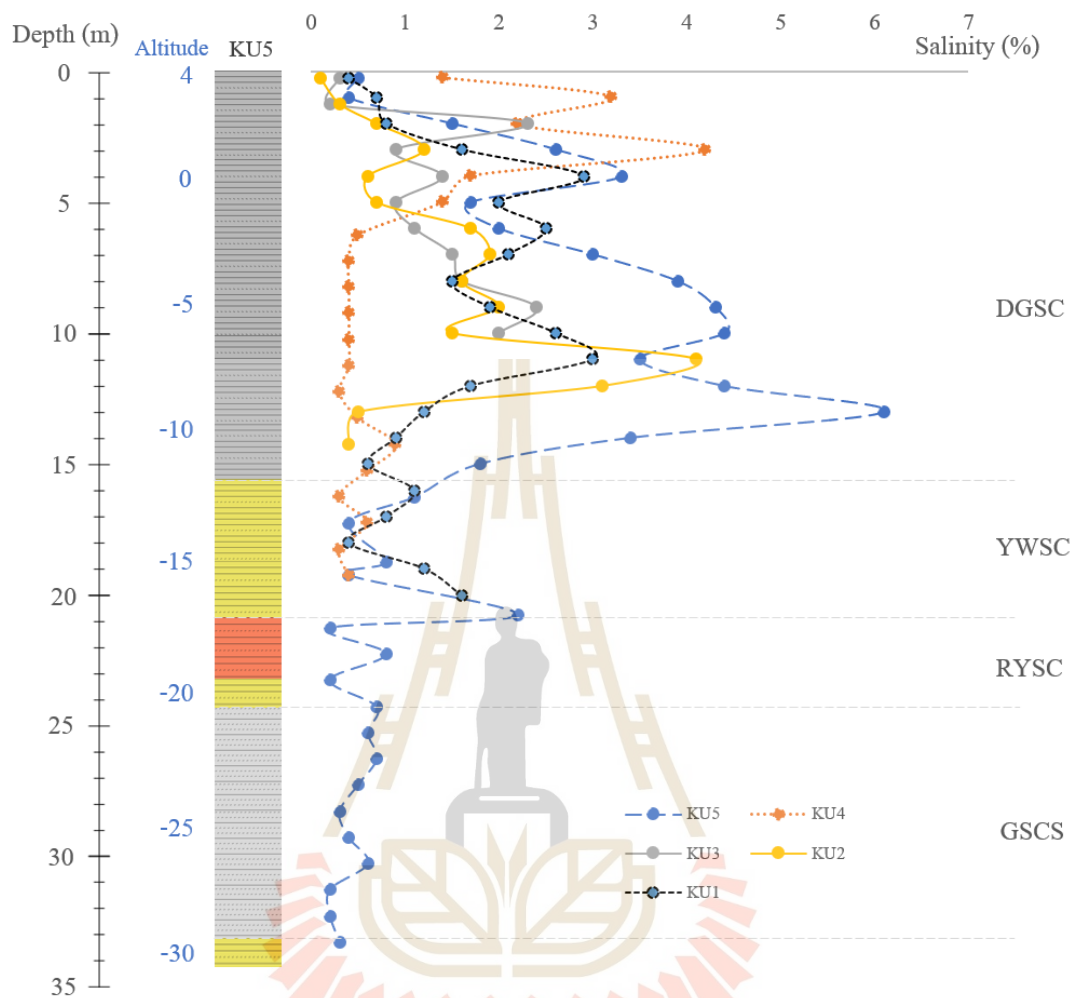


Figure 4.3 Salinity levels of 5 boreholes with lithostratigraphic column of Borehole KU5 (representing a composite column) from Samut Sakhon Province

However, at a depth of 3 meters, there is a notable jump in salinity to 1.2%. From 4 to 6 meters, the salinity levels fluctuate within a relatively narrow range, with values ranging from 0.6% to 1.7%. However, at 7 meters, there is a significant increase in salinity to 1.9%. From 8 to 10 meters, the salinity levels remain relatively stable, fluctuating between 1.5% and 2%. At 11 meters, there is a sharp increase in salinity to 4.1%, indicating a sudden change in the composition of the water at that depth. Beyond 11 meters, the salinity levels gradually decrease, with values ranging from 3.1% at 12 meters to 0.4% at 14.25 meters.

The trend of salinity levels with depth shows both gradual and sudden changes, suggesting variations in the sources and composition of the water at different depths within the studied section.

3) Salinity measurement of Borehole KU3

The salinity levels in Borehole KU3 display some variations as the depth increases. From the surface to a depth of 2 meters, there is a significant increase in salinity percentage, with values ranging from 0.3% to 2.3%. This suggests a notable change in the composition of the water between these depths. At a depth of 3 meters, there is a slight decrease in salinity to 0.9%. From 4 to 6 meters, the salinity levels remain relatively consistent, fluctuating within a narrow range of 0.9% to 1.4%. At 7 meters, there is a slight increase in salinity to 1.5%, followed by a further increase to 1.6% at a depth of 8 meters. From 9 to 10 meters, there is a gradual increase in salinity, with values ranging from 2.0% to 2.4%.

The trend of salinity levels with depth in Borehole KU3 indicates both gradual and discrete changes, suggesting variations in the composition of the water at different depths. These variations could be attributed to factors such as groundwater inflow, geological formations, or hydrological processes specific to this borehole.

4) Salinity measurement of Borehole KU4

From the surface to a depth of 3 meters, there is a significant increase in salinity percentage, with values ranging from 1.4% to 4.2%. This indicates a substantial change in the composition of the water during this initial portion of the borehole. Between 4 to 6.25 meters, there is a gradual decrease in salinity levels, with values ranging from 1.4% to 0.5%. The depth of 7.25 to 10.25 meters, the salinity levels remain relatively stable and low, consistently at 0.4%. From 11.25 to 14.25 meters, there is a slight increase in salinity levels, with values ranging from 0.4% to 0.9%. From 15.25 to 18.25 meters, the salinity levels show some fluctuations, with values ranging from 0.3% to 0.6%. Beyond 18.25 meters, the salinity levels decrease again, with values of 0.3% observed at 16.25 and 18.25 meters.

The trend of salinity levels with depth in Borehole KU4 suggests a combination of fluctuations and gradual changes. The initial portion of the

borehole exhibits a notable increase in salinity, followed by a gradual decrease and relatively stable low levels. The subsequent depths show some variability but generally maintain lower salinity levels. These variations may be indicative of changes in the hydrological conditions or the presence of different water sources at various depths within Borehole KU4.

5) Salinity measurement of Borehole KU5

From the surface to a depth of 3 meters, there is a gradual increase in salinity percentage, with values ranging from 0.5% to 2.6%. This indicates a noticeable change in the composition of the water during this initial portion of the borehole. From 4 to 10 meters, there is a relatively steady increase in salinity levels, with values ranging from 3.3% to 4.4%. At 11 meters, there is a slight decrease in salinity to 3.5%. From 12 to 13 meters, there is a temporary increase in salinity, reaching a peak of 6.1% at 13 meters. From 14 to 16.25 meters, the salinity levels decrease, ranging from 3.4% to 1.1%. From 17.25 to 21.25 meters, the salinity levels remain relatively stable, with values ranging from 0.4% to 2.2%. Beyond 21.25 meters, there are fluctuations in the salinity levels, but they generally remain at lower values, ranging from 0.2% to 0.8%.

The trend of salinity levels with depth in Borehole KU5 demonstrates both gradual changes and intermittent fluctuations. The initial portion of the borehole shows an increasing salinity trend, followed by a relatively stable range, and then a decrease in salinity. These variations could be attributed to changes in the hydrological conditions, water sources, or geological formations encountered at different depths within Borehole KU5.

4.2.2 XRD analysis

The X-ray diffraction (XRD) analysis of sediment samples collected at different depths revealed the presence of various minerals (Figure 4.4). Ten samples were selected to be the representative sediment from five units. The KU1 sample taken from depth of 2.25 meters, is consisted of quartz, calcite, kaolinite, muscovite, illite, montmorillonite, aragonite, pyrite, microcline, albite, and gypsum (Figure 4.5).

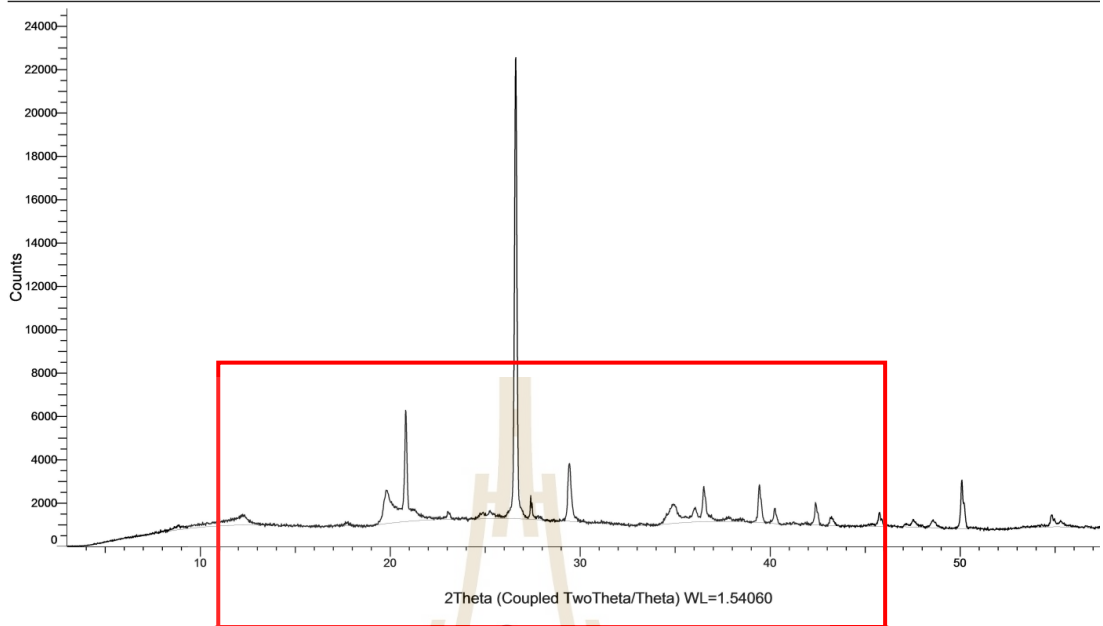
The KU2 sample obtained from 8.25 meters depth (Unit 4) contain quartz, calcite, kaolinite, muscovite, montmorillonite, aragonite, pyrite, gypsum, halite,

microcline, and albite (Figure 4.6). 18.75 meters depth (Unit 3) in the KU1 sample, the mineral composition consisted of quartz, calcite, kaolinite, muscovite, montmorillonite, aragonite, pyrite, gypsum, microcline, and albite (Figure 4.7). Analyzing the KU3 sample collected at 6.25 meters depth (Unit 4) contain quartz, calcite, kaolinite, muscovite, illite, montmorillonite, aragonite, pyrite, gypsum, halite, microcline, and albite (Figure 4.8). The KU4 sample taken from 1.00 meters depth (Unit 4) is consisted of quartz, microcline, calcite, kaolinite, muscovite, aragonite, pyrite, and montmorillonite (Figure 4.9). 19.75 meters depth (Unit 3) in the KU4 sample, contain quartz, kaolinite, calcite, microcline, aragonite, muscovite, illite, montmorillonite, and albite (Figure 4.10).

The KU5 sample obtained at 13.00 meters depth (Unit 4), the minerals observed contain quartz, kaolinite, microcline, aragonite, muscovite, montmorillonite, albite, gypsum, halite, and pyrite (Figure 4.11). 21.25 meters depth (Unit 3) in the KU5 sample, is consisted of quartz, calcite, kaolinite, muscovite, montmorillonite, aragonite, pyrite, microcline, and albite (Figure 4.12).

24.25 meters depth (Unit 3) in the KU5 sample, the identified minerals included quartz, kaolinite, microcline, aragonite, muscovite, montmorillonite, albite, gypsum, and calcite (Figure 4.13). At 28.25 meters depth (Unit 1), the mineral composition is consisted of quartz, calcite, kaolinite, muscovite, montmorillonite, aragonite, microcline, albite, gypsum (Figure 4.14).

(Coupled TwoTheta/Theta)



(Coupled TwoTheta/Theta)

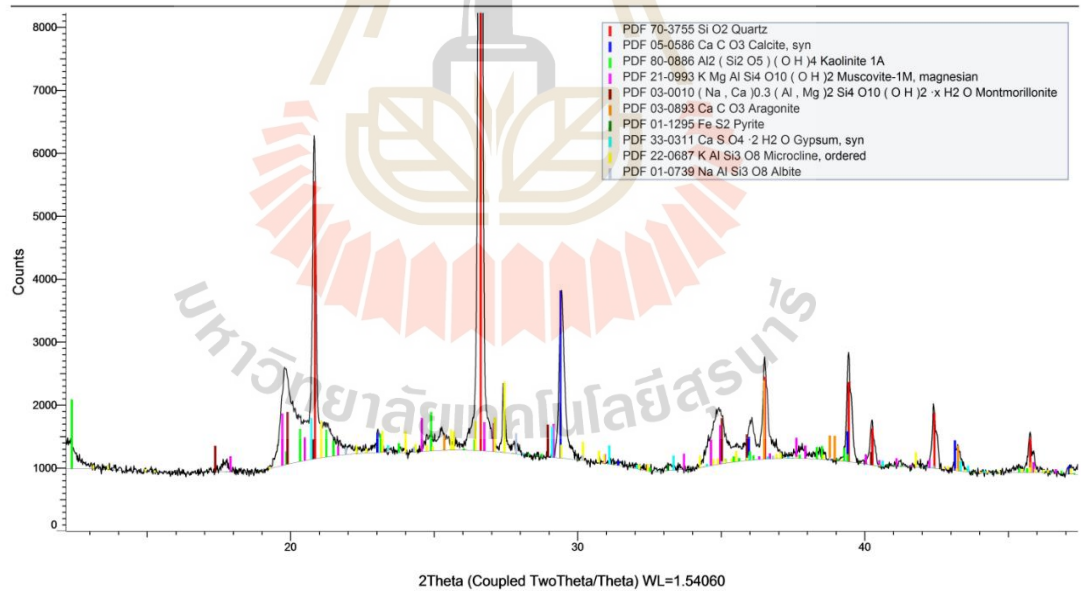


Figure 4.4 X-ray Diffractogram of sediment at 18.75-meter depth (Borehole KU1)

(Coupled TwoTheta/Theta)

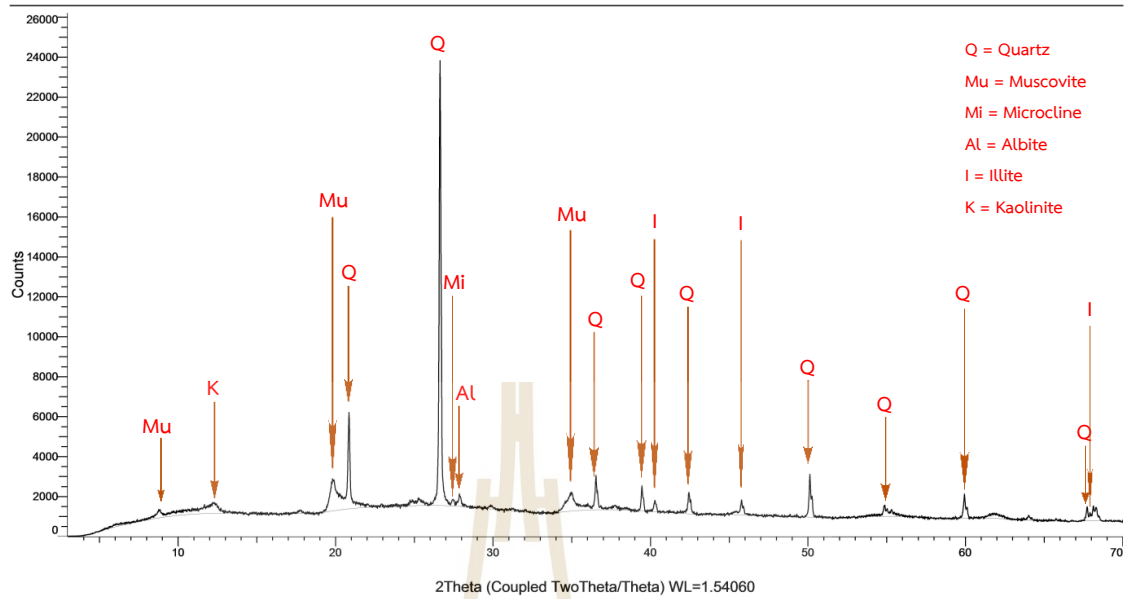


Figure 4.5 X-ray Diffractogram of sediment at 2.25-meter depth (Borehole KU1)

(Coupled TwoTheta/Theta)

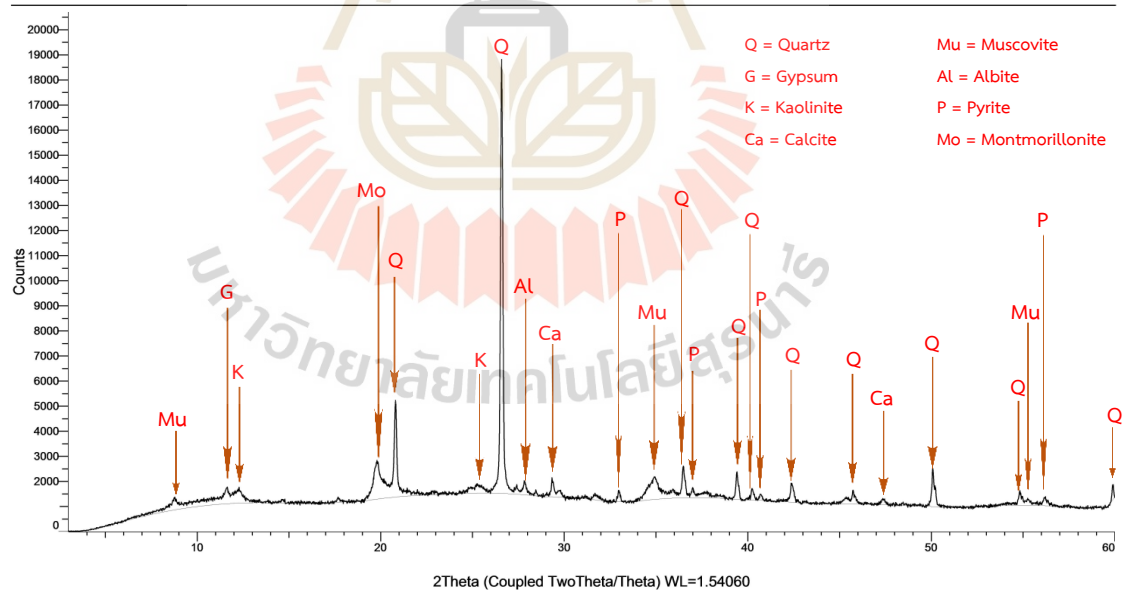


Figure 4.6 X-ray Diffractogram of sediment at 8.25-meter depth (Borehole KU2)

(Coupled TwoTheta/Theta)

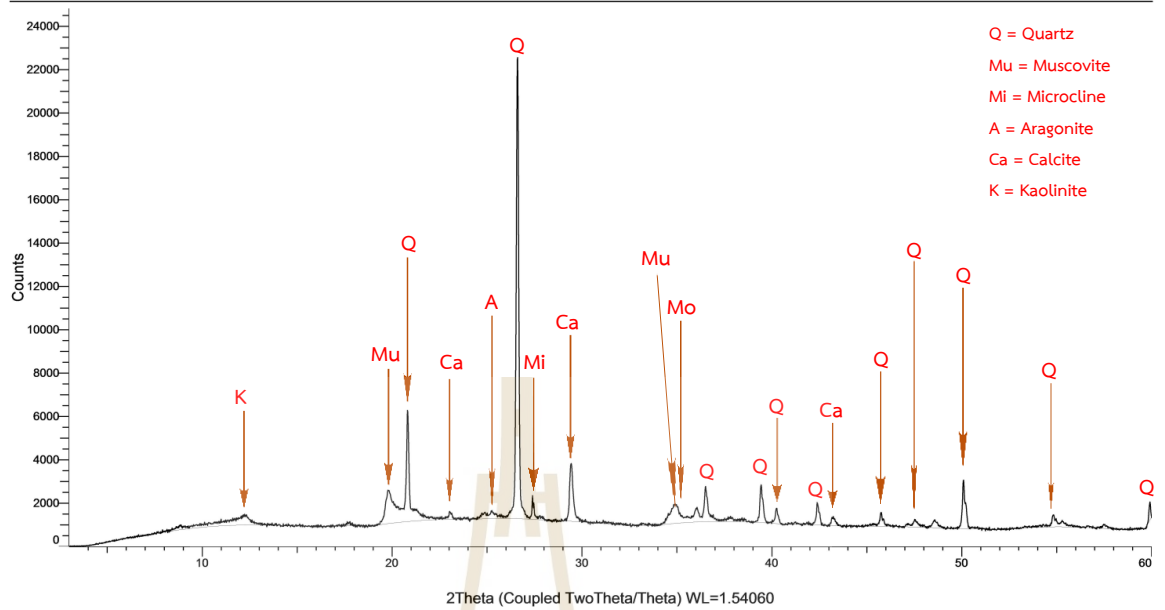


Figure 4.7 X-ray Diffractogram of sediment at 18.75-meter depth (Borehole KU1)

(Coupled TwoTheta/Theta)

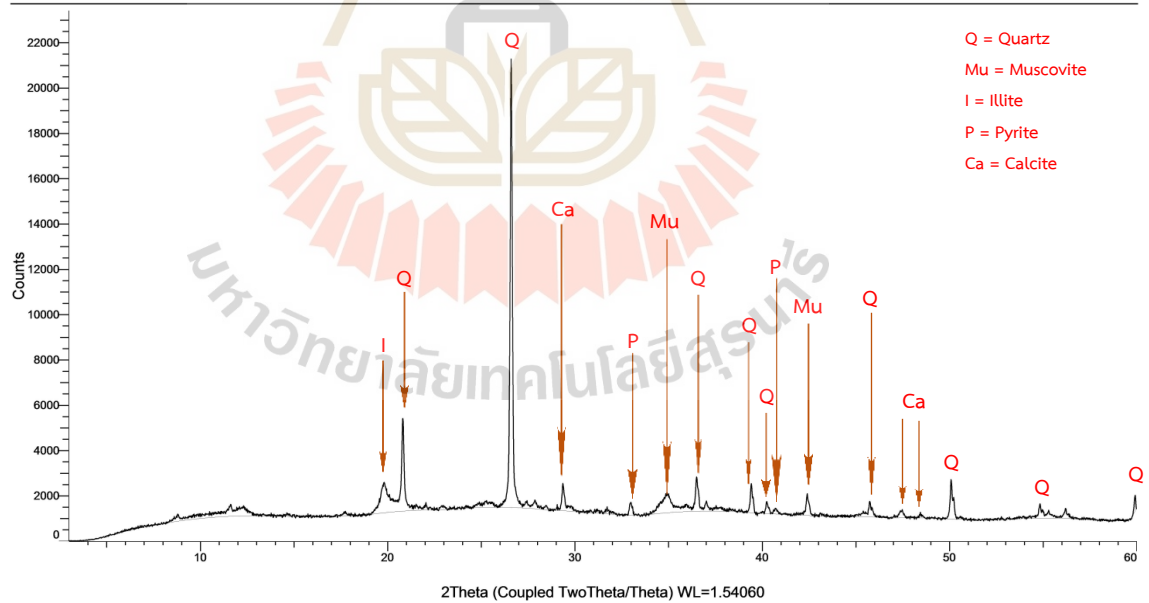


Figure 4.8 X-ray Diffractogram of sediment at 6.25-meter depth (Borehole KU3)

(Coupled TwoTheta/Theta)

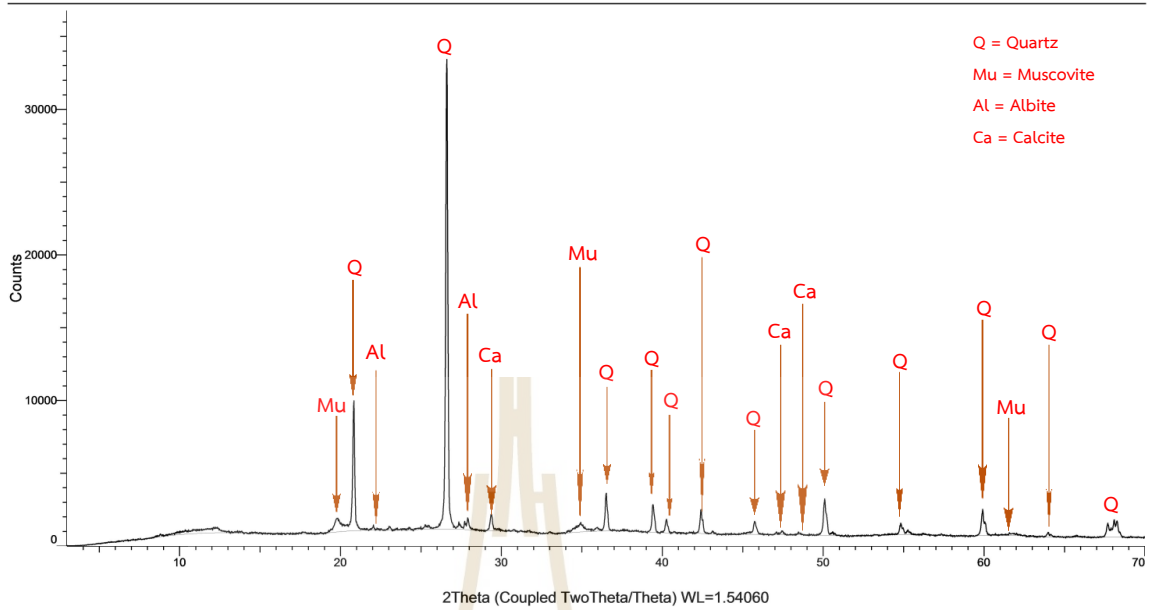


Figure 4.9 X-ray Diffractogram of sediment at 1.00-meter depth (Borehole KU4)

(Coupled TwoTheta/Theta)

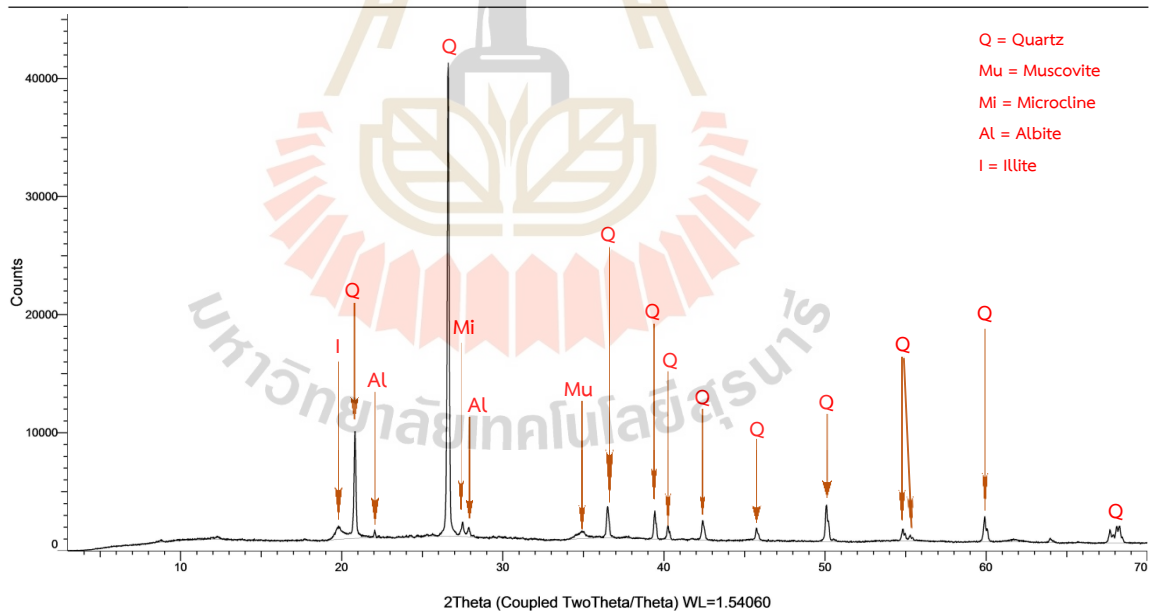


Figure 4.10 X-ray Diffractogram of sediment at 19.75-meter depth (Borehole KU4)

(Coupled TwoTheta/Theta)

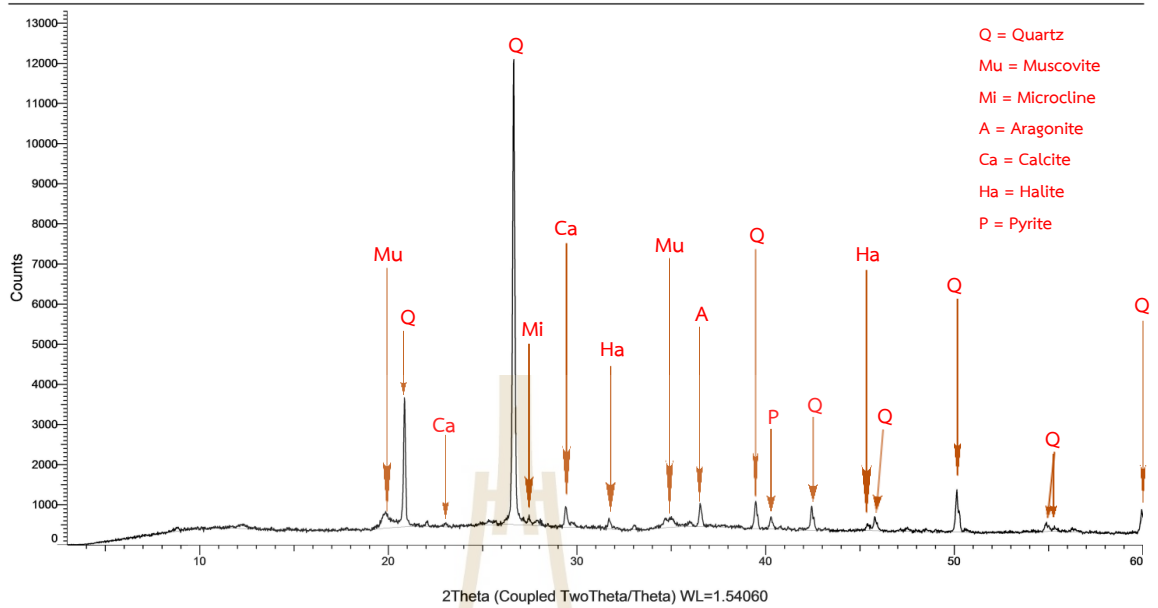


Figure 4.11 X-ray Diffractogram of sediment at 13.00-meter depth (Borehole KU5)

(Coupled TwoTheta/Theta)

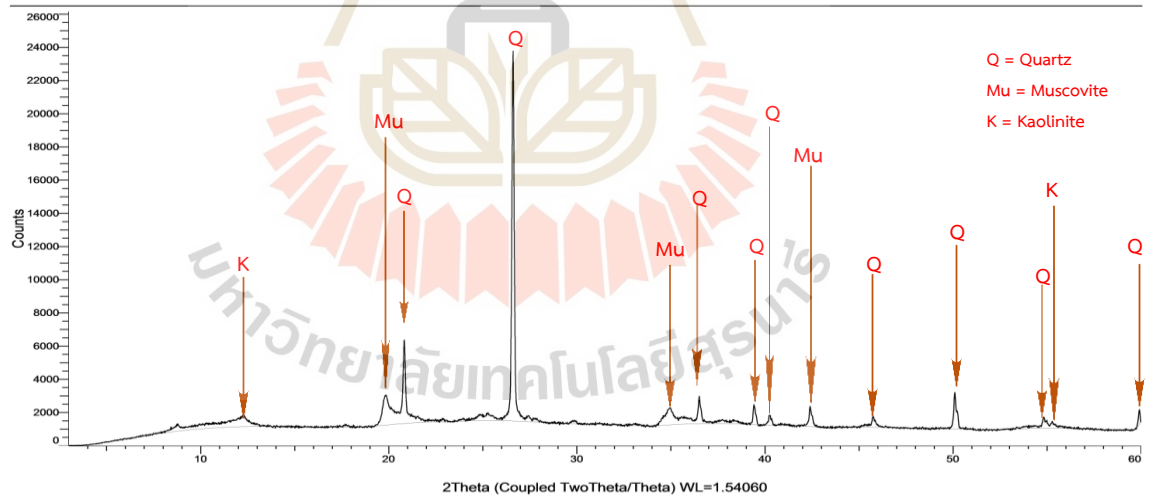


Figure 4.12 X-ray Diffractogram of sediment at 21.25-meter depth (Borehole KU5)

(Coupled TwoTheta/Theta)

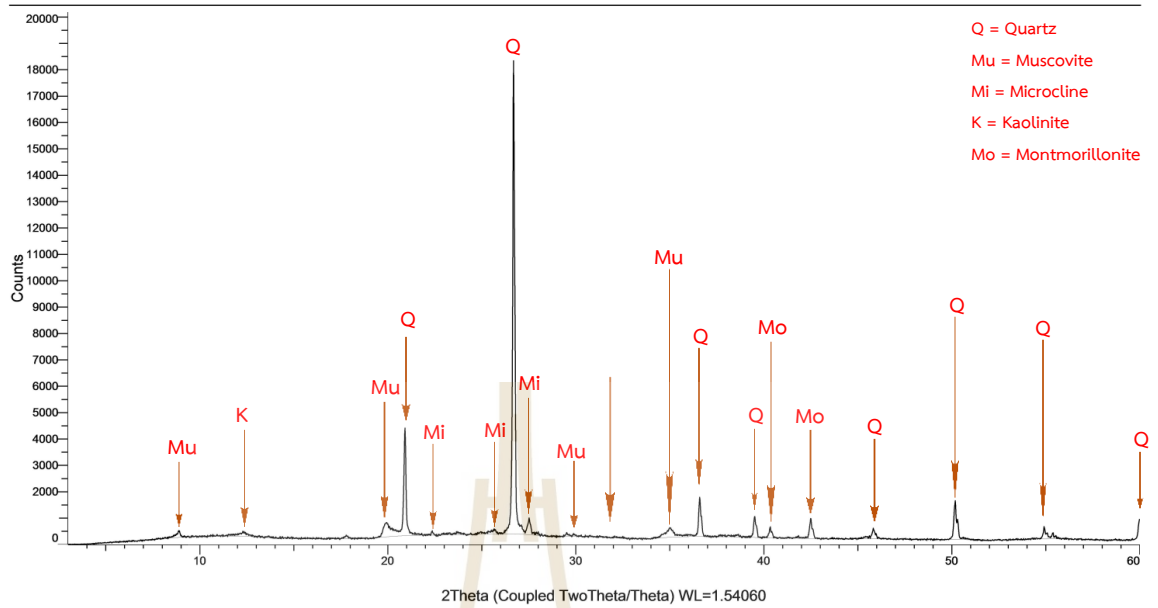


Figure 4.13 X-ray Diffractogram of sediment at 24.25-meter depth (Borehole KU5)

(Coupled TwoTheta/Theta)

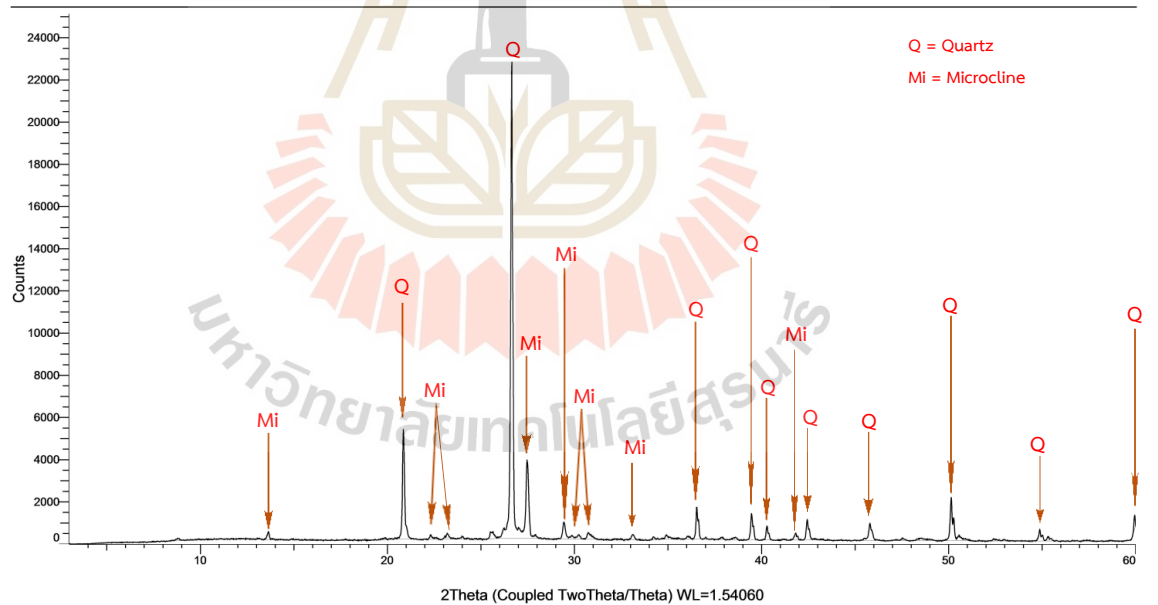


Figure 4.14 X-ray Diffractogram of sediment at 28.25-meter depth (Borehole KU5)

CHAPTER V

SYSTEMATIC PALEONTOLOGY

This chapter presents the results of the study, focusing on classification and identification of the recovered ostracods (section 5.1), and providing distribution of the ostracods (Section 5.2).

5.1 Systematic paleontology

In this thesis, the classification of ostracod is altered Moore (1961) and Martens and Horne (2009). In this part, the SEM photographs were used to identify fossil ostracods and to compare with previous works of the Holocene ostracods. 2,097 ostracods specimens (valves and carapaces) are obtained from 99 clay samples from Boreholes KU1 to KU5. They are identified to 15 species, belonged to ten genera and seven families.

Forty clay samples from Phanom Surin shipwreck site were processed for ostracods, and yielded 92 specimens which can be classified to seven genera and nine species (Figure 5.1 - 5.6)

Abbreviations: DB: dorsal border; AB: anterior border; ADB: anterior dorsal border; AVB: anterior ventral border; VB: ventral border; PB: posterior border; PVB: posterior ventral border; PDB: posterior dorsal border; H: height; L: length.

Suborder CYTHEROCOPINA Baird, 1850

Superfamily CYTHEROIDEA Baird, 1850

Family CYTHERIDEIDAE Baird, 1850

Subfamily CYTHERIDEINAE Sars, 1925

Genus Neocyprideis Apostolescu, 1956

Type-species. Cyprideis (Neocyprideis) durocortoriensis Apostolescu, 1956

Neocyprideis agilis (Guan, 1978)

Figure 5.1 A-F

Materials. 11 complete valves from Borehole KU1, 34 complete valves from Borehole KU3, and three complete carapaces and 16 complete valves from Phanom Surin shipwreck site.

Dimensions. H = 0.44 – 0.55 mm; L = 0.71 – 0.85 mm; H/L = 0.62 – 0.64.

Occurrence. Modern distribution: Neocyprideis spinulosa (Brady, 1868b) is one of the most widespread shallow water species known from the eastern coast of South Africa across India, Malaysia, Solomon Islands, Australia, New Caledonia and French Polynesia (summarised in Titterton et al., 2001); southwestern coast of Peninsular Thailand, Ao nun, Satun Province, Andaman Sea (Forel, 2021). Fossil distribution: Late Pliocene of Timor (Fyan, 1916), Pliocene-Pleistocene of India (Guha, 1968), Quaternary of Solomon Islands (Williams, 1980) and Fiji (Malz and Ikeya, 1986). This study: Samples SUT-22-P73 to SUT-22-P91, Phanom Surin shipwreck site; sample SUT-KU1-165 to SUT-KU1-175, Borehole KU1, SUT-KU3-001 to SUT-KU3-034, Borehole KU3, Samut Sakhon Province, central Thailand, Holocene, Quaternary.

Remarks. N. agilis is characterized by dorsal margin strongly convex, with distinct posterior cardinal angle, particularly in the left valve; anterior margin broadly rounded, posterior margin obliquely rounded; ventral margin straight in the right valve, and slightly convex in the left valve. Left valves markedly larger than right ones (Wouters, 2005). Neocyprideis was found in Southern part of Thailand (Fig. 3. J.-N. p. 4. in Forel, 2021), NW Gulf of Thailand (Fig. 2. 1. p. 233. in Montenegro et al., 2004), Hong Kong (Fig. 5. C., L. p. 143. and Fig. 7. I. p. 145. in Hong, 2016), and living species in Indonesia (Fig. 3. p. 92. in Wouter, 2005).

Genus Sinocytheridea Hou in Hou et al., 1982

Type-species. Sinocytheridae latiovata Hou in Hou et al. 1982, junior synonym of Sinocytheridea impressa (Brady, 1869) following the revision of Whatley and Zhao (1988a).

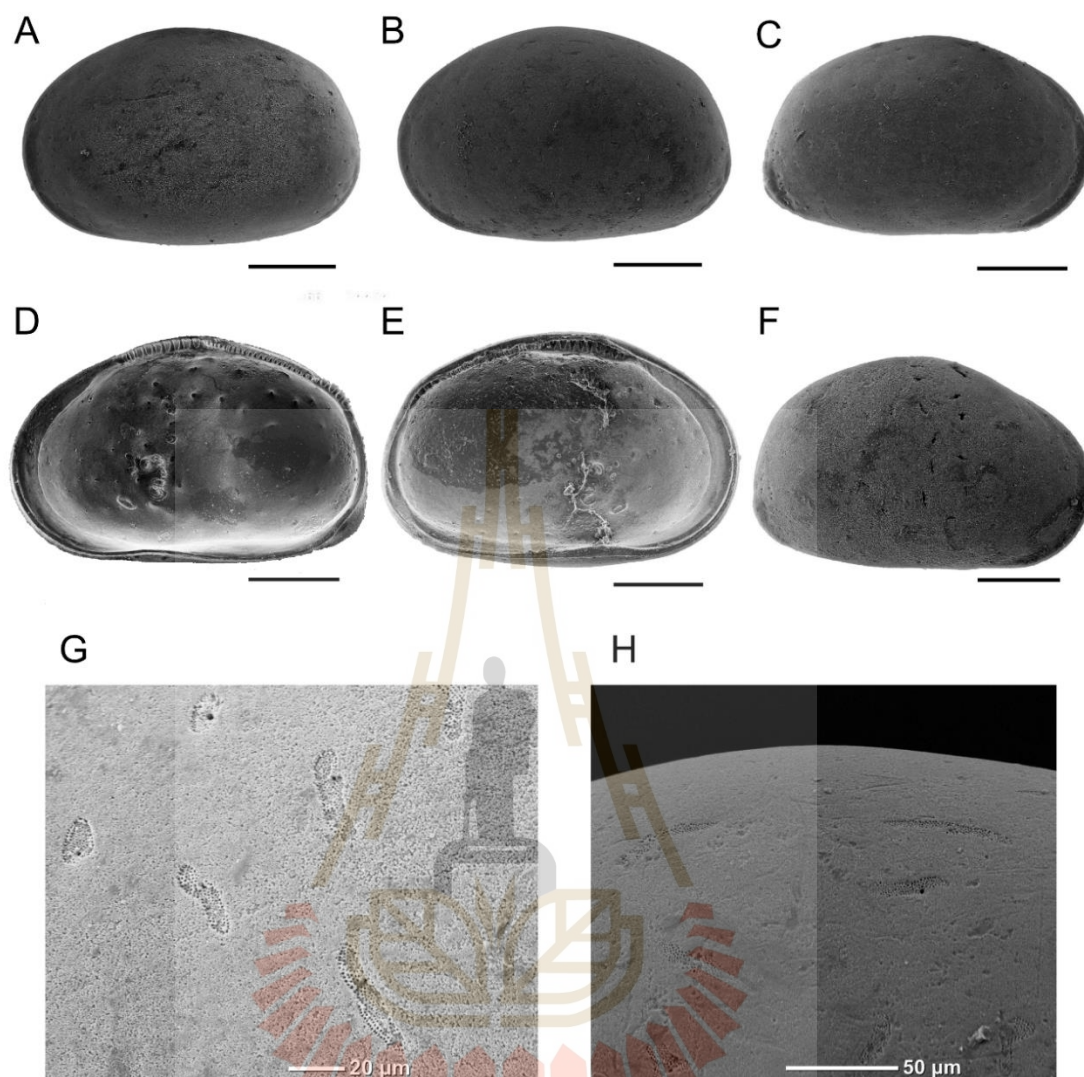


Figure 5.1 Late Holocene ostracods from Samut Sakhon Province: A-F, *Neocyprideis agilis* (Guan, 1978); G-H, elongate and rounded sieve pores of *N. agilis*. See description of the specimen in text. Scale bars are 200 µm, except for G-H

***Sinocytheridea impressa* (Brady, 1869)**

Figure 5.2 A-G

Materials. 42 complete valves from Borehole KU2, three complete carapaces and 52 complete valves from Borehole KU3, 51 complete valves from Borehole KU4, 73 complete valves from Borehole KU5, and one complete valve from Phanom Surin shipwreck site.

Dimensions. H = 0.24 – 0.35 mm; L = 0.43 – 0.59 mm; H/L = 0.47 – 0.60.

Occurrence. East China Sea to Indo-Pacific (Hong et al., 2019); Japan Sea to South China Sea (Tanaka et al., 2009); Vietnam (Tanaka et al., 2009; Tan et al., 2021); Mae Khlong river mouth, north west Peninsular Thailand (Montenegro et al., 2004); Andaman Sea coasts (Yamada et al., 2014); Samut Sakhon Province, Central Thailand (Chitnarin et al., 2023). This study: SUT-KU2-198 to SUT-KU2-239, SUT-KU3-266 to SUT-KU3-320, SUT-KU4-050 to SUT-KU4-100, and SUT-KU5-435 to SUT-KU5-507 (Borehole KU). SUT-22-P04 (Phanom Surin shipwreck site).

Remarks. *S. impressa* (Brady, 1869) carapaces exhibit distinctive features, including a flat and elongated to oval lateral outline, a long hinge, and a slightly concave ventral margin. The carapace surface is adorned with scattered sieve-like pores. Sexual dimorphism is evident, with males being longer and slender, having similar-sized anterior and posterior parts, and an indistinct anterior height maximum.

Family HEMICYTHERIDAE Puri, 1953

Genus *Hemicytheridea* Kingma, 1948

Type-species. *Hemicytheridea reticulata* Kingma, 1948

Hemicytheridea reticulata Kingma, 1948

Figure 5.2 H-J

Materials. Two complete valves from Borehole KU4, and one complete carapace and one complete valve from Phanom Surin shipwreck site.

Dimensions. H = 0.29 – 0.33 mm; L = 0.61 – 0.65 mm.; H/L = 0.46 – 0.55.

Occurrence. Australia (Bentley, 1988); southeast India (e.g., Hussain, 1998); east India (e.g., Hussain and Mohan, 2001); Sri Lanka (Iwatani et. al., 2014); Java Sea (e.g., Dewi, 1993, 2000; Fauzielly, 2013; Fauzielly et. al., 2012, 2013); Celebes Sea (Dewi and Illahude, 2005); Malaysia (e.g., Kingma, 1948 Zhao and Whatley, 1989; Ramlan and Noraswana, 2009; Omar et al., 2017); Hong-Kong (Hong et al., 2019); China Sea (Gu et al., 2017); Vietnam (Ten et al., 2021); southwestern coast of Peninsular Thailand, Ao

nun, Satun Province, Andaman Sea (Forel, 2021). This study: SUT-KU4-104 to SUT-KU4-105 (Borehole KU). SUT-22-P71 to SUT-22-P72 (Phanom Surin shipwreck site).

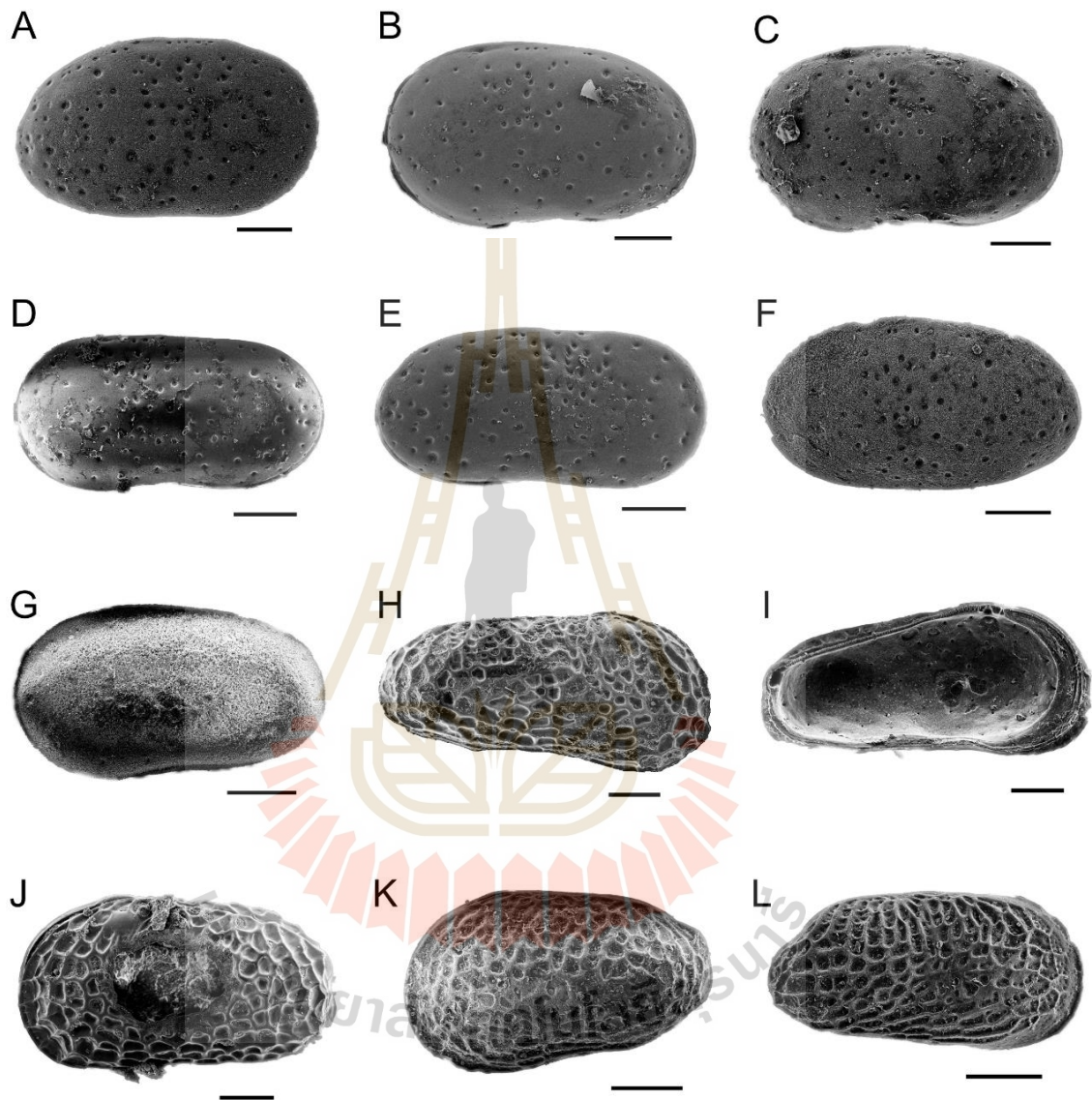


Figure 5.2 Late Holocene ostracods from Samut Sakhon Province: A-G, *Sinocytheridea impressa* (Brady, 1869); H-J, *Hemiccytheridea reticulata* Kingma, 1948; K-L, *Hemiccytheridea cancellata* (Brady, 1868). See description of the specimen in text. Scale bars are 100 μm

Remarks. The distribution of *H. reticulata* has been recently summarized and discussed in the study by Iwatani et al. (2014). According to the literature, this species has been

reported in shallow waters of the Indo-Pacific region (Zhao and Whatley, 1989; Hong et al., 2019). Another related species, *H. reticulata*, has been documented in marshland in southern Iraq (Issa, 2016). This species was found in southwestern coast of Thailand (Forel, 2021).

Hemicytheridea cancellata (Brady, 1868)

Figure 5.2 K-L

Materials. One complete valve from Borehole KU1, one complete valve from Borehole KU3, and three complete valves from Borehole KU5.

Dimensions. H = 0.20 – 0.25 mm; L = 0.41 – 0.43 mm; H/L = 0.49 – 0.58.

Occurrence. Phetchaburi area, NW Gulf of Thailand (Pugliese et al., 2006); Pahang River Delta, Pahang Darul Makmur (Noraswana, N. F. and Ramlan, O, 2014); Pulau Perhentian, Terengganu, Malaysia (OMAR, 2017). This study: SUT-KU2-698, SUT-KU3-581, and SUT-KU5-706 to SUT-KU5-708.

Remarks. The specimen of *H. cancellata* found in North West Gulf of Thailand (Pugliese et al., 2006), occur in scattered way and are represented by a reduced number of specimens. This species showed great dominance in Pulau Perhentian, Terengganu in Malaysia (Omar, 2017). Description of *H. cancellata*: Medium in size and has strong reticulate ornamentation. The dorsal margin is straight and ventral margin is sinuous. The posterior end is turned upwards and the anterior end is rounded (Omar, 2017).

Superfamily CYTHEROIDEA Baird, 1850

Family TRACHYLEBERIDIDAE Sylvester-Bradley, 1948

Genus *Keijella* Ruggieri, 1967

Type species. *Cythere hodgii* Brady, 1866 subsequently designated by Ruggieri (1967).

Keijella multisulcus Whatley and Zhao, 1988

Figure 5.3 A-F

Materials. 71 complete valves from Borehole KU1, three complete carapaces and 134 complete valves from Borehole KU2, four complete carapaces and 155 complete

valves from Borehole KU3, 26 complete carapaces from Borehole KU4, three complete carapaces and 265 complete valves from Borehole KU5, and one complete carapace and seven complete valves from Phanom Surin shipwreck site.

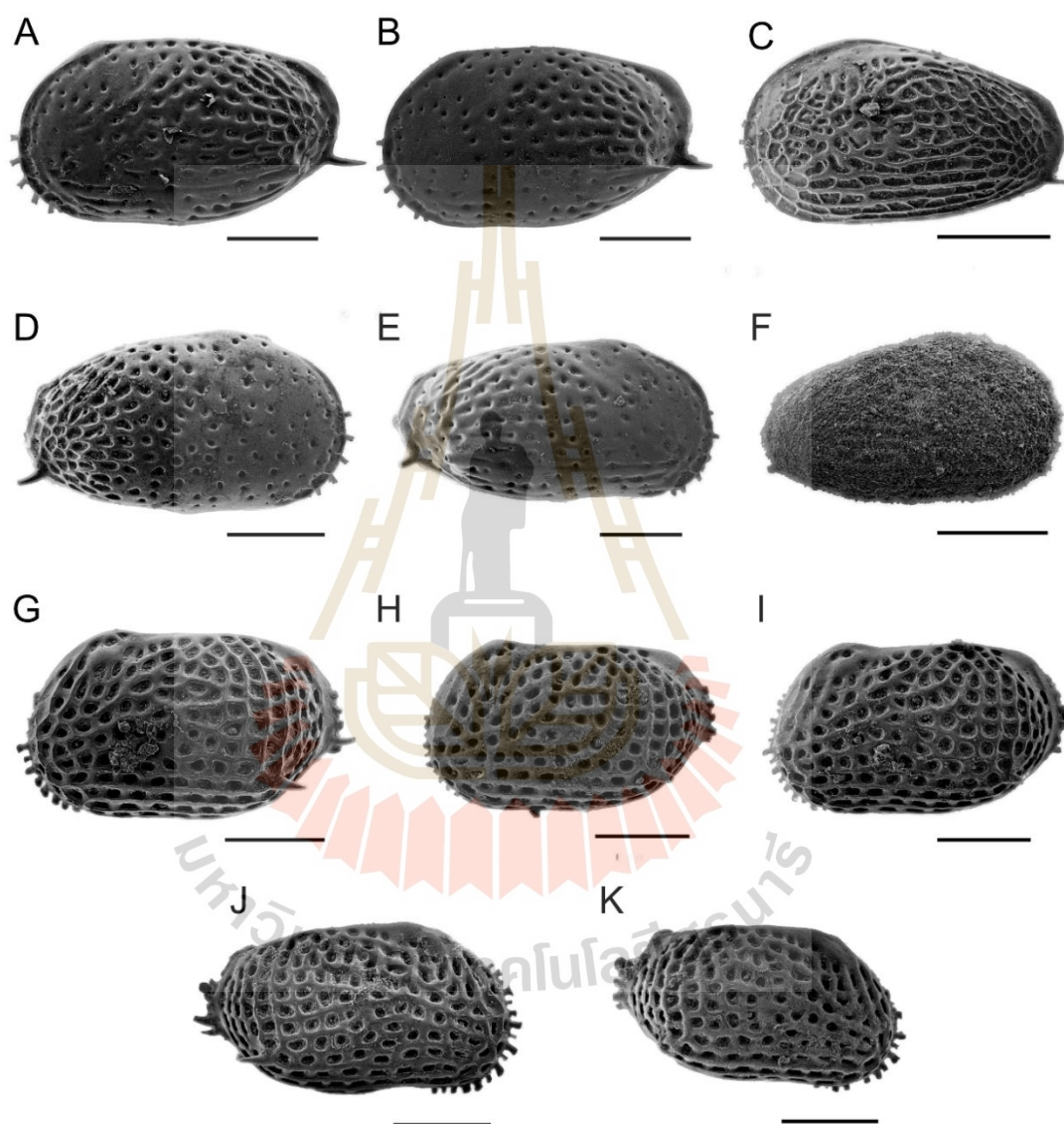


Figure 5.3 Late Holocene ostracods from Samut Sakhon Province: A-F, *Keijella multisulcus* Whatley and Zhao, 1988; G-K, *Keijella gonia* Zhao and Whatley, 1989. See description of the specimen in text. Scale bars are 200 μm

Dimensions. H = 0.31 – 0.42 mm; L = 0.54 – 0.84 mm; H/L = 0.46 – 0.60.

Occurrence. Malacca Straits (Whatley and Zhao, 1988); Malaysia (Omar et al., 2017); Mae Khlong river mouth, north west Gulf of Thailand (Montenegro et al., 2004); southwestern coast of Peninsular Thailand, Ao nun, Satun Province, Andaman Sea (Forel, 2021); whale-fall excavation site, Chao Phraya delta, Central Thailand (Chitnarin et al., 2023). This study: SUT-KU2-001 to SUT-KU2-137, SUT-KU3-035 to SUT-KU3-193, SUT-KU4-001 to SUT-KU4-026, and SUT-KU5-001 to SUT-KU5-268 (Borehole KU). SUT-22-P62 to SUT-22-P69 (Phanom Surin shipwreck site).

Remarks. This species is characterized by medium size with almost smooth surface and subovate in lateral view. This samples have small posteroventral spine with denticles in both posterior and anteroventral area, without posterior cardinal angle in lateral view of dorsal area. External valves pitted and punctate.

This species is restricted to Thailand and Malaysia (Zhao and Whatley, 1988a, 1988b; Montenegro et al., 2004; Yamada et al., 2014; Omar et al., 2017; Forel, 2021; Chitnarin et al., 2023).

Keijella gonia Zhao and Whatley, 1989

Figure 5.3 G-K

Materials. 15 complete valves from Borehole KU1, two complete carapaces and 58 complete valves from Borehole KU2, 72 complete valves from Borehole KU3, 23 complete valves from Borehole KU4, two complete carapaces and 164 complete valves from Borehole KU5, and eight complete carapaces and 34 complete valves from Phanom Surin shipwreck site.

Dimensions. H = 0.29 – 0.39 mm; L = 0.49 – 0.69 mm; H/L = 0.48 – 0.61.

Occurrence. Java Sea (Fauzielly, 2013; Fauzielly et al., 2012, 2013); Malaysia (Whatley and Zhao, 1989); Vietnam (Tan et al., 2021); Mae Khlong river mouth, north west Peninsular Thailand (Montenegro et al., 2004), southwestern coast of Peninsular Thailand, Ao nun, Satun Province, Andaman Sea (Forel, 2021), Whale-fall excavation site, Chao Phraya delta, Central Thailand (Chitnarin et al., 2023). This study: SUT-KU2-138 to SUT-KU2-197, SUT-KU3-194 to SUT-KU3-265, SUT-KU4-027 to SUT-KU4-049, and

SUT-KU5-269 to SUT-KU5-434 (Borehole KU). SUT-22-P20 to SUT-22-P61 (Phanom Surin shipwreck site).

Remarks. *K. gonia* Zhao and Whatley, 1989 was dominant in Chao Phraya delta area at Whale-fall excavation site (Chitnarin et al., 2023) near Phanom Surin shipwreck site. The size of specimens from this works represented adults.

Family SCHIZOCYTHERIDAE Howe in Moore, 1961

Subfamily SCHIZOCYTHERINAE Mandelstam, 1960

Genus *Neomonoceratina* Kingma, 1948

Type-species. *Neomonoceratina columbiformis* Kingma, 1948 by original designation.

Neomonoceratina iniqua (Brady, 1868)

Figure 5.4 A-E

Materials. Five complete valves from Borehole KU1, one complete carapace and 146 complete valves from Borehole KU2, 97 complete valves from Borehole KU3, 45 complete valves from Borehole KU5, and three complete carapaces and 16 complete valves from Phanom Surin shipwreck site.

Dimensions. H = 0.30 – 0.32 mm; L = 0.56 – 0.62 mm; H/L = 0.51 – 0.54.

Occurrence. Iraq (Al-Jumaily and Al-Sheikhly, 1999); Java Sea (Brady, 1868a; Dewi, 1993, 2000; Fauzielly, 2013; Fauzielly et al., 2012, 2013); east India (e.g., Hussain and Mohan, 2001; Hussain et al., 2007); southeast India (e.g., Hussain et al., 2004, 2007, 2013a; Baskar et al., 2013; Hussain and Kalaiyarasi, 2013; Hussain, 1998); southwest India (e.g., Hussain et al., 2013b; Gopalakrishna et al., 2007); west India (e.g., Bhatia and Kumar, 1979); Sri Lanka (Iwatani et al., 2014); Persian Gulf (Paik, 1977; Mostafawi, 2003; Mostafawi et al., 2010); Malaysia (e.g., Zhao and Whatley, 1989; Ramlan and Noraswana, 2009, 2010); Japan (Ishizako and Kato, 1976); Vietnam (Tan et al., 2021); Mae Khlong river mouth, north west Gulf of Thailand (Montenegro et al., 2004); southwestern coast of Peninsular Thailand, Ao nun, Satun Province, Andaman Sea (Forel, 2021); whale-fall excavation site, Chao Phraya delta, Central Thailand (Chitnarin et al., 2023). This study:

SUT-KU2-534 to SUT-KU2-680, SUT-KU3-475 to SUT-KU3-571, and SUT-KU5-634 to SUT-KU5-678.

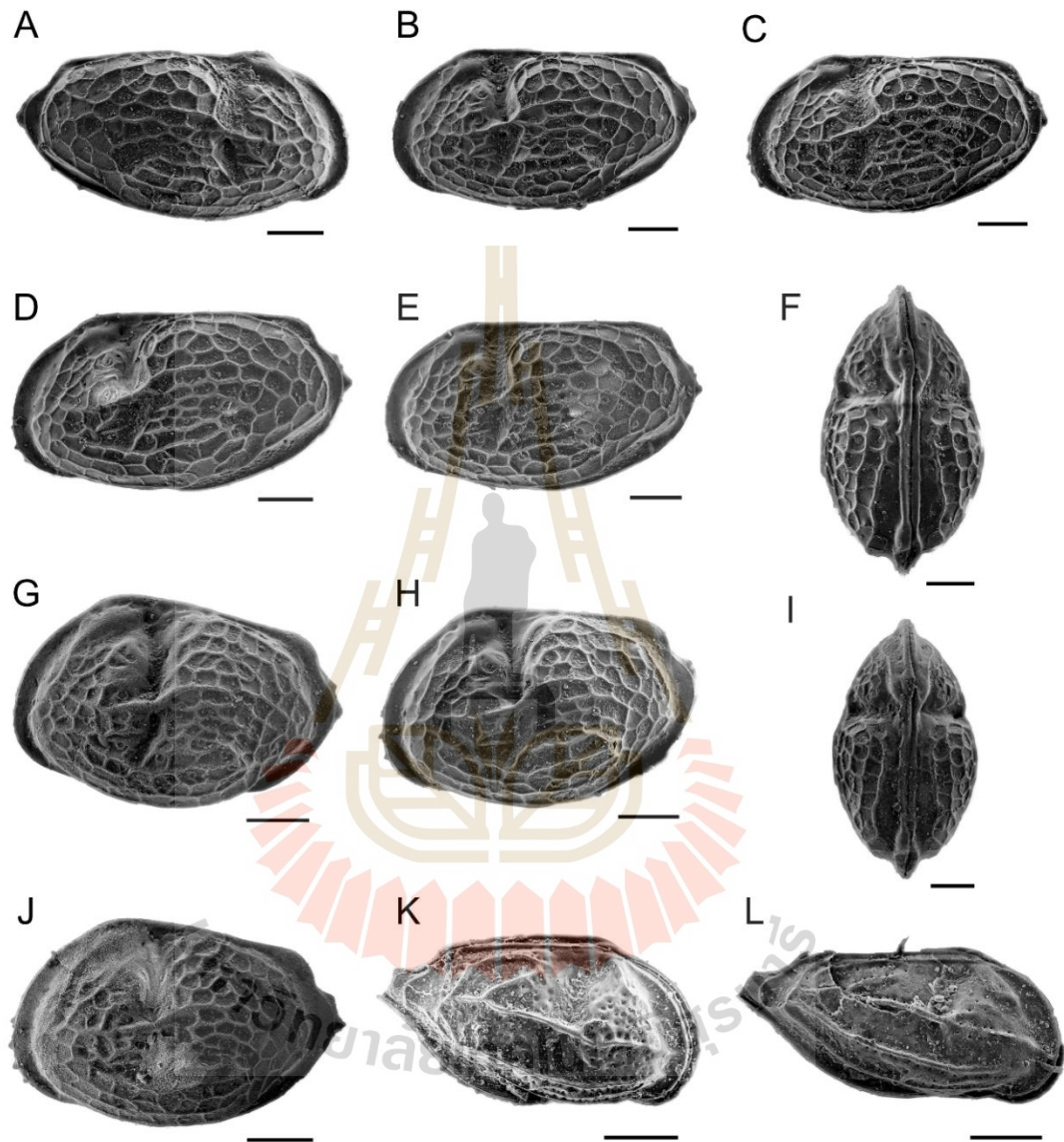


Figure 5.4 Late Holocene ostracods from Samut Sakhon Province: A-E, *Neomonoceratina iniqua* (Brady, 1868); F-J, *Neomonoceratina rhomboidea* (Brady, 1968); K, *Neomonoceratina mediterranea malayensis* Zhao and Whatley, 1988; L, *Neomonoceratina mediterranea mediterranea* (Ruggieri, 1953). See description of the specimen in text. Scale bars are 100 μ m

Remarks. *N. iniqua*, identified by Brady in 1868, can be distinguished by its reticulate surface adorned. The species displays a short and indistinct posterodorsal rib, accompanied by a long median rib extending from the anterior to the posteroventral region. Additionally, a venterolateral rib terminates in a simple spine. There is clear sexual dimorphism, with male carapaces exhibiting a longer and more slender morphology, while female carapaces are shorter and higher.

Neomonoceratina rhomboidea (Brady, 1968)

Figure 5.4 F-I

Materials. Eight complete valves from Borehole KU1, nine complete carapaces and 285 complete valves from Borehole KU2, four complete carapaces and 150 complete valves from Borehole KU3, two complete valves from Borehole KU4, four complete carapaces and 122 complete valves from Borehole KU5, and one complete carapace from Phanom Surin shipwreck site.

Dimensions. H = 0.29 – 0.34 mm; L = 0.47 – 0.53 mm; H/L = 0.60 – 0.65.

Occurrence. Modern distribution: Batavia, Java, Indonesia (Brady 1968); Jason Bay, southeast Malaysia (Zhao and Whatley 1988). Fossil distribution: Bangkok Clay, whale excavation site, Samut Sakhon Province, Thailand, Late Holocene (Chitnarin et al., 2023). This study: SUT-KU2-240 to SUT-KU2-533, SUT-KU3-321 to SUT-KU3-474, SUT-KU4-101 to SUT-KU4-102, and SUT-KU5-508 to SUT-KU5-633 (Borehole KU). SUT-22-P92 (Phanom Surin shipwreck site).

Remarks. *N. rhomboidea* Brady in 1968, is distinguished by its inflated carapace and exhibits a weak and shallow reticulation pattern. It features a thin median rib and a posteroventral region that is similar to the shape of an ala. Additionally, this species displays relatively large sieve-type pore canals. The anterior margin of the carapace is denticulate, and the intercostal surface is reticulate with polygonal fossae. The muri of *N. rhomboidea* are relatively thin, and the sola is finely punctate.

Neomonoceratina mediterranea malayensis Zhao and Whatley, 1988

Figure 5.4 L

Materials. One complete valve from Borehole KU1, 14 complete carapaces from Borehole KU2, five complete valves from Borehole KU5, and 13 complete carapaces and two complete valves from Phanom Surin shipwreck site.

Dimensions. H = 0.21 mm; L = 0.45 mm; H/L = 0.47.

Occurrence. Recent distribution: Jason Bay, southeastern Malay Peninsula, Malaysia (Zhao and Whatley 1989); Southwestern coast of Peninsular Thailand, Ao Nun, Satun Province, Andaman Sea (Forel 2021). Fossil distribution: Bangkok Clay, whale excavation site, Samut Sakhon Province, Thailand, Late Holocene (Chitnarin et al., 2023). This study: SUT-KU2-681 to SUT-KU2-695, and SUT-KU5-679 to SUT-KU5-683 (Borehole KU). SUT-22-P05 to SUT-22-P19 (Phanom Surin shipwreck site).

Remarks. N. mediterranea malayensis, punctae, or small dots, on the carapace surface are primarily located at the base of the ribs, while they are infrequent on the smooth intercostal surface. The discovery of N. mediterranea malayensis initially occurred in shallow water sediments of Jason Bay, located in the Malay Peninsula, as reported by Zhao and Whatley in 1988. Additionally, this species has been found along the Andaman coast of Thailand, as depicted in Figure 4f of the study conducted by Forel in 2021 and whale fall excavation site in Chitnarin et al., 2023.

Neomonoceratina mediterranea mediterranea (Ruggieri, 1953)

Figure 5.4 K

Materials. One complete carapace from Borehole KU2.

Dimensions. H = 0.23 mm; L = 0.44 mm; H/L = 0.53.

Occurrence. Modern distribution: Southwestern coast of Peninsular Thailand, Ao Nun, Satun Province, Andaman Sea (Forel 2021). Fossil distribution: Pliocene of southeast China, Quaternary of east China, East of Australia, Recent of Eastern Mediterranean, the Philippines, Indonesia, Australia, the Caribbean and Gulf of Mexico (see details in Zhao and Whatley 1989); Bangkok Clay, whale excavation site, Samut Sakhon Province, Thailand, Late Holocene (Chitnarin et al., 2023). This study: SUT-KU2-699.

Remarks. N. mediterranea mediterranea, as described by Ruggieri in 1953, is characterized by its small carapace size and the presence of two short oblique posterodorsal ribs, a long median rib, one venterolateral rib, and one ventral rib. The posterodorsal and venterodorsal ribs connect with the median rib in the posterior region. The carapace surface of this species is finely punctate.

Superfamily PONTOCYPRIDOIDEA Müller, 1894

Family PONTOCYPRIDIDAE Müller, 1894

Genus Propontocypris Sylvester-Bradley, 1947

Type-species. Pontocypris trigonella Sars, 1866 by original designation.

Propontocypris bengalensis Maddocks, 1969

Figure 5.5 A-H

Materials. Two complete valves from Borehole KU2, one complete carapace and five complete valves from Borehole KU3, one complete carapace and eight complete valves from Borehole KU5, and three complete carapaces from Phanom Surin shipwreck site.

Dimensions. H = 0.17 – 0.24 mm; L = 0.35 – 0.48 mm; H/L = 0.45 – 0.53.

Occurrence. Modern distribution: Persian Gulf (Maddocks 1969; Mostafawi 2003); Bay of Bengal and Sri Lanka (Maddocks 1969); Persian Gulf (Bate 1971; Paik 1977); Red Sea (Bonaduce et al. 1983). Fossil distribution: Hang Hau Formation, Lei Yue Mun, Hong Kong, Holocene (Wang et al. 2018); Bangkok Clay, whale excavation site, Samut Sakhon Province, Thailand, Late Holocene (Chitnarin et al., 2023). This study: SUT-KU2-695 to SUT-KU2-696, SUT-KU3-572 to SUT-KU3-577, and SUT-KU5-684 to SUT-KU5-692 (Borehole KU). SUT-22-P01 to SUT-22-P03 (Phanom Surin shipwreck site).

Remarks. Propontocypris (Schedopontocypris) bengalensis Maddocks, 1969 appears in endemic east and west coast of India (Hussain, 1998).

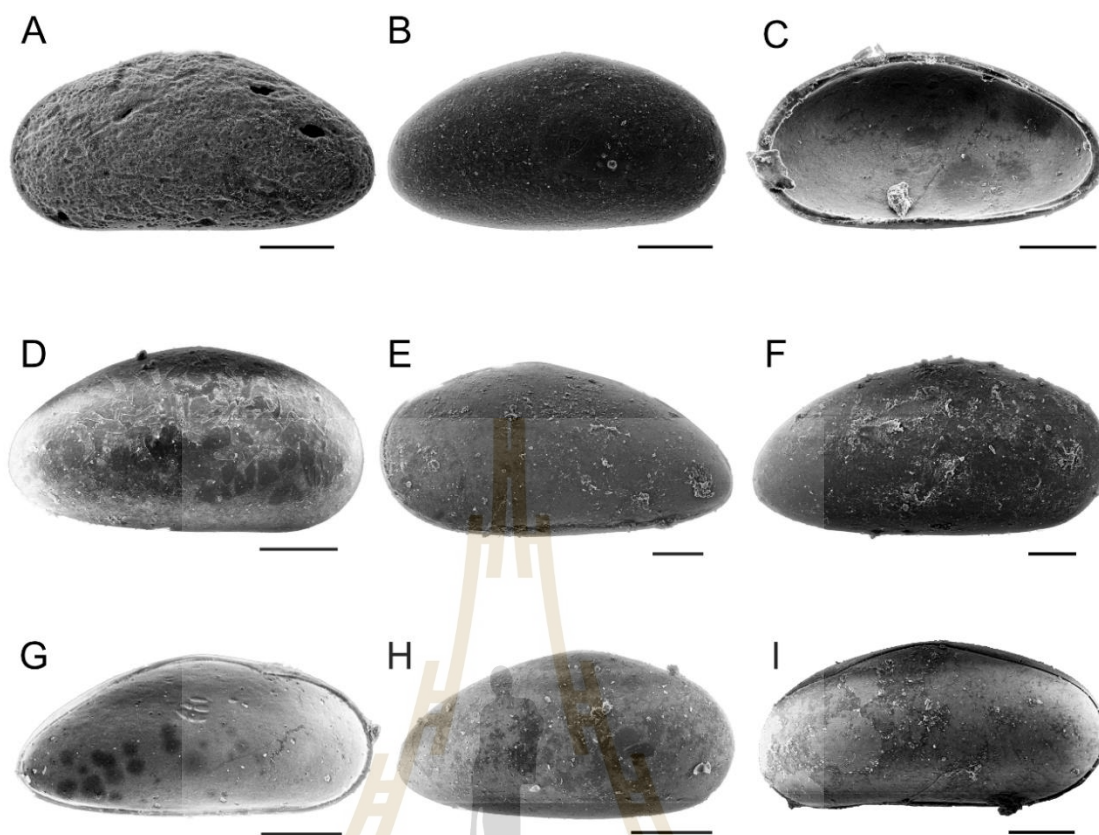


Figure 5.5 Late Holocene ostracods from Samut Sakhon Province: A-H, *Propontocypris bengalensis* Maddocks, 1969; I, *Aglaiocypris pellucida* Mostafawi, 2003. See description of the specimen in text. Scale bars are 100 μ m

Superfamily Cypridoidea Baird, 1845

Family Candonidae Kaufmann, 1900

Genus *Aglaiocypris* Sylvester-Bradley, 1947

Type species. *Aglaiocypris pulchella* (Brady, 1868) subsequently designated by Sylvester-Bradley (1947).

Aglaiocypris pellucida Mostafawi, 2003

Figure 5.5 I

Materials. One complete valve from Borehole KU5.

Dimensions. H = 0.25 – 0.27 mm; L = 0.52 mm; H/L = 0.49.

Occurrence. Modern distribution: West coast of India, Recent (Jain 1978); Persian Gulf, Recent (Maddocks 1969; Paik 1977; Mostafawi 2003). Fossil distribution: Hang Hau Formation, Lei Yue Mun, Hong Kong, Holocene (Wang et al. 2018); Bangkok Clay, whale excavation site, Samut Sakhon Province, Thailand, Late Holocene (Chitnarin et al., 2023). This study: SUT-KU5-705.

Remarks. A. pellucida Mostafawi, 2003 can be identified by its distinct characteristics, including a thin, flat, and obtuse carapace with a triangular lateral outline. The anterior and posterior margins (AB and PB) are largely rounded, and the highest point is centrally located. The dorsal border is convex on the left valve (LV) and slightly angulated on the right valve (RV), with moderate overlapping of RV on LV all around. The ventral border (VB) is straight on the right valve and concave on the left valve, and numerous normal pores are present. The first occurrence of A. pellucida in Thailand is in Chitnarin et al. (2023), expanding its known distribution beyond the Persian Gulf (Maddocks 1969; Paik 1977; Mostafawi 2003), the western coast of India (Jain 1978), and Holocene deposits of Hong Kong (Wang et al. 2018). The size of the examined specimens is similar to the Holocene specimens found in Hong Kong (Wang et al. 2018), but they are smaller than the extant type material from the Persian Gulf (Mostafawi 2003).

Genus Lankacythere Bhatia and Kumar, 1979

Type species. Lankacythere coralloides (Brady, 1886)

Lankacythere coralloides (Brady, 1886)

Figure 5.6 A-D

Materials. 16 complete valves from Borehole KU1, and four complete valves from Borehole KU4.

Dimensions. H = 0.27-0.43 mm; L = 0.52-0.80 mm; H/L = 0.52-0.60.

Occurrence. Malacca Straits (Whatley and Zhao, 1988); west India (Jain, 1978; Bhatia and Kumar, 1979); southeast India (e.g., Hussain, 1998; Hussain et al., 2004); Sri Lanka (Brady, 1886. Iwatani et al., 2014); Andaman Islands (Hussain et al., 2006); southwest India (e.g., Gopalakrishna et al., 2007; Hussain et al., 2013b); Malaysia (e.g., Noraswana

and Ramlan, 2014; Omar et al., 2017); Persian Gulf (Bate, 1971; Paik, 1977); Gulf of Oman (Paik, 1977; Mostafawi et al., 2010) southwestern coast of Peninsular Thailand, Ao nun, Satun Province, Andaman Sea (Forel, 2021). This study: SUT-KU4-106 to SUT-KU4-109.

Remarks. *L. coralloides* was originally reported by Brady (1886). *Lankacythere* has deep concentric fossae but the posterodorsal ridge, one diagnostic feature of this genus, is not so prominent. This species are common to Jason Bay, south eastern Peninsular Malaysia (Noraswana and Ramlan, 2014). This species was found in Southwestern coast of Peninsular Thailand, Ao Nun, Satun Province, Andaman Sea (Forel 2021).

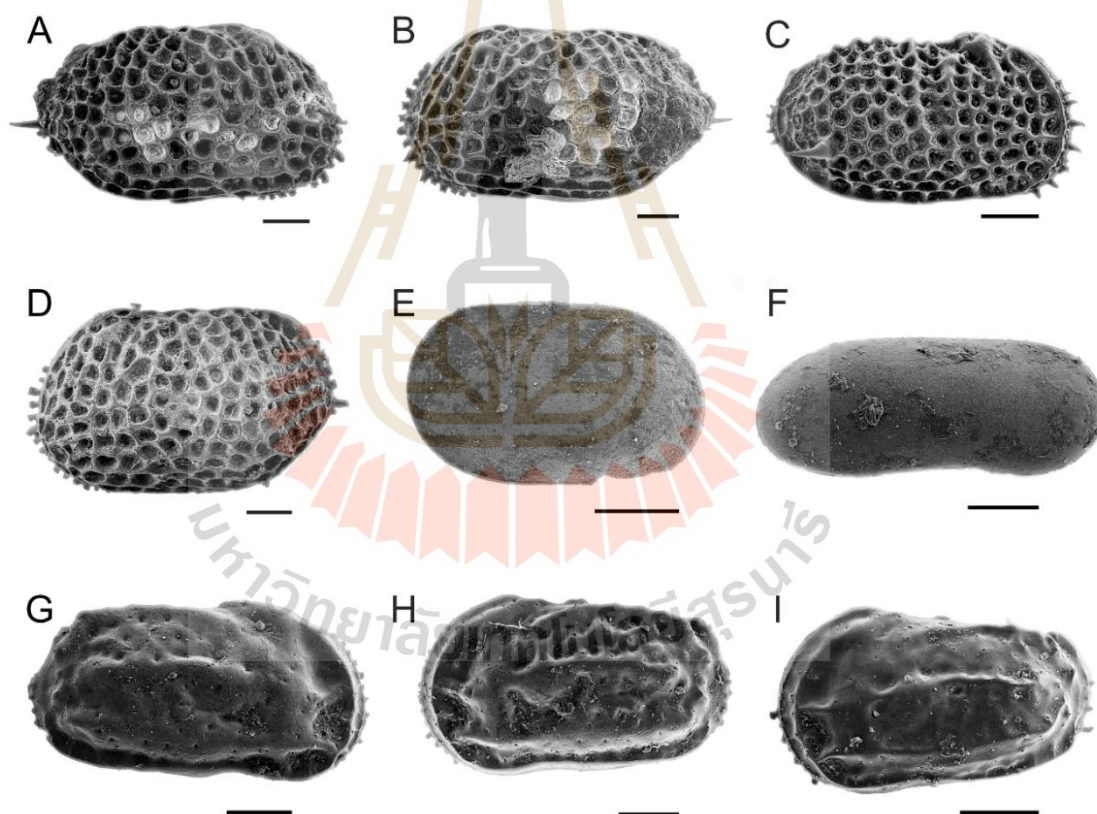


Figure 5.6 Late Holocene ostracods from Samut Sakhon Province: A-D, *Lankacythere coralloides* (Brady, 1886); E, *Cytherella* sp.; F-I, *Stigmatocythere bona* Chen in Hou et al., 1982. See description of the specimen in text. Scale bars are 100 μm

Order PLATYCOPIDA Sars 1866
 Superfamily CYTHERELLOIDEA Sars 1886
 Family CYTHERELLIDAE Sars 1866
 Genus Cytherella Jones 1849

Type species. Cytherella ovata (Roemer, 1841)

Cytherella sp.

Figure 5.6 E

Materials. One complete valve from Borehole KU4, and one complete valve from Borehole KU5.

Dimensions. H = 0.22 mm; L = 0.36 mm; H/L = 0.60.

Occurrence. Java Sea (Brady, 1868a ; Kingma, 1948 ; Fauzielly, 2013 ; Fauzielly et al., 2012, 2013 ; Dewi, 1997, 2000); Celebes Sea (Dewi and Illahude, 2005); Sulu Sea (Noraswana et al., 2014); western India (Jain, 1978); Papua New Guinea (Brady, 1880); Solomon Islands, Pacific Ocean (Titterton et al., 2001 ; Titterton and Whatley, 2006); New Caledonia and Fiji (Brady 1890); Malaysia (e.g., Omar and Noraswana, 2010 ; Ramlan and Noraswana, 2009 ; Omar et al., 2017); Australia (Chapman, 1941 ; Howe and McKenzie, 1989); Torres Straits (Brady, 1880); Andaman and Nicobar Islands (Hussain et al., 2006); southwestern coast of Peninsular Thailand, Ao nun, Satun Province, Andaman Sea (Forel, 2021). Fossil distribution: Lower Miocene of New Zealand (Swanson, 1969); Lower Pliocene of Java (Kingma, 1948); Upper Pliocene? of Timor (Fyan, 1916); Pliocene of Solomon Islands (Hughes, 1977) and Sumatra (LeRoy, 1940; Kingma, 1948); offshore Quaternary marine sediments from Guadalcanal (Williams, 1980). This study: SUT-KU4-110, and SUT-KU5-704.

Remarks. The specimens are distinguished by its thick shelled ovate, usually smooth or punctate carapace. The specimens are similar with Cytherella hemipuncta which has hinge adont, adductor muscle scar pinnate or feather-shaped, aggregate and sexual dimorphism, but with only two specimens with poorly observed of internal valve, so it cannot be identified at specific level.

Genus Stigmatocythere Siddiqui, 1971

Type-species. Stigmatocythere obliqua Siddiqui, 1971 by original designation.

Stigmatocythere bona Chen in Hou et al., 1982

Figure 5.6 F-I

Materials. Four complete valves from Borehole KU1, three complete valves from Borehole KU3, one complete valve from Borehole KU4, one complete carapace and ten complete valves from Borehole KU5, and one complete carapace from Phanom Surin shipwreck site.

Dimensions. H = 0.24 – 0.30 mm; L = 0.42 – 0.58 mm; H/L = 0.52 – 0.58.

Occurrence. Java Sea (Dewi, 1993, 2000); Malacca Straits (Whatley and Zhao, 1988); Vietnam (Tan et al., 2021); Sri Lanka (Iwatani et al., 2014); Mae Klong river mouth, north west Gulf of Thailand (Montenegro et al., 2004); southwestern coast of Peninsular Thailand, Ao nun, Satun Province, Andaman Sea (Forel, 2021); whale-fall excavation site, Chao Phraya delta, Central Thailand (Chitnarin et al., 2023). This study: SUT-KU3-578 to SUT-KU3-580, SUT-KU4-103, and SUT-KU5-693 to SUT-KU5-703 (Borehole KU). SUT-22-P70 (Phanom Surin shipwreck site).

Remarks: Stigmatocythere is characterized by the presence of two ridges springing from the eye tubercle, one to form a high anterior marginal rim, the other curving sharply round to join the subcentral tubercle. Left valve slightly over-reaches right valve in the region of the anterior cardinal angle and at the posterodorsal slope, and hinge structure. In the right valve, the hinge consists of a strongly projecting anterior tooth followed by an anteromedian socket. The distribution of this species has recently been summarized and discussed in Iwatani et al. (2014).

5.2 Distribution of ostracods

5.2.1 Distribution of ostracods along the Borehole KU1

Total number of 191 ostracods were recovered, the distribution provided in Figure 5.7, K. multisulcus was observed at depths ranging from 6.00 to 9.00 meters, with the highest count of 48 individuals observed at 8.00 meters. This species

was not found at depths beyond 9.00 meters. *K. gonia* was observed at depths ranging from 1 to 9.00 meters. The highest count of 9 individuals was observed at 9.00 meters. This species was not found at depths deeper than 9.25 meters.

S. impressa was observed at depths ranging from 8.25 to 10.00 meters and at 13.00 meters. The highest count of 29 individuals was observed at 10.00 meters. *N. rhomboidea* was observed at depths ranging from 4.00 and 7.00 to 8.00 meters. The highest count of 3 individuals was observed at 4.00 and 7.00 meters, and was not found at depths beyond 8.00 meters. *N. iniqua* was observed at depths 6.00 and 10.00 meters. The highest count of 4 individuals was observed at 10.00 meters. *N. mediterranea malayensis* was observed only at a depth of 6.00 meters, with a count of one individual.

S. bona was observed at depths ranging from 9.00 to 10.00 meters. The highest count of 2 individuals was observed at both depths. *N. agilis* was observed at depths of 2.00 and 7.00 meters, with a count of 10 and 1 individuals. *L. coralloides* was observed at depths of 10.00 to 13.00 meters. The highest count of 13 individuals was observed at 10.00 meters. This species was not found at depths beyond 13.00 meters. Number of valve and carapace is shown in Figure 5.8, valve: carapace ratio are high in all species.

5.2.2 Distribution of ostracods along the Borehole KU2

The distribution and abundance of ostracod species at various depths in the Borehole KU2 shows in Figure 5.9, with total number of 698 ostracods were recovered (Figure 5.10). Each species is listed along with the number of individuals observed at each depth increment. *K. multisulcus* did not show any presence or abundance until a depth of 6.25 meters, where four individuals were found. The counts increased gradually at subsequent depths, with the highest count of 55 individuals observed at 8.25 meters. The species persisted until a depth of 14.25 meters, where two individuals were recorded. Similarly, *K. gonia* was not present until a depth of 6.25 meters, where seven individuals were observed. The counts fluctuated at different depths, reaching a peak of 26 individuals at 8.25 meters. After that, the numbers gradually decreased until only one individual was recorded at 13.00 meters.

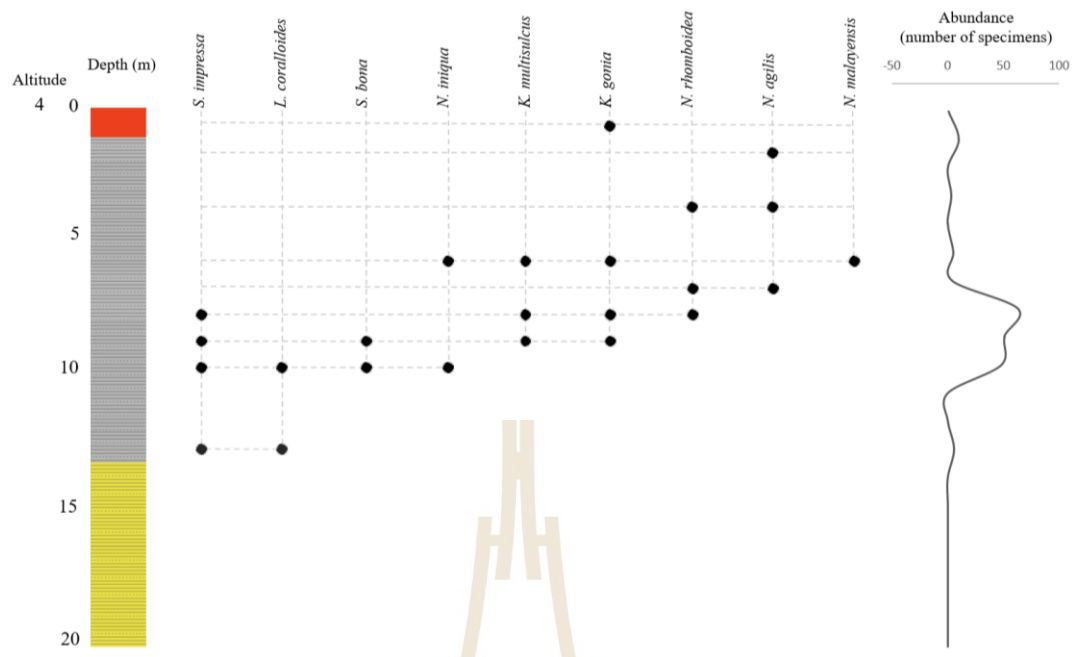


Figure 5.7 Distribution of ostracod species from Borehole KU1

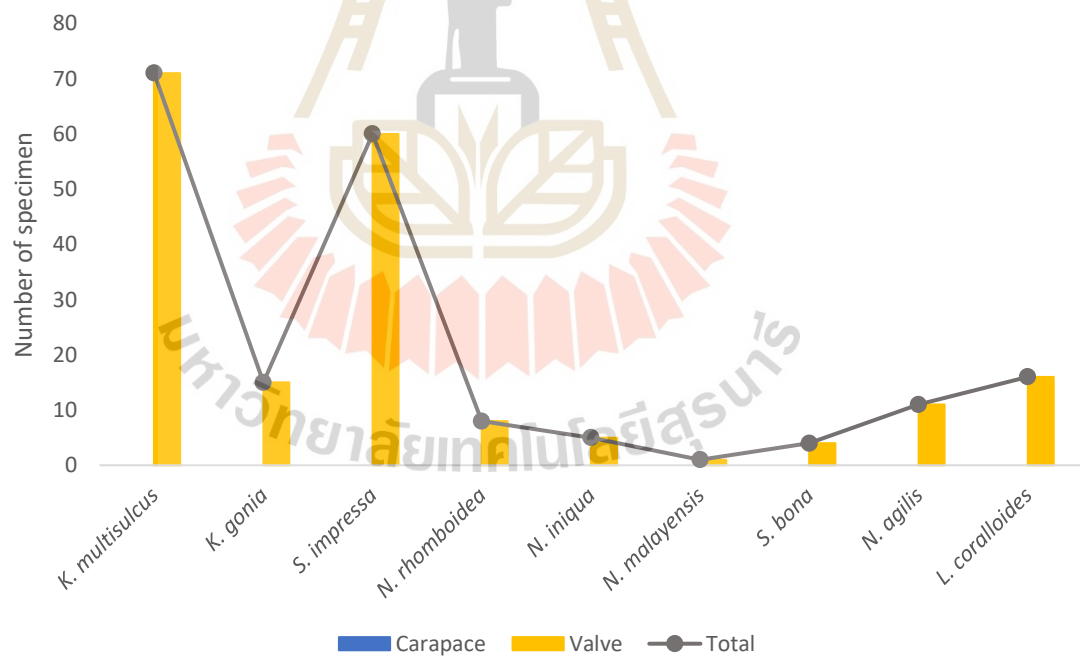


Figure 5.8 Number of valve and carapace of ostracods from Borehole KU1

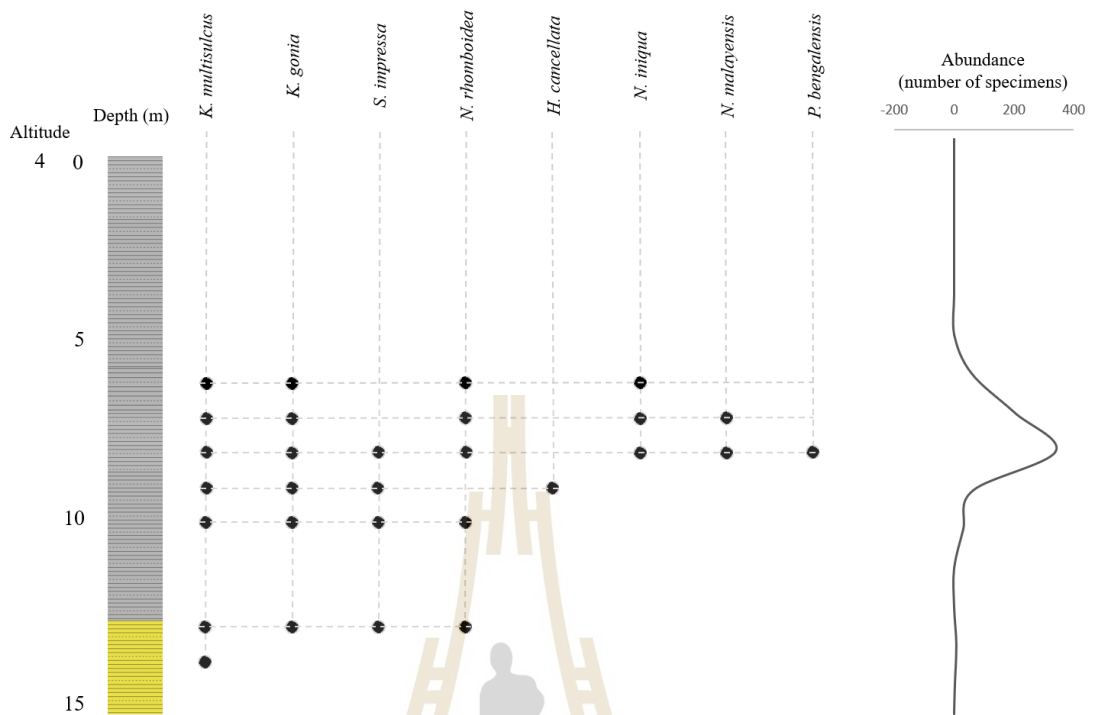


Figure 5.9 Distribution of ostracod species from Borehole KU2

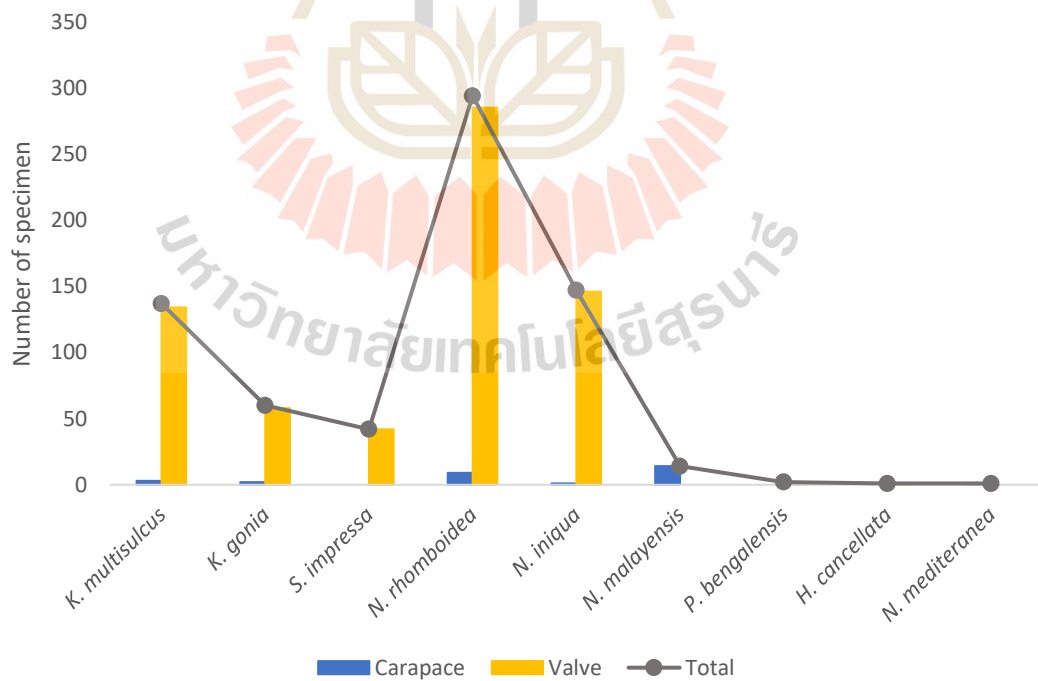


Figure 5.10 Number of valve and carapace of ostracods from Borehole KU2

S. impressa showed a scattered presence starting at a depth of 8.25 meters, with one individual observed. The abundance peaked at a depth of 9.25 meters, where 25 individuals were recorded. Subsequently, the numbers declined, with one individual observed at a depth of 13.00 meters. N. rhomboidea appeared at a depth of 6.25 meters, with 32 individuals observed. The counts increased significantly at 8.25 meters, reaching 173 individuals, the highest count for this species. It was also present at 10.25 meters, with two individuals, and at 13.00 meters, with one individual.

N. iniqua was found starting from a depth of 6.25 meters, with 14 individuals observed. The species persisted until a depth of 8.25 meters, where the highest count of 76 individuals was recorded. After that, no individuals were found at the remaining depths. N. mediterranea malayensis was only observed at two depths, 7.25 and 8.25 meters, with eight and seven individuals, respectively. P. bengalensis was present exclusively at a depth of 8.25 meters, with two individuals. H. cancellata was found at a single depth, 9.25 meters, with one individual recorded. Number of valve and carapace is shown in Figure 5.10.

The abundance of ostracod species varied across different depths in the Borehole KU2. Some species were absent or showed minimal presence at certain depths, while others displayed higher abundances at specific depths. The data provides valuable insights into the distribution patterns of these ostracod species in the borehole.

5.2.3 Distribution of ostracods along the Borehole KU3

Total number of 581 ostracods were recovered, the distribution provided in Figure 5.11, K. multisulcus appeared at 0.25 meters, with three individuals. The counts fluctuated at different depths, reaching a peak of 81 individuals at 8.25 meters. After that, the numbers gradually decreased until 10 individuals were recorded at 10 meters. K. gonia was not present until a depth of 6.25 meters, where 32 individuals were observed. The counts varied at subsequent depths, with the count of 22 individuals at 8.25 meters. The numbers decreased towards the deeper depths, with five individuals recorded at 10 meters.

S. impressa was absent until a depth of 6.25 meters, where nine individuals were observed. The abundance peaked at 10.00 meters, with 25 individuals.

This species showed a preference for the intermediate depths. *N. rhomboidea* was present at multiple depths, with the highest abundance observed at 6.25 meters (116 individuals). The species persisted at various depths, showing varying counts, and was absent at 10 meters. *N. iniqua* appeared starting from a depth of 6.25 meters, with 66 individuals observed. The counts fluctuated at different depths, reaching a peak of 27 individuals at 7.25 meters. After that, the numbers gradually decreased, and only three individuals were found at 10 meters.

P. bengalensis was observed at 5.25 and 6.25 meters, with one individual each. Another species, *S. bona*, was found at a depth of 6.25 meters, with two individuals. A species identified as *N. agilis* was present at 1.25 and 2.25 meters, with 29 and four individuals, respectively. *H. cancellata* was found exclusively at a depth of 9.25 meters, with one individual recorded. Number of valve and carapace is shown in Figure 5.12. The abundance of ostracod species varied across different depths in the Borehole KU3. Some species showed preferences for specific depths, while others had broader distributions. The data provides valuable information about the distribution patterns and relative abundances of these ostracod species within the borehole.

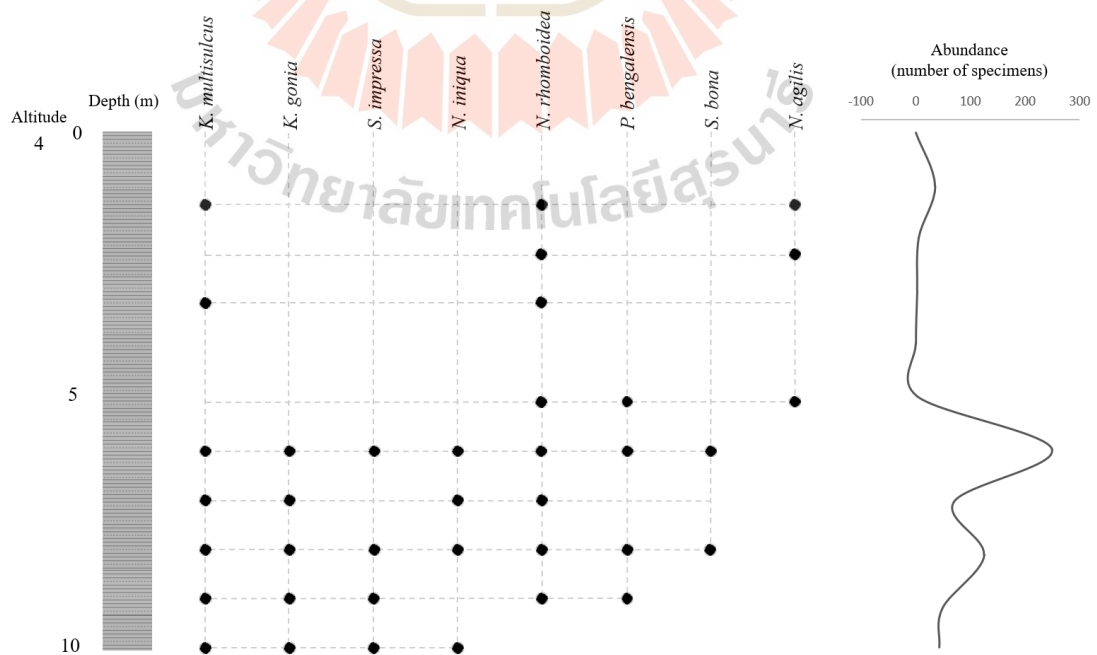


Figure 5.11 Distribution of ostracod species from Borehole KU3

5.2.4 Distribution of ostracods along the Borehole KU4

Total number of 110 ostracods were recovered, the distribution provided in Figure 5.13, *K. multisulcus* had the highest abundance at the shallowest depth of 0.25 meters, with 22 individuals observed. Three and one samples were counted at 2.25 and 3.25 meters, respectively. *K. gonia* was observed at depths ranging from 0.25 to 2.25 meters, with the highest count of 19 individuals at 0.25 meters. After 2.25 meters, this species was not found at any subsequent depths.

S. impressa displayed an abundance pattern where the highest count of 46 individuals was observed at 0.25 meters. This species was present at depths ranging from 0.25 to 3.25 meters and was not found at deeper depths. *N. rhomboidea* had a small abundance of two individuals observed only at 0.25 meters. *S. bona* was observed at 1.25 meters, with a count of one individual.

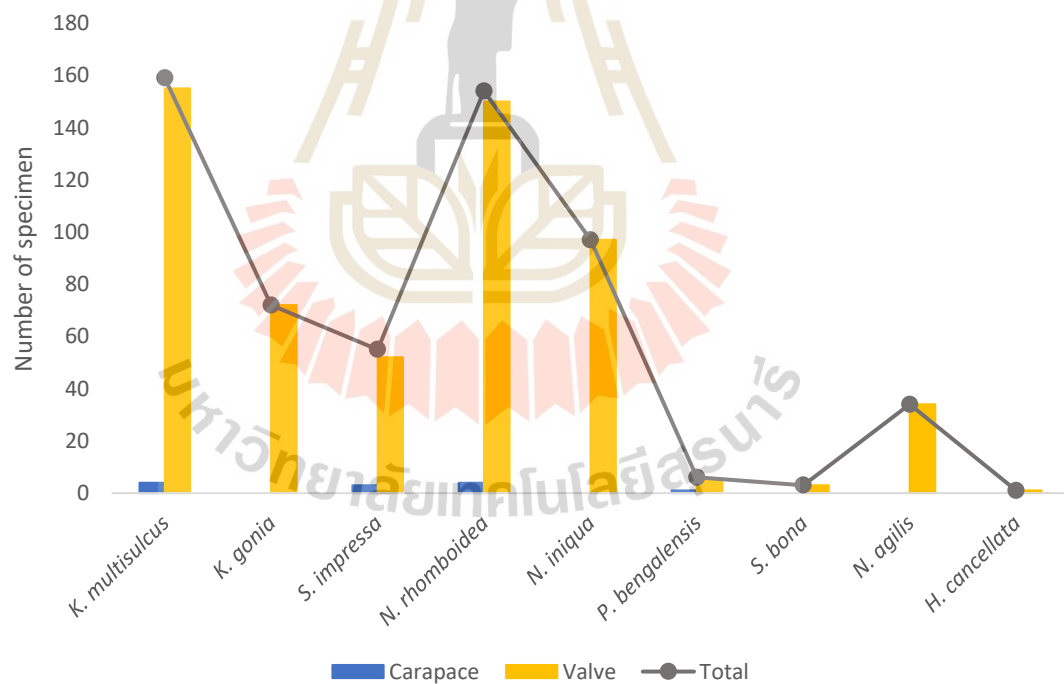


Figure 5.12 Number of valve and carapace of ostracods from Borehole KU3

A single valve of *H. cancellata* was found at 0.25 and at 1.25 meters depth. *L. coralloides* (4 valves) was found at 2.25 meters depth, and *C. hemipuncta* (a single valve) presented at 3.25 meters depth. Number of valve and carapace is shown in

Figure 5.14. The abundance of ostracod species varied across different depths in the borehole. Some species exhibited preferences for specific depths, while others were found only at shallow depths. The result provides insights into the distribution patterns and relative abundances of these ostracod species within the borehole.

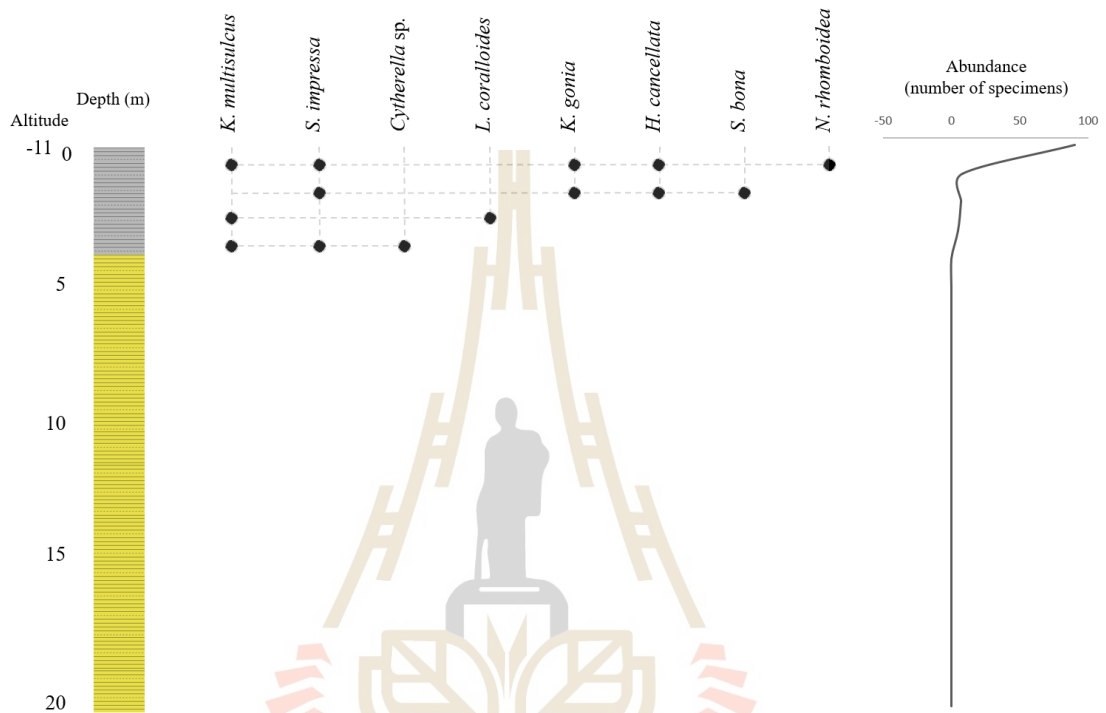


Figure 5.13 Distribution of ostracod species from Borehole KU4

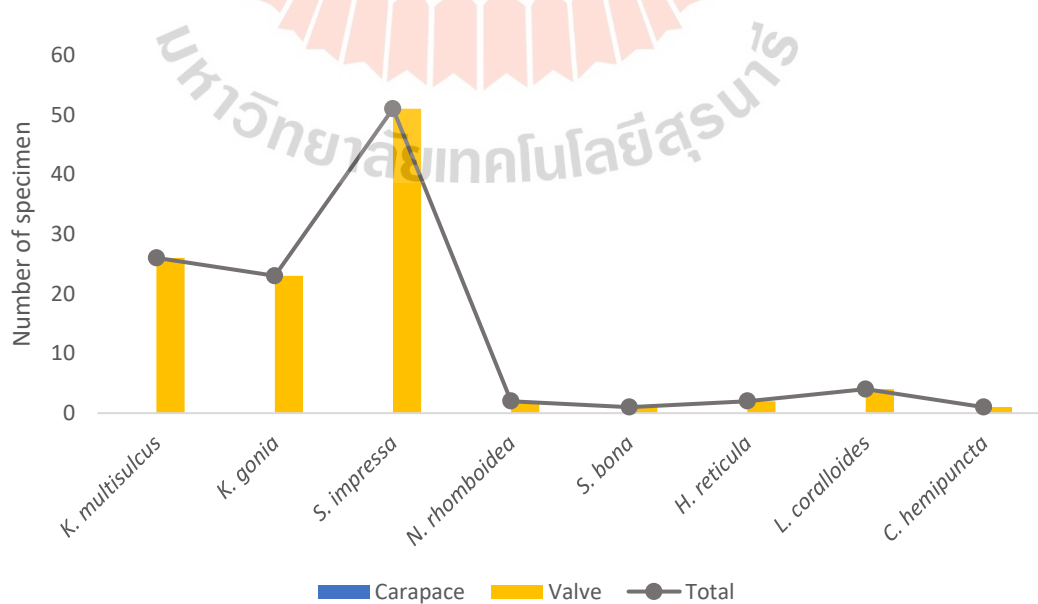


Figure 5.14 Number of valve and carapace of ostracods from Borehole KU4

5.2.5 Distribution of ostracods along the Borehole KU5

Total number of 708 ostracods were recovered, the distribution provided in Figure 5.15, *K. multisulcus* was observed at depths ranging from 8.00 to 28.25 meters, with varying abundances. The highest count of 208 individuals was observed at 13.00 meters. *K. gonia* was observed at depths ranging from 7.00 to 29.25 meters. The highest count of 113 individuals was observed at 13.00 meters. *S. impressa* was observed at depths ranging from 8.00 to 13.00 meters and 27.25 to 29.25 meters. The highest count of 59 individuals was observed at 13.00 meters.

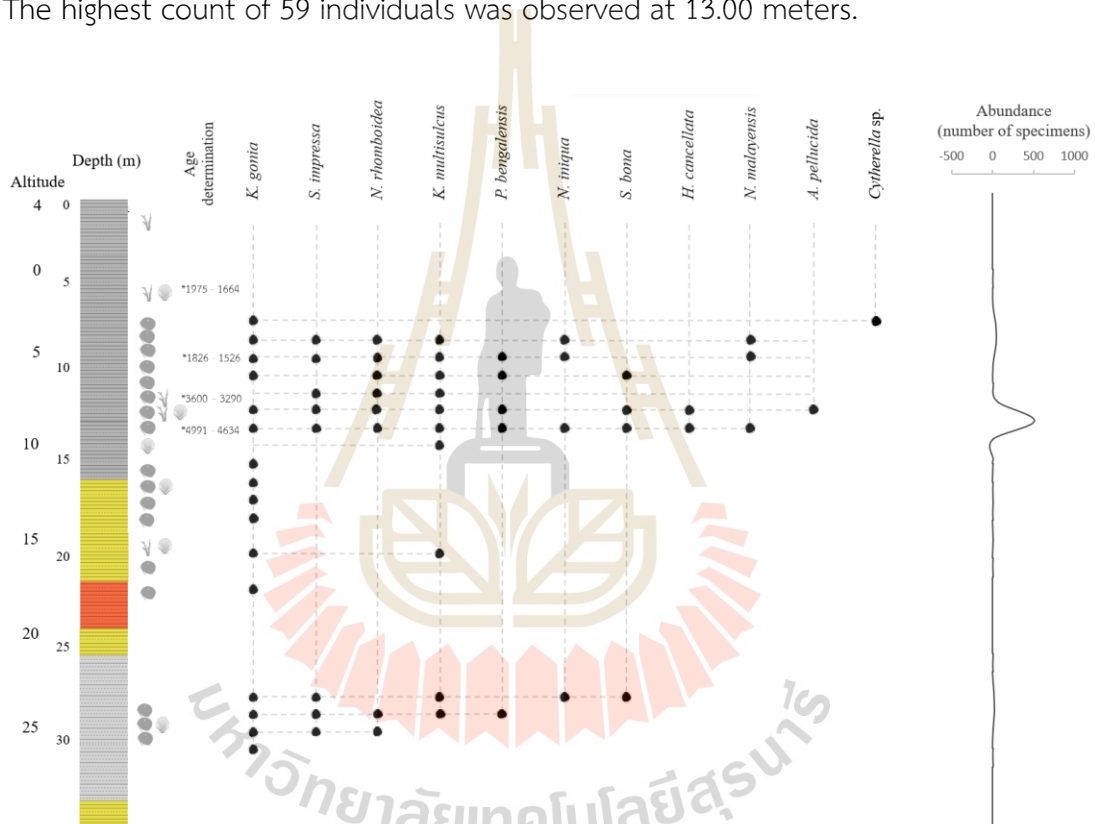


Figure 5.15 Distribution of ostracod species from Borehole KU5

N. rhomboidea was observed at depths ranging from 8.00 to 19.25 meters and 28.25 to 29.25 meters. The highest count of 80 individuals was observed at 13.00 meters. *N. iniqua* was observed at depths from 8.00 to 9.00 meters with each one individual. The highest count of 42 individuals was observed at 13.00 meters and one sample was founded at 27.25 meters. *N. mediterranea malayensis* was observed at depths 8.00 with three. At the depth of 9.00 and 13.00 meters with each one specimen was recovered.

P. bengalensis was observed at depths ranging from 9.00 to 13.00 meters. The highest count of 3 individuals was observed 9.00 and 12.00 meters. One specimen of this species was found at depths 27.25 meters. *S. bona* was observed at depths 10.00, 12.00, 13.00 and 27.25 meters. The highest count of 8 individuals was observed at 13.00 meters. *C. hemipuncta* was observed only at depth 7.00 meters of 1 individual. This species was not found at other depths.

Another species, *A. pellucida*, was found at a depth of 12.00 meters, with a count of 1 individual. *H. cancellata* was observed at depths ranging from 12.00 to 13.00 meters. The highest count of 2 individuals was observed at 13.00 meters. This species was not found at depths beyond 13.00 meters. Number of valve and carapace is shown in Figure 5.16.

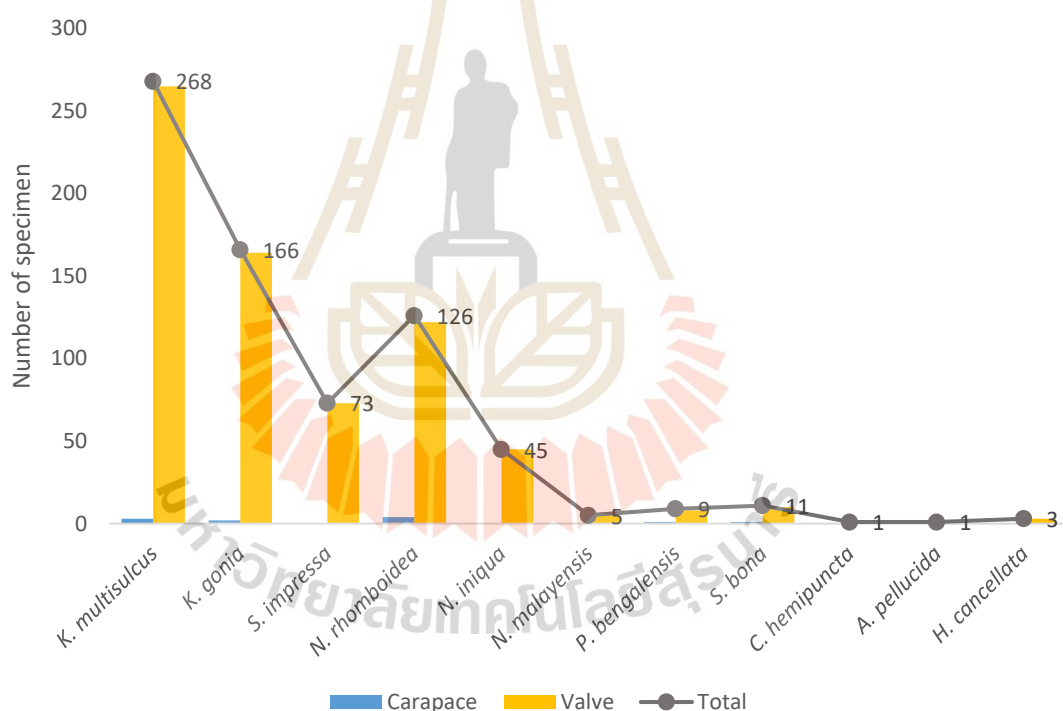


Figure 5.16 Number of valve and carapace of ostracods from Borehole KU5

5.2.6 Distribution of ostracods along the Phanom Surin shipwreck site

Total number of 92 specimens of ostracods were recovered, including 32 carapaces and 60 valves. The occurrence of ostracods shows in Figure 5.17, in the depth range of 20-30 cm (Sample P01), one individual of *N. agilis* and one individual of *K. multsulcus* were observed. Moving to the depth range of 30-40 cm (Sample P02), one individual of *K. gonia* was present.

Similarly, in the depth range of 40-50 cm (Sample P03), one individual of N. mediterranea malayensis was identified. Samples P04 to P06 do not have any recorded occurrences of ostracods. At a depth of 80-90 cm (Sample P07), one individual of N. agilis was observed. Moving further, in the depth range of 190-200 cm (Sample P14), one individual of N. agilis and one individual of H. reticulata were identified. Sample P17 (220-230 cm) displayed relatively higher diversity. It contained three individuals of N. agilis, one individual of K. multisulcus, and one individual of K. gonia. Sample P20 (250-260 cm) had one individual of N. agilis. Sample P21 (260-270 cm) displayed the presence of one individual of N. mediterranea malayensis. Sample P28 (370-380 cm) exhibited two individuals of N. agilis, four individuals of K. gonia, and one individual of H. reticulata.

Sample P29 (380-390 cm) demonstrated a diverse range with five individuals of N. agilis, 15 individuals of K. multisulcus, seven individuals of K. gonia, one individual of N. mediterranea malayensis, and one individual of N. rhomboidea. The occurrences continue to vary across the remaining samples, including species such as S. impressa, H. reticulata, and others.

N. agilis, K. multisulcus, K. gonia, and N. mediterranea malayensis have a wide depth range, they can be found in the shallow depth along the deeper depth. S. impressa was found only one individual valve at the depth of 460–470 cm. Number of valve and carapace is shown in Figure 5.18.

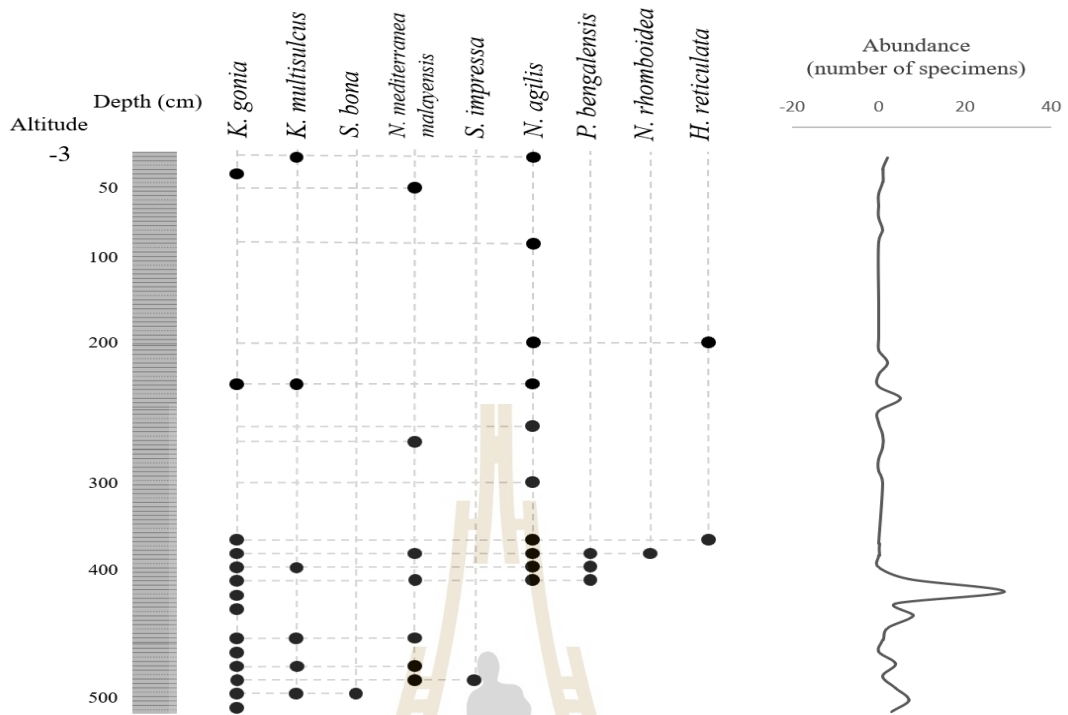


Figure 5.17 Distribution of ostracod from Phanom Surin shipwreck site

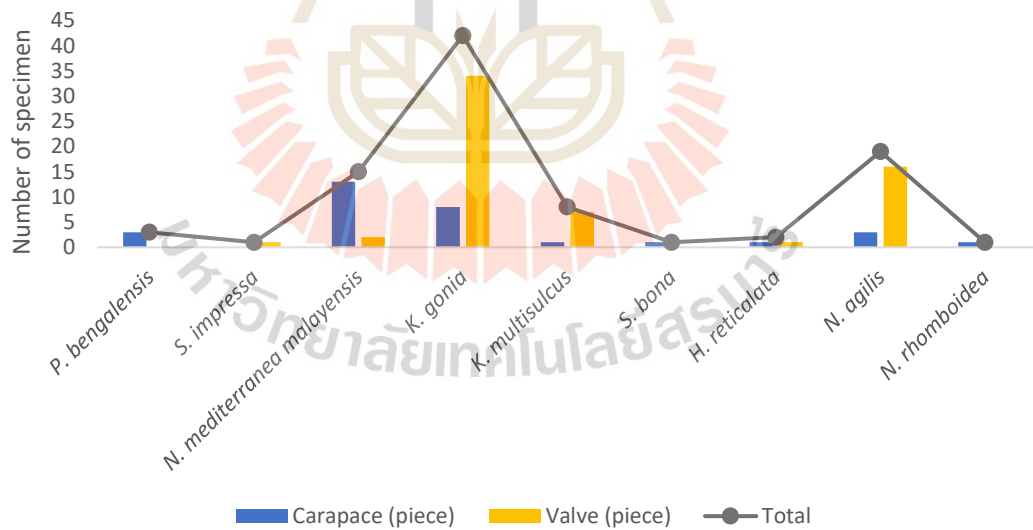


Figure 5.18 Number of valve and carapace of ostracods from Phanom Surin shipwreck site

CHAPTER VI

DISCUSSIONS AND CONCLUSION

This chapter presents discussions and conclusion of the study, focusing on the lithostratigraphy and geochemical analysis of the Late Quaternary sediments from the study area (section 6.1.1), and provides the paleoenvironmental interpretation based on ostracod assemblages (section 6.1.2). Recommendations for future studies are also provided (section 6.2).

6.1 Discussions

6.1.1 Paleoenvironmental interpretation on basis of lithostratigraphy and geochemical analysis

Five lithologic units are interpreted to two sedimentary facies: Facies I (Tidal flat and Tidal channel) consisting of Units 1, 2, and 3; Facies II (Prodelta) coming from Unit 4, in ascending order. The study area is covered by topsoils of the recent floodplain, however the topsoil is found only in Borehole KU1.

As shown in Figure 6.1, a boundary between the two facies lies at 15 meters depth (at the base of Unit 4 in Borehole KU5), and the age determination at the base of Unit 4 is approximately 4,991 years BP (see section 4.1). Thus, the sediments of Facies II should represent deposition during Late Holocene. Each facies is characterized by lithology, and geochemical data as described below:

1) **Facies I:** Tidal flat and tidal channel

Units 1, 2, and 3 are categorized to Facies I which is distinguished by fine- to coarse-grained sediment and having low salinity level (Figure 6.2) and lacking minerals typically associated with marine environments, such as aragonite and halite.

Unit 1 (GSCS) consists of light-colored, fine- to coarse-grained sands with pebbles. These characteristics align with the description of channel-bottom deposits in tidal systems (Barwis, 1978; Smith, 1987; James and Dalrymple, 2010).

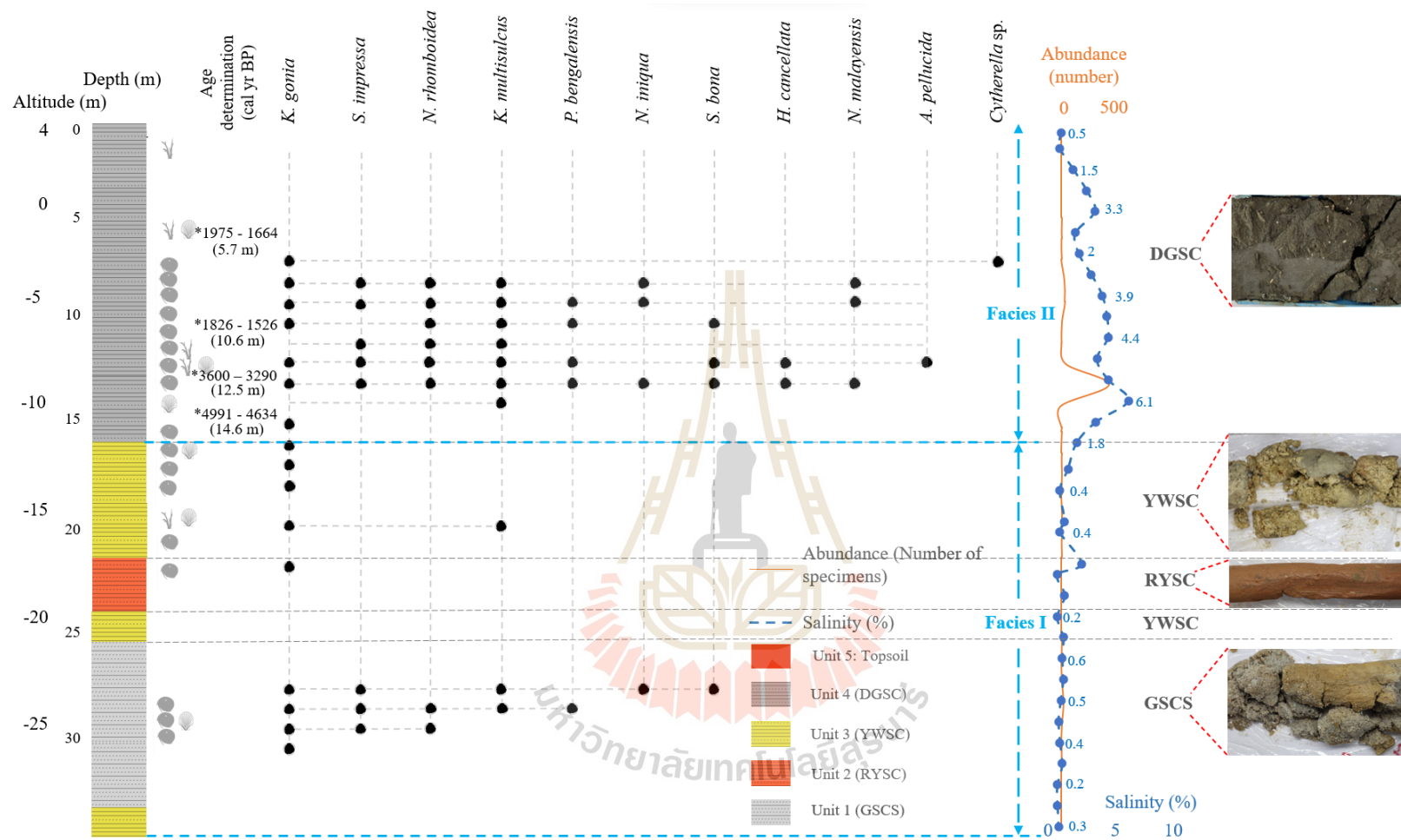


Figure 6.1 Lithostratigraphy, salinity level, and distribution and abundance of ostracods from Borehole KU5

Tidal currents play a significant role in transporting sediments within the tidal channels (Fenies and Faugères, 1998), leading to the presence of coarse-grained sediments in this unit. Besides, certain layers exhibit finer size of quartz, mica, calcareous fragments, and yellowish-brown silts. According to James and Dalrymple (2010), the channel-bottom deposit in the more seaward region may contain a substantial amount of shell debris, and an abundance of mud clasts. Therefore, Unit 1 represents tidal channel deposits of either estuarine or deltaic systems. This unit is found only in Borehole KU5 at the depth of 34.5 to 24.5 meters.

Unit 2 (RYSC) consists of silt, silty clay and less amount of very fine-grained sand. This unit is composed of reddish brown interbedded with yellow stiff silty clay. The lithology of this unit is similar to the overlying Unit 3, but different in color. The reddish color suggests the occurrence of oxidation and laterization processes, which involve the weathering and alteration of minerals (Parton et al., 1995).

Unit 3 (YWSC) contains yellowish white to brown silty clays. The sediments found in Units 2 and 3 correspond to intertidal zone as they typically consist of sandy materials, gradually transitioning into mud which are common in sheltered areas connected to tidal channels (James and Dalrymple, 2010). This type of tidal flat extends seaward, it undergoes a transition from being influenced by river-dominated conditions to marine conditions. Based on the lithology of the sediment, both Units 2 and 3 are identified as intertidal deposits. In Borehole KU2, the age of the shell materials found in Unit 3 ranges from 4,440 – 4,095 cal yr B.P. distinguishing the facies boundary observed in Borehole KU5.

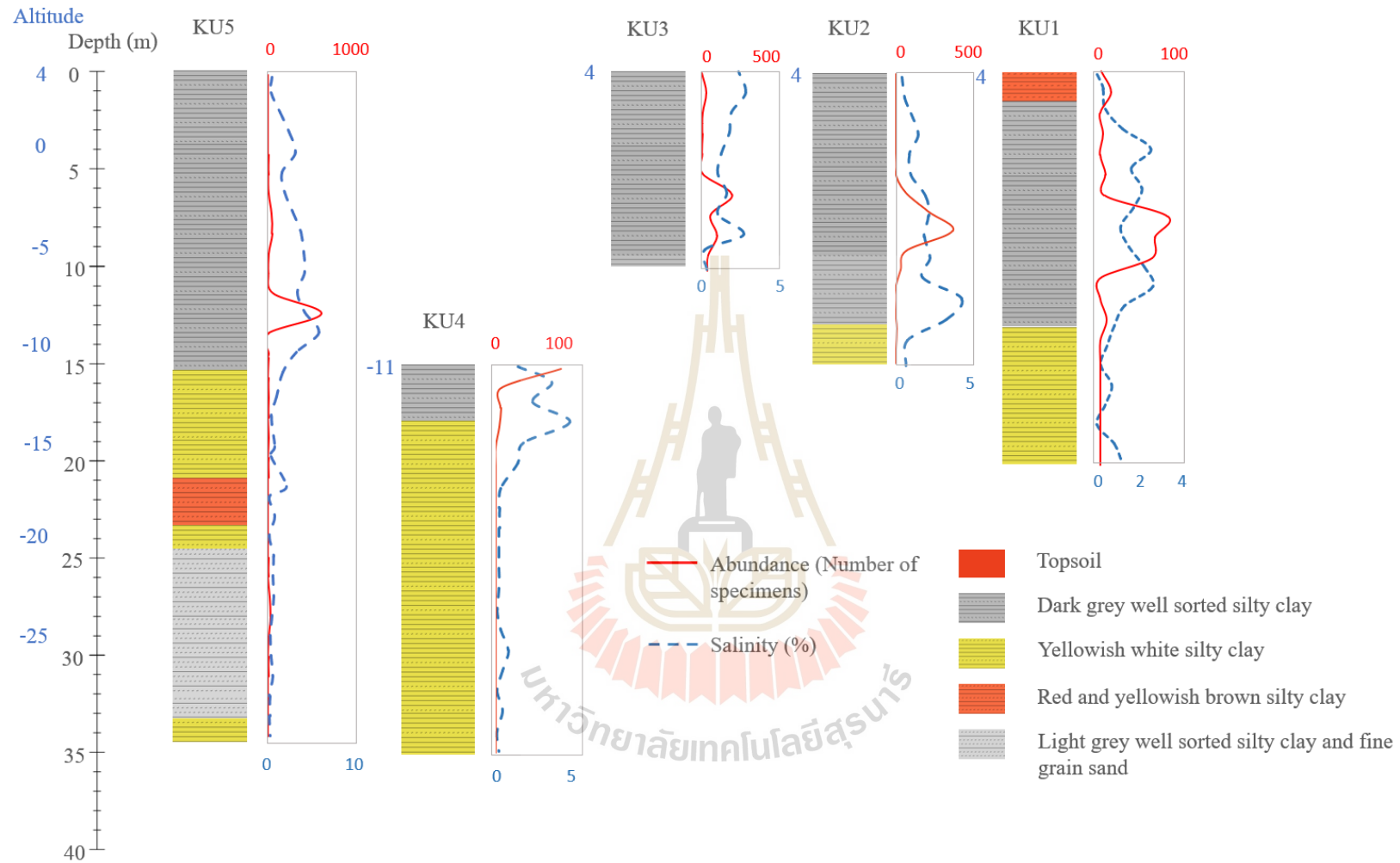


Figure 6.2 Salinity level of the sediments and abundance of ostracods in each borehole

The difference in color between Unit 2 and Unit 3 in the intertidal zone can be influenced by the sea level and the exposure of the sediments to the air. In certain intertidal environments, when the sea level drops during low tide, the sediments are exposed to the air. This exposure can lead to oxidation processes, where iron minerals in the sediments react with oxygen.

2) Facies II: Prodelta

Facies II encompasses Unit 4, which represents the fine-grain sedimentary deposits during the Late Holocene. Facies II exhibits variations in sediment salinity and is characterized by the presence of marine clay minerals (calcite, aragonite, and halite).

Unit 4 (DGSC) is observed in all 6 boreholes. The sedimentary material is predominantly composed of well-sorted calcareous dark grey silty clay, with a lesser proportion of fine-grained sand. Following James and Dalrymple (2010), this unit is interpreted as prodelta muds, which extend towards the sea and gradually transition into fine-grained sediments on the distal basin floor. These sediments often contain calcareous components and may evolve into delta-front facies as they approach the landward direction. The absence of burrowing structures in this study, can be attributed to the high sedimentation rates and fluctuations in salinity in the prodelta region, which may have hindered bioturbation processes (James and Dalrymple, 2010). The sediments of this unit align with the lithostratigraphic description of Unit IIb (Deltaic and shallow marine sediments), subunit 1 (prodelta and seafloor sediments), as documented by Tanabe et al. (2003). Furthermore, the study conducted by Chitnarin et al. (2023) at a whale-fall excavation site reported similar lithostratigraphic units, which correspond to the sediment observed in this unit. These findings suggest that Unit 4 is associated with marine environments. Supporting evidence for the interpretation of shallow marine deposits at whale fall excavation site, conducted by Ketwetsuriya and Dumrongrojwattana (2021), who investigated marine microgastropods. The agreement between this sediment unit, and mentioned studies strengthens the interpretation of Unit 4 as a representative of prodelta (deltaic and shallow marine sediments).

The occurrence of calcite, aragonite, and halite suggests the likelihood of deposition in a marine environment in the past (Schwab, 2003). Aragonite, typically found in corals, is commonly associated with tropical seas, while calcite is more widespread throughout the ocean (Kastner, 1999). These two calcium carbonate minerals, calcite and aragonite, are commonly encountered in the open ocean (Kastner, 1999; Sulpis et al., 2022).

Overlain the Unit 4, though observed only two-meter thick in Borehole KU1 is the topsoil which is classified as the Unit 5 in this study (section 4.1.1). The sediments are characterized by red and yellowish-brown silty clays with a distinctive oxidized silty-clay layer containing the shell fragments. These characteristics indicate the occurrence of laterization and oxidation processes on a land surface subjected to lateritic weathering conditions (Parton et al., 1995).

The interpretation of this study introduces two models, including Model I (Holocene Sequence) and Model II (Pleistocene and Holocene Sequence). According to age determination of Borehole KU5 (Unit 4), suggests the first model of this study. The sediments of Facies I represents deposition during Early Holocene, and Facies II represents Late Holocene sediments.

The second model of this study suggests that the sediment in Facies I represents Pleistocene sediment (below 15.50 meters, Figure 6.1), while Facies II consists of marine clay in the Holocene. Based on DGR (2012), Pleistocene stiff clay can have a considerable thickness of over 20 meters. Within these clay layers, additional layers of medium to dense or very dense sand may interlace. The research conducted by Planchareon (1976), Planchareon and Chuamthaisong (1976), Wongsomsak and Theyapunte (1987), and Sinsakul (2000), indicate that an uppermost layer of stiff clay, located at a depth ranging from approximately 15 to 20 meters, corresponds to the Late Pleistocene Epoch within the Central Plain of Thailand. The low electrical conductivity, and low concentration of chloride ions indicate a freshwater or low-salinity environment. The salinity level documented in this study is consistently low and nearly negligible, which aligns with the conditions typically associated with the Pleistocene period.

Tanabe et al. (2003) identified the Late Pleistocene shallow marine and fluvial deposits (Unit I) in Site 3 core, Pits 1, and Pits 2 (see Figures 2.3 and 2.4), which are characterized by molluscan shells and shelly layers dating from 36,290 to >50,240 yr BP. The sediments distributed between 12.5 and 24.9 meters below MSL. However, it is important to note that in the present study, the absence of age determination in Facies I does not provide conclusive evidence to confirm that the sediment in this facies represents the Pleistocene Epoch.

6.1.2 Palaeoenvironmental interpretation based on ostracod assemblages

Fifteen species of the ostracods belonged to ten genera and seven families are recovered from ninety-nine samples of the Borehole KU1 to Borehole K U 5 . The ostracod genera, include Neocyprideis, Sinocytheridea, Propontocypris, Hemicytheridea, Keijella, Neomonoceratina, Aglaioocypris, Lankacythere, Cytherella, and Stigmatocythere. On the other hand, 92 ostracod specimens are recovered from forty samples from the Phanom Surin shipwreck site, and can be classified to seven genera and nine species. These seven genera include Neocyprideis, Sinocytheridea, Propontocypris, Hemicytheridea, Keijella, Neomonoceratina, and Stigmatocythere. The presence of similar faunal compositions can be observed among the Cenozoic to Recent ostracod assemblages in the Indo-Pacific and South China region, as indicated by previous studies (e.g., Montenegro et al. 2004; Pugliese et al. 2006; Hong et al. 2019; Tanaka et al. 2019; Forel 2021; Tan et al. 2021; Chitnarin et al. 2023). These genera have been found in various locations, such as the Indian Ocean, Persian Gulf, South China Sea, and Thailand. The salinity analysis conducted along the depth of the cores reveal that salinity levels ranging from 1.5% to 4.0% exhibit a relatively high abundance of species and specimens, as depicted in Figure 6.1.

It should be noted that the oldest part of the studied samples belongs to Unit 1, and the Units 2 and 3 are also found only in Borehole KU5. Lithology and salinity levels of these units are unique which can be differentiated clearly from Unit 4. However, ostracods found from Units 1 – 4 are similar to those in the upper part. They consist of K. gonia, S. impressa, N. rhomboidea, K. multisulcus, P. bengalensis, N. iniqua, and S. bona. The presence of a high ratio of valve : carapace in the recovered

specimens indicates the likelihood of transportation prior to deposition (Boomer et al., 2003). Tidal currents, particularly in high-energy zones where tidal waves impact the shelf, have played a role in the transportation process (James and Dalrymple, 2010). This suggests that these faunas may have migrated from shallow marine environments to the tidal channel environment through tidal currents.

Unit 2 and Unit 3 exhibited low salinity levels that were insufficient to support the presence of ostracods, except for K. gonia and K. multisulcus. These two species have the remarkable ability to adapt to a wide range of environmental conditions, allowing them to persist even in salinity-limited environments (Montenegro et al., 2004).

In Unit 4, all ten genera of ostracods were recovered, with high abundance of specimens and species richness observed. The substrate type played a crucial role, as silty clay and clay sediment were conducive to the preservation of ostracod specimens, while sandy and coarse sediment were less favorable (Montenegro et al., 2004). Within the identified species, species like K. multisulcus, K. gonia, S. bona, N. iniqua, N. rhomboidea, N. mediterranea malayensis, P. bengalensis and S. impressa have previously been reported from whale fall excavation site, Samut Sakhon Province, Thailand (Chitnarin et al., 2023). This indicates their persistence and wide distribution in the region.

K. gonia, K. multisulcus, S. impressa, S. bona, and N. iniqua recovered from unit 1 and 4, can be considered opportunistic since they are generalists and adapted to a wide range of environmental conditions (Dodd and Stanton, 1991; Montenegro et al., 2004; Pugliese et al., 2006). K. gonia exhibits the broadest distribution among the species studied, being present throughout the depth range from 1 to 32 meters. This suggests its ability to thrive in diverse environmental conditions.

S. impressa, which has been recovered from Unit 1 and Unit 4, is a good bioindicator of benthic marine ecosystems. It is known to thrive in euryhaline and eurythermal conditions, preferring nutrient-rich mud substrates. Its presence suggests the influence of muddy to fine sandy environments with moderate to high nutrient levels in the study area (Hong et al., 2021a, 2021b; Tan et al., 2021; Chitnarin

et al., 2023). However, the occurrence of separated valves of S. impressa in Facies I (Tidal flat and tidal channel) may involve with tidal process that the specimens were transported by tides from shallow marine environments to tidal channel.

N. agilis which is restricted to Unit 4, (see the distribution in Figures 5.7; 5.11; 5.17), has distributed in Yingli, Haikang County, China, Pliocene (Guan, 1978); Delta of the river Mahakam, Kalimantan, Indonesia (Carbonel, Hoiblan and Moyes, 1985); Mae Khlong river mouth, Thailand (Montenegro et al., 2004); Pantai Kenjeran, Surabaya, Java (Wouters, 2005). According to Keen (1990) and Keen and Racey (1991), genus Neocyprideis has been observed in diverse habitats ranging from low salinity to high salinity environments, and has been observed to develop tubercles in low-salinity environments (Siddiqui, 2000). However, tubercles have not been found among the specimen discussed here, indicating the potential presence of medium to higher salinity conditions in specific layers where N. agilis occurs.

Genus Cytherella, recovered from Unit 4, has been found in Thailand (Montenegro et al. 2004; Pugliese et al., 2006; Yamada et al. 2014; Forel, 2021). Some studies suggest that ostracod fossil assemblages in which cytherellids (especially Cytherella) are the dominant taxa indicate a marine environment (Bergue, 2007). This aligns with the characteristics of Cytherella sp. recovered from Facies II, which is interpreted as the prodelta environment.

S. bona is a marine ostracod species commonly observed in the middle and outer shelf regions of the contemporary East China Sea and South China Sea, inhabiting euryhaline waters (Zhao et al., 1986; Cai, 1988; Wang et al., 1988; Zhao and Wang, 1988; Liu et al., 2002). This species has previously been reported from Recent sediments of Thailand (Montenegro et al. 2004; Pugliese et al., 2006; Forel et al., 2021; Chitnarin et al., 2023). In this study, the presence of S. bona in Facies II corresponds with the lithological analysis, supporting the interpretation of a marine environment.

6.2 Conclusion

Based on the lithostratigraphic and geochemical data analyzed in this study, two sedimentary facies are identified in the study area. Facies I include Units 1 -3;

Unit 1 correspond to Early Holocene to Middle Holocene sediments consisting of sand, silt, clay, and gravel, suggesting tidal channel deposit with low sediment salinity level; Unit 2 exhibits reddish-brown interbedded silty clay, indicating the occurrence of oxidation and laterization processes; Unit 3 characterized by yellowish-white-brown silty clay and shell fragments. The Unit 2 and 3 represent intertidal deposits. Facies II (Unit 4) consists of calcareous dark grey silty clay and fine-grained sand, interpreted as prodelta deposits. The presence of specific minerals, such as calcite, halite, and aragonite further support the interpretation of marine clay in Units 4.

Ostracod assemblages were also clarified, with fifteen species identified across the boreholes. The presence of genera like Neocyprideis, Sinocytheridea, Propontocypris, Hemicytheridea, Keijella, Neomonoceratina, Aglaioocypris, Lankacythere, Cytherella, and Stigmatocythere indicates a common faunal composition in the Indo-Pacific and South China region. The presence of ostracods in Unit 1 suggests transportation by tidal currents from shallow marine environments to the tidal channel. Units 2 and 3 exhibit low salinity levels that limit ostracod presence, except for some adaptable species. In Unit 4, all ten genera of ostracods were recovered, indicating a favorable environment for ostracod preservation. The presence of species found in the study supports the interpretation of a marine environment. The dominance of Cytherella in Unit 4 further suggests a marine prodelta environment. The occurrence of N. agilis and S. bona within specific salinity ranges indicates medium to higher salinity conditions in certain layers. The high ratio of valve : carapace in the recovered specimens suggests that they were shortly transported before being deposited.

The lithostratigraphic, geochemical, and ostracod analyses provide the paleoenvironmental conditions of tide dominated environment in the study area. The identified sedimentary facies, comprises of the upward-fining succession with an interplay of fluvial, tidal, and marine processes in the Holocene Epoch. These can be concluded that the paleoenvironment of this study area might be tidal deposits in Early Holocene and deltaic environment from intertidal to prodelta environment in Middle to Late Holocene.

6.3 Recommendations for future studies

To confirm the conclusion drawn in this study, more research are recommended as follows:

1) This study was carried out in a North – South trend of sampling localities. Therefore, lithologic and paleontological information in East – West direction are missed. It is recommended to further investigation in the East – West trend across the Chao Phraya floodplain.

2) Conduct comparative studies with similar sedimentary environments or regions to validate the findings and interpretations.

3) Investigate long-term palaeoecological trends and their implications for present and future environmental changes.

4) Apply statistical analyses, such as multivariate analysis, and cluster analysis, to identify patterns, correlations, and environmental gradients within the datasets.

5) Combine multiple proxies, such as different types of microfossils, to strengthen the interpretation.

6) Incorporate dating techniques to determine the age of the sediment samples, especially the Units 1 to 3 in order to testify the whole range of the Quaternary deposits.

REFERENCES

- Aiello, G., Barra, D., Parisi, R., Isaia, R., & Marturano, A. (2018). Holocene benthic foraminiferal and ostracod assemblages in a paleo-hydrothermal vent system of Campi Flegrei (Campania, South Italy). *Palaeontologia Electronica*, 21.
- Aiello, G., Barra, D., Parisi, R., Arienzo, M., Donadio, C., Ferrara, L., Toscanesi, M., & Trifuoggi, M. (2021). *Aquatic Ecology*, 55:955–998.
- Ainsworth, N. R. (1985). Upper Jurassic and Lower Cretaceous ostracoda from the Fastnet Basin, Offshore Southwest Ireland. *Irish Journal of Earth Sciences*, 7(1), 15–33.
- Alexseev, M. N., & Takaya, Y. (1967). An outline of the Upper Genozoic deposits in the Chao Phraya Basin, Central Thailand. *Southeast Asian Studies*, 5, 106-124.
- Apostolescu, V. (1956). Contribution à l'étude des ostracodes de l'Eocène inférieur (s.l.) du Bassin de Paris. *Revue de l'Institut Français du Pétrole et Annales des Combustibles Liquides* 11, 1327–1352.
- Ayress, M., Neil, H., Passlow, V., & Swanson, K. (1997). Benthonic ostracods and deep watermasses: Aqualitative comparison of Southwest Pacific, Southern and Atlantic Oceans. *Palaeogeography, Palaeoclimatology, Palaeoecology*, 131:287-302.
- Baird, W. (1850). *The Natural History of the British Entomostraca*. Ray Society, London, p. 364.
- Bergue, C., Coimbra, J., & Cronin, T. (2007). Cytherellid species (Ostracoda) and their significance to the Late Quaternary events in the Santos Basin, Brazil. *Marine Biodiversity*, 37, 5-12.
- Boomer, I., Horne, D., & Slipper, I. (2003). The Use of ostracods in palaeoenvironmental studies, or what can you do with an ostracod shell? *The Paleontological Society Papers*, 9, 153-180.

- Boyd, W. E., Highman, C. F. W., & Thosarat, R. (1996). The Holocene paleogeography of the southeast margin of the Bangkok Plain, Thailand, and its archaeological implications. *Asian Perspectives* 35, 193–207.
- Brady, G. S. (1868b). Contributions to the study of the Entomostraca II. Marine Ostracoda from the Mauritius. *Annals and Magazine of Natural History* 4 (2), 178–184.
- Brenchley, P. J., & Harper, D. A. T. (1998). Palaeoecology: Ecosystems, environments and evolution. *Chapman and Hall*. 402 pp.
- Brown, G. F., Buravas, S., Charaljavanaphet, N., Johnston, W. D., Sresthaputra V., & Taylor, G. (1951). Geologic reconnaissance of the mineral deposits of Thailand, U.S. *Geological Survey Bulletin*, No. 984. 183p.
- Centhonglang, C. (2022). Facies analysis and reservoir characteristics of 2E unit in North Malay Basin, Gulf of Thailand. *Bulletin of Earth Sciences of Thailand*, 14(2), 105–120.
- Chataro, C., Choowong, M., & Phantuwongraj, S. (2022). Initial report on OSL dating from Pailin Beach Ridge Plain, Trat Province, Eastern Gulf of Thailand with special highlight to record of the Holocene Sea Level Change. *Bulletin of Earth Sciences of Thailand*, 14(1), 62-68.
- Chitnarin, A., Forel M., & Tepnarong P. (2023). Holocene ostracods (Crustacea) from whale-fall excavation site from the Chao Phraya delta, Central Thailand. *European Journal of Taxonomy*, 856(1), 120–151.
- Chonglakmani, C., Ingavat, R., Piccoli, G., & Robba, E. (1983). The last marine submersion of the Bangkok area in Thailand. In: *Memorie Di Scienze Gologiche* XXXVI, pp. 343–352.
- Choowong, M. (2002). The geomorphology and assessment of indicators of sea-level changes to study coastal evolution from the Gulf of Thailand. *Proceedings of the Symposium on Geology of Thailand*, pp. 208-220.
- Choowong, M., U., Charoentitirat, Charusiri, P., Daorerk, Songmuang, & Ladachart, R. (2004). Holocene biostratigraphical records in coastal deposit from Sam Roi Yod National Park, Prachuap Khiri Khan, Western Thailand. *Journal of Natural History of Chulalongkorn University*, 4, 1-18.

- Dalrymple, R. W., & Choi, K. (2007). Morphologic and facies trends through the fluvial–marine transition in tide-dominated depositional systems: A schematic framework for environmental and sequence-stratigraphic interpretation. *Earth-Science Reviews*, 81(3), 135-174.
- Debenay, J.P., Bénéteau, É., Zhang, J., Stouff, V., Geslin, E., Redois, F., & Fernandez-Gonzalez, M. (1998). *Ammonia beccarii* and *Ammonia tepida* (Foraminifera): morphofunctional arguments for their distinction. *Marine Micropaleontology*, 34, 235-244.
- Department of Mineral Resources. (2016). การจำแนกเขตเพื่อการจัดการด้านธรณีวิทยา และทรัพยากรธรณี จังหวัดสมุทรสาคร.
- Department of Groundwater Resources. (2012). ศึกษาผลกระทบตอโครงสร้างใต้ดิน เนื่องจากการคืบตัวของแรงดันน้ำในชั้นน้ำบาดาล บริเวณกรุงเทพมหานครและปริมณฑล.
- Derya, P., & Atike, N. (2016). Ostracods of The Mediterranean (The Gulf of Antalya) and The Aegean Sea (Ayvalik and Kuşadası) and Their Biogeographical Distributions. *Bulletin of The Mineral Research and Exploration*, 152:63-83
- Dheeradilok, P. (1992). Quaternary geological formations of Thailand: Their depositional environments, economic significance and tectonics. *Proceedings of National Conference on Geological Resources of Thailand: Potential for future development*, Department of Mineral Resources, Bangkok, 600.
- Dheeradilok, P. (1995). Quaternary coastal morphology and deposition in Thailand. *Quaternary International*, 26, 49-54.
- Dheeradilok, P. (1986). Review of Quaternary geological mapping and research in Thailand. In: Wezel, F.W., Rau, J.L. (Eds.), *Proceeding on developments in Quaternary geological research in east and south east Asia during the last decade*, Bangkok, Thailand, pp. 141-167.
- Dingle, R. Y., & Lord, A. R. (1990). Benthic ostracods and deep water-masses in the Atlantic Ocean. *Palaeogeography, Palaeoclimatology, Palaeoecology*, 80:213-235.

- Dingle, R. V., Lord, A. R., & Boomer, I. D. (1989). Ostracod faunas and water masses across the continental margin off southwestern Africa. *Marine Geology*, 87:323-328.
- Dupuy, C., Rossignol, L., Geslin, E., & Pascal, P. (2010). Predation of mudflat meio-macrofaunal metazoans by a calcareous foraminifer, *Ammonia tepida* (CUSHMAN, 1926). *Journal of Foraminiferal Research*, 40, 305-312.
- Fenies, H., & Faugères, J. C. (1998). Facies and geometry of tidal channel-fill deposits (Arcachon Lagoon, SW France). *Marine Geology*, 150(1), 131-148.
- Forel, M. B. (2021). Recent ostracods (Crustacea) from the southwestern coast of Peninsular Thailand (Satun Province), Andaman Sea Ostracodes (Crustacea) *Revue de Micropaleontologie*, 72, 100526.
- Frenzel, P., & Boomer, I. (2005). The use of ostracods from marginal marine, brackish waters as bioindicators of modern and Quaternary environmental change. *Palaeogeography, Palaeoclimatology, Palaeoecology*, 225(1), 68-92.
- Fyan, E. C. (1916). Eenige-jong Pliocene Ostracoden van Timor. In: *Proceedings of the Section of Sciences*, 24. Koninklijke Nederlandse Akademie van Wetenschappen te Amsterdam, pp. 1175–1186.
- Gebhardt, H., Ćorić, S., Darga, R., Briguglio, A., Schenk, B., Werner, W., & Sames B. (2013). Middle to Late Eocene paleoenvironmental changes in a marine transgressive sequence from the northern Tethyan margin (Adelholzen, Germany). *Australian Journal of Earth Sciences*, 106:45–72.
- Goodbred, S., & Saito, Y. (2011). Tide-Dominated Deltas. In book: *Principles of Tidal Sedimentology*, pp. 129-149.
- Guha, D. (1968). On the Ostracoda from Neogene of Andaman Islands. *Journal of the Geological Society of India* 2, 208–217.
- Haynes, J. R. (1992). Supposed pronounced ecophenotypy in foraminifera. *Journal of Micropalaeontology*, 11, 59 - 63.
- Holmes, J. A., & Chivas, A. R. (2002). The Ostracoda: applications in Quaternary research. Geophysical Monograph Series, 131. American Geophysical Union: Washington DC.

- Horne, D. J., & Siveter, D. J. (2016). Collecting and processing fossil ostracods. *Journal of Crustacean Biology*, 36(6), 841-848.
- Hattori, T. (1969). Mineral composition of clay fractions in some Quaternary deposits in the Chao Phraya Basin, central Thailand. *The Center for Southeast Asian Studies*. Vol.6, No.4. March, pp. 241-246.
- Hattori, T. (1971). The Quaternary Stratigraphy in the Northern Basin of the Central Plain, Thailand. *The Center for Southeast Asian Studies*. Vol.9. No.3, pp. 398-420.
- Iwatani, H., Young, S. M., Irizuki, T., Sampei, Y., & Ishiga, H., (2014). Spatial variations in recent ostracode assemblages and bottom environments in Trincomalee Bay, northeast coast of Sri Lanka. *Micropaleontology* 60 (6), 509–518.
- Jain, S. (1978). Recent Ostracoda from Mandvi Beach, west coast of India. *Bulletin of the Indian geologists Association* 11 (2): 89–139.
- Jain, S. (2020). Fundamentals of Invertebrate Palaeontology. *Springer Geology*.
- James, P. N., & Dalrymple, R. W. (2010). *Facies models 4*. St. John's, Nfld.: Geological Association of Canada.
- Jedrum, S., Thanachit, S., Anusontpornperm, S., & Wiriyakitnatekul, W. (2014). Soil amendments effect on yield and quality of jasmine rice grown on typical natraqualfs, Northeast Thailand. *International Journal of Soil Science* 9 (2): 37-54.
- Jorissen, F. J. (1988). *Benthic foraminifera from the Adriatic Sea: principles of phenotypic variation*. Dept. of Stratigraphy and Paleontology State University of Utrecht.
- Jumprom, P. (2019). Recovery of a lost Arab-styled ship at PhanomSurin, the wetland excavation site in Central Thailand. In: Srisuchat A, Giessler W (Eds.). *Ancient Maritime Cross-cultural Exchanges: Archaeological Research in Thailand*. The Fine Arts Department, Ministry of Culture, Bangkok, pp 227–247.
- Kastner, M. (1999). Oceanic minerals: Their origin, nature of their environment, and significance. *Proceedings of the National Academy of Sciences*, 96(7), 3380-3387.

- Kawira, A. & Saethien, P. (2021). Excavation and taxonomic study on Holocene whale from Am Pang Subdistrict, Ban Peaw District, Samut Sakhon Province. In: Suvapak, I., Apsorn, S., Thawatchai, C., Prachya, B., Siripond, S., Denchak, M., Angsumalin, P., Sakda, K., Veerachat, V., Metha, Y., Prodit, N., Phornpen, C. and Sirirat, P. (eds) *Abstract Book of Geothai Webinar 2021*: 47. Royal Department of Mineral Resources of Thailand, Bangkok.
- Keen, M. C. (1990). The ecology and evolution of the Palaeogene ostracod Neocyprideis. *Cow. Forsch. Inst. Senckenberg*, 123: 217-228.
- Keen, M. C., & Racey, A. (1991). Lower Eocene ostracods from the Rusayl Shale Formation of Oman. *Journal of Micropalaeontology*, 10: 227-233.
- Ketwetsuriya, C., & Dumrongrojwattana, P. (2021). A new microgastropod species, Orbitestella amphaengensis, (Gastropoda: Heterobranchia: Orbitestellidae) from Bangkok clay of Samut Sakorn Province, Thailand. *The Raffles Bulletin of Zoology*, 69, 304-308.
- Kheoruenromne, I., & Suddhiprakarn, A. (1998). Mineralogy and micromorphology of salt affected soils in central plain, Thailand. *Thai Journal of Agricultural Science*, 31(1), 3-20.
- Kheoruenromne, I. (2007). Saline soil in Thailand. Publisher Kasetsart University, Bangkok, 173: 143-167
- Lamb, A. L., Wilson, G. P., & Leng, M. J. (2006). A review of coastal palaeoclimate and relative sea-level reconstructions using $\delta^{13}\text{C}$ and C/N ratios in organic material. *EarthScience Reviews*, 75: 29-57.
- Maddocks, R. (1969). Recent ostracodes of the Family Pontocyprididae chiefly from the Indian Ocean. *Smithsonian Contributions to Zoology* 7: 1-56.
- Maddock, R. (1982). Unification of Income Taxes in Australia. *Australian Journal of Politics & History*, 28(3), 354-366.
- Malz, H., & Ikeya, N. (1986). In: Miocyprideis and Bishopina, related but different Cyprideidine Ostracoda, 20. Reports of the Faculty of Science, Shizuoka University, pp. 175-187.

- Mandur, M. M. M., Hewaidy, A. G. A., Farouk, S., & Agroudy, I. S. E. (2023). An approach to using foraminifera in sequence stratigraphic analysis of Wadi Qena, Central Eastern Desert, Egypt. *Arabian Journal of Geosciences*, 16(3), 190.
- Martens, K. & Horne, D. J. (2009). Ostracoda. In: Likens G.E. (Ed.) *Encyclopedia of Inland Waters*: 405– 414. Elsevier, Oxford.
- Moh, Z., C. (1969). Strength and deformation behavior of Bangkok clay. In: *Proceeding on 7th International Conference on Soil Mechanics Foundation Engineering*, pp. 287-296.
- Montenegro, M., Nevio, P., & Sciuto, F. (2004). Shallow water ostracods near the Mae Khlong river mouth (NW Gulf of Thailand). *Bollettino della Societa Paleontologica Italiana*, 43, 225-234.
- Moore, R. C. (1961). *Treatise on invertebrate paleontology, Part Q, Arthropoda 3*. Geological Society of America and University of Kansas Press, Lawrence and Boulder, p. 442.
- Mostafawi, N. (2003). Recent ostracods from the Persian Gulf. *Senckenbergiana Maritima* 32 (1/2): 51– 75.
- Murray, J. W. (2006). Ecology and applications of benthic foraminifera. *Environmental Science, Geography*. Cambridge University Press, New York, 1-426.
- Negri, M. (2009). An experimental mapping method by means of fossil mollusk faunas: the Holocene Thai paleogulf. *Bollettino della Societa Paleontologica Italiana*, 48, 41-50.
- Nimnate, P., Chutakositkanon, V., Choowong, M., Pailoplee, S., & Phantuwongraj, S. (2015). Evidence of Holocene sea level regression from Chumphon coast of the Gulf of Thailand. *Scienceasia*, 41, 55.
- Noraswana, N. F., & Ramlan, O. (2014). Recent benthic ostracoda of Pahang River Delta, Pahang Darul Makmur. AIP Conference Proceedings. *Proceedings of the Universiti Kebangsaan Malaysia*, Faculty of Science and Technology 2014 Postgraduate Colloquium - Selangor, Malaysia, 610–615.

- Nutalaya, P., & Rau, J. L. (1984). Structural framework of the Chao Phraya Basin, Thailand. *Proceedings of the Symposium on Cenozoic Basins Thailand*. Department of Mineral Resources, Bangkok, 106 - 129.
- Oliver, G. J. H., & Terry, J. P. (2019). Relative sea-level highstands in Thailand since the Mid-Holocene based on ^{14}C rock oyster chronology. *Palaeogeography, Palaeoclimatology, Palaeoecology*, 517, 30-38.
- Omar, R. (2017). Recent benthic ostracoda in offshore sediment of Pulau Perhentian, Terengganu. *Malaysian Applied Biology*, 46 (1), 15-19.
- Paik, K. H. (1977). Regionale Untersuchungen zur Verteilung der Ostracoden im Persischen Golf und im Golf von Oman. "Meteor" Forschungsergebnisse, Reihe C: *Geologie und Geophysik* 23: 37-76.
- Parton, T. R., Humphrays, G. S., & Mitchell, P. B. (1995). *Soils—a New Global View*. UCL Press, London, 213 pp.
- Pirazzoli, A. P. (1991). World Atlas of Holocene Sea level Changes. *Elsevier*, 300 pp.
- Pirazzoli, A. P. (1996). Sea-level change: The last 20,000 years. John Wiley and Sons, 211 pp. pp. 106-129. *Proceeding of the Symposium of Cenozoic Basins*, Chiang Mai University, Thailand, *Quaternary International*, 26, 49-54.
- Planchareon, G. (1976). Ground water and land subsidence in Bangkok, Thailand, *Proceedings of the 2nd International Symposium on Land Subsidence*, Anaheim, California., pp.355-364.
- Pianchareon, C., & Chuamthaisong, C. (1976). Groundwater of Bangkok Metropolis, Thailand, *Proceedings of International Hydrogeology Conference*, Budapest, pp.510-526.
- Puckett, M. (2012). Paleogeographic significance of muscle scars in global populations of Late Cretaceous ostracodes. *Micropaleontology*, 58, 259-271.
- Pugliese, N., Montenegro, M., & Sciuto, F. (2006). Environmental monitoring through the shallow marine ostracods of Phetchaburi area (NW Gulf of Thailand). In. *Proceedings of the Second and Third Italian Meetings on Environmental Micropaleontology*, 11, 85-90.

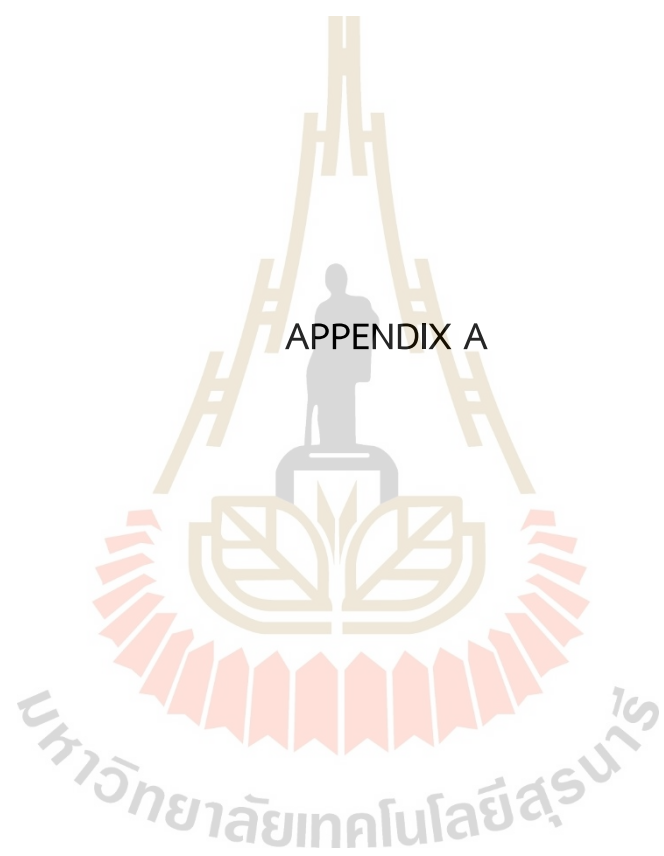
- Reijnenstein, H., Posamentier, H., & Bhattacharya, J. (2011). Seismic geomorphology and high-resolution seismic stratigraphy of inner-shelf fluvial, estuarine, deltaic, and marine sequences, Gulf of Thailand. *AAPG Bulletin*, 95, 1959-1990.
- Robinson, M. K. (1974). The Physical oceanography of the Gulf of Thailand. The University of California Scripps Institution of Oceanography, La Jolla, California, NAGA REPORT. Volume 3. Part, 5-109.
- Rosenfeld, A., & Vesper, B., (1977). The variability of the sieve-pores in recent and fossil species of *Cyprideis torosa* (Jones, 1850) as an indicator for salinity and palaeosalinity. In *Aspects of ecology and zoogeography of Recent and fossil Ostracoda*, Loffler H., Danielopol D. (Eds.): Junk, The Hague; pp, 55–67.
- Ruiz, F., González-Regalado, M. L., Baceta, J. I., & Muñoz, J. M. (2000). Comparative ecological analysis of the ostracod faunas from low-and high-polluted southwestern Spanish estuaries: a multivariate approach. *Marine Micropaleontology*, 40: 345–376.
- Ruiz, F., Abad, M., Bodergat, A. M., Carbonel, P., Rodríguez-Lázaro, J., & Yasuhara, M. (2005). Marine and brackish-water ostracods as sentinels of anthropogenic impacts. *Earth-Science Reviews*, 72: 89–111.
- Saethien, P. (2021). Protection and conservation management of Holocene whale skeleton from Am Pang Subdistrict, Ban Peaw District, Samut Sakhon Province. In: Suvapak, I., Apsorn, S., Thawatchai, C., Prachya, B., Siripond, S., Detchak, M., Angsumalin, P., Sakda, K., Veerachat, V., Metha, Y., Prodit, N., Phornpen, C., & Sirirat, P. (Eds.) Abstract Book of Geothai Webinar 2021: 207. Royal Department of Mineral Resources of Thailand. Bangkok.
- Sars, G. O. (1922-1925). An account of the Crustacea of Norway with short descriptions and figures of all species. Crustacea of Norway: *Cypridinidae*, *Conchoeciidae*, *Polycopidae* (1922) *Polycopidae*, *Cytherellidae*, *Cypridae* (1923) *Cypridae* (1925) *Cypridae*, *Cytheridae* (1925). 9th edition, Bergen, p. 277.

- Savatenalinton, S. (2014). Ostracods (Crustacea: Ostracoda) from the floodplain of the Chi River, Mahasarakham Province, Northeast Thailand, with the first record of male Tanycypris siamensis Savatenalinton and Martens, 2009. *Zootaxa*, 3838(2), 195-206.
- Savatenalinton, S. (2015). On three new species of non-marine ostracods (Crustacea: Ostracoda) from Northeast Thailand. *Zootaxa*, 3914(3), 275-300.
- Savatenalinton, S., & Suttajit, M. (2016). A checklist of Recent non-marine ostracods (Crustacea: Ostracoda) from Thailand, including descriptions of two new species. *Zootaxa*, 4067(1), 1-34.
- Savatenalinton, S. (2017). Species diversity of ostracods (Crustacea: Ostracoda) from rice fields in Northeast Thailand, with the description of a new Tanycypris species. *Zootaxa*, 4362(4), 499-516.
- Savatenalinton, S. (2018). Two new species of Cypretta Vávra, 1895 (Crustacea, Ostracoda) from Thailand and discussion of genus. *Zootaxa*, 4532(4), 483-502.
- Savatenalinton, S. (2022). Redescription of Neocypridella fossulata (Daday, 1910) (Crustacea: Ostracoda) and description of a new subfamily. *Zootaxa*, 5093(1), 83-93.
- Savatenalinton, S. (2023). Songkhramodopsis gen. nov., a new genus of Cypridopsinae (Crustacea: Ostracoda) from Thailand. *Zootaxa*, 5254(1), 51-68.
- Schnitker, D. (1974). Ecotypic variation in Ammonia beccarii (Linne). *Journal of Foraminiferal Research*, 4, 217-223.
- Siddiqui, Q. A. (2000). Some species of the genus Neocyprideis in the early Tertiary of Pakistan. *Journal of Micropalaeontology*, 19(1), 1-7.
- Sinsakul, S. (1992). Evidence of Quaternary sea level changes in the coastal areas of Thailand: a review. *Journal of Southeast Asian Earth Sciences*, 7, 23-37.
- Sinsakul, S. (2000). Late Quaternary geology of the Lower Central Plain, Thailand. *Journal of Asian Earth Sciences*, 18(4), 415-426.
- Sinsakul, S., Chaimanee, N., & Tiyaipairach, S. (2002). Quaternary Geology of Thailand. *Proceedings of the Symposium on Geology of Thailand*, 170-180.

- Shan, Y., Wang, X., Cui, J., Mo, H., & Li, Y. (2021). Effects of clay mineral composition on the dynamic properties and fabric of Artificial Marine Clay. *Journal of Marine Science and Engineering*, 9(11), 1216.
- Somboon, J. R. P. (1988). Paleontology study of the recent marine sediments in the lower central plain, Thailand. *Journal of Southeast Asian Earth Science*, 2, pp.201-210.
- Somboon, J. R. P., & Thiramongkol, N. (1992). Holocene highstand shoreline of the Chao Phraya delta, Thailand. *Journal of Southeast Asian Earth Science*. 7, 53-60. Southeastern Malay Peninsula. *Micropaleontology* 35, 168–187.
- Sulpis, O., Agrawal, P., Wolthers, M., Munhoven, G., Walker, M., & Middelburg, J. J. (2022). Aragonite dissolution protects calcite at the seafloor. *Nature Communications*, 13(1), 1104.
- Surakiatchai, P., Choowong, M., Charusiri, P., Charoentitirat, T., Chawchai, S., Pailoplee, S., Chabangborn, A., Phantuwongraj, S., Chutakositkanon, V., Kongsen, S., Nimnate, P., & Bissen, R. (2018). Paleogeographic Reconstruction and History of the Sea Level Change at Sam Roi Yot National Park, Gulf of Thailand. *Tropical Natural History*, 18(2), 112-134.
- Takata, H., Dettman, D. L., Seto, K., Kurata, K., Hiratsuka, J., & Khim, B. (2009). Novel habitat preference of *Ammonia* “*beccarii*” forma 1 in a macrobenthos community on hard substrates in the Ohashi River, Southwest Japan. *Journal of Foraminiferal Research*, 39, 87-96.
- Takaya, Y. (1972a). Quaternary outcrops in the Central Plain of Thailand. *The Center for Southeast Asian Studies*. Kyoto University, pp. 7-68.
- Takaya, Y. (1972b). Quaternary outcrops of the Southern Part of the Central Plain of Thailand. *The Center for Southeast Asian Studies*. 10, September, pp. 298-320.
- Tanabe, S., Saito, Y., Sato, Y., Suzuki, Y., Sinsakul, S., Tiyaipairach, S., & Chaimanee, N. (2003). Stratigraphy and Holocene evolution of the mud-dominated Chao Phraya delta, Thailand. *Quaternary Science Reviews*, 22, 789-807.

- Titterton, R., Whatley, R. C., & Whittaker, J. E. (2001). A review of some key species of mainly Indo-Pacific Ostracoda from the collections of G.S. Brady. *Journal of Micropalaeontology* 20, 111–142.
- Van de Plassche, O. (1986). Sea-level research: a manual for the collection and evaluation of data. Wezel, F. W., Rau, J. L. (Eds.), *Proceeding on developments in Quaternary geological research in East and South East Asia during the last decade*, Bangkok, Thailand, pp. 141-167.
- Van Morkhoven, F. P. C. M. (1963). Post–Paleozoic Ostracoda, Volume II. Amsterdam: Elsevier Publishing Company, 478 pp.
- Waleed, Y. A. L., Ubide & Saleh, K., Khalaf. (2010). New Species of Ostracoda Genus *Cytherella* Jones, 1849 from the Upper Cretaceous of Hamrin Area North Eastern Iraq. *Journal of Earth Sciences*, 10(2), pp. 25 -34.
- Wang, H., Zhang, H., Cao, M., & Horne, D. (2018). Holocene ostracods from the Hang Hau Formation in Lei Yue Mun, Hong Kong, and their palaeoenvironmental implications. *Alcheringa: An Australasian Journal of Palaeontology* 43(2): 320–333.
- Whatley, R. C., & Zhao, Q. (1987). The recent ostracods of Malacca Straits (Part I). *Revista Española de Micropaleontología* 19(3), 327–366.
- Whatley, R. C., & Zhao, Q. (1988). The recent ostracods of Malacca Straits (Part II). *Revista Española de Micropaleontología* 20(1), 5–37.
- Williams, E. U. (1980). Some Quaternary ostracods from the Solomon Islands. University College of Wales, p. 198.
- Wongsomsak, S., & Theyapunte, S. (1987). Geology of Pak Hai and Lad Lum Kaow map sheet. Ayutthaya province. Geological Survey Report, DMR, Bangkok, pp 115.
- Wouters, K. (2005). On an extant species of the genus *Neocyprideis* Apostolescu from Java (Indonesia) with the description of the appendages (Crustacea, Ostracoda). *Bulletin de l'Institut Royal des Sciences Naturelles de Belgique*, 75, 89-95.

- Yamada, K., Terakura, M., & Tsukawaki, S. (2014). The impact on bottom sediments and ostracods in the Khlong Thom River Mouth following the 2004 Indian Ocean tsunami. *Paleontological Research*, 18(2), 104-117.
- Yasuhara, M., Hunt, G., Breitburg, D., Tsujimoto, A., & Katsuki, K. (2012). Human-induced marine ecological degradation: micropaleontological perspectives. *Ecology and Evolution*, 2: 3242–3268.
- Yasuhara, M., & Seto, K. (2006). Holocene relative sea-level change in Hiroshima Bay, Japan: a semi-quantitative reconstruction based on ostracodes. *Paleontological Research*, 10, 99–116.
- Yasuhara, M., & Yamazaki, H. (2005). The impact of 150 years of anthropogenic pollution on the shallow marine ostracode fauna, Osaka Bay, Japan. *Marine Micropaleontology*, 55, 63–74.
- Yümün, Z. Ü., Meriç, E., Avşar, N., Nazik, A., Barut, İ. F., Yokeş, B., Sagular, E. K., Yıldız, A., Eryilmaz, M., Kam, E., Başsarı, A., Sonuvar, B., Diñer, F., Baykal, K., & Kaya, S. (2016). Meiofauna, microflora and geochemical properties of the late Quaternary (Holocene) core sediments in the Gulf of Izmir (Eastern Aegean Sea, Turkey). *Journal of African Earth Sciences*, 124, 383-408.
- Zhao, Q., & Whatley, R. C. (1989). Recent podocopid ostracods of the Sedili River and Jason Bay, southeastern Malay Peninsula. *Micropaleontology* 35, 168–187.



APPENDIX A

Table A1. Lithology and pictures of core samples from Borehole KU1.

| Sample No. | Core samples | Depth (m) | Sediment |
|------------|---|-----------|---|
| KU1 |  | 0.0 - 0.5 | Grey silty clay with lateritic sediment |
| KU1 |  | 0.5 - 1.0 | Grey silty clay with lateritic sediment |
| KU1 |  | 1.0 - 1.5 | Grey silty clay with lateritic sediment |
| KU1 |  | 1.5 - 2.0 | Dark grey clay, well sorted silty clay |
| KU1 |  | 2.0 - 2.5 | Dark grey clay, well sorted silty clay |
| KU1 |  | 2.5 - 3.0 | Dark grey clay, well sorted silty clay |

Table A1. Lithology and pictures of core samples from Borehole KU1 (continued).

| Sample No. | Core samples | Depth (m) | Sediment |
|------------|---|-----------|--|
| KU1 |  | 3.0 – 3.5 | Dark grey clay, well sorted silty clay |
| KU1 |  | 3.5 – 4.0 | Dark grey clay, well sorted silty clay |
| KU1 |  | 4.0 – 4.5 | Dark grey clay, well sorted silty clay |
| KU1 |  | 4.5 – 5.0 | Dark grey clay, well sorted silty clay |
| KU1 |  | 5.0 – 5.5 | Dark grey clay, well sorted silty clay |
| KU1 |  | 5.5 – 6.0 | Dark grey clay, well sorted silty clay |

Table A1. Lithology and pictures of core samples from Borehole KU1 (continued).

| Sample No. | Core samples | Depth (m) | Sediment |
|------------|---|-----------|--|
| KU1 |  | 6.0 – 6.5 | Dark grey clay, well sorted silty clay |
| KU1 |  | 6.5 – 7.0 | Dark grey clay, well sorted silty clay |
| KU1 |  | 7.0 – 7.5 | Dark grey clay, well sorted silty clay |
| KU1 |  | 7.5 – 8.0 | Dark grey clay, well sorted silty clay |
| KU1 |  | 8.0 – 8.5 | Dark grey clay, well sorted silty clay, and carbonate fragment |
| KU1 |  | 8.5 – 9.0 | Dark grey clay, well sorted silty clay |

Table A1. Lithology and pictures of core samples from Borehole KU1 (continued).

| Sample No. | Core samples | Depth (m) | Sediment |
|------------|---|-------------|--|
| KU1 |  | 9.0 – 9.5 | Dark grey clay, well sorted silty clay |
| KU1 |  | 9.5 – 10.0 | Dark grey clay, well sorted silty clay |
| KU1 |  | 10.0 – 10.5 | Dark grey clay, well sorted silty clay |
| KU1 |  | 10.5 – 11.0 | Dark grey clay, well sorted silty clay |
| KU1 |  | 11.0 – 11.5 | Dark grey clay, well sorted silty clay |
| KU1 |  | 11.5 – 12.0 | Dark grey clay, well sorted silty clay |

Table A1. Lithology and pictures of core samples from Borehole KU1 (continued).

| Sample No. | Core samples | Depth (m) | Sediment |
|------------|---|----------------|--|
| KU1 |  | 12.0 – 12.5 | Dark grey clay, well sorted silty clay |
| KU1 |  | 12.5 – 13.0 | Dark grey clay, well sorted silty clay |
| KU1 |  | 13.0 – 13.5 | Yellowish brown and light grey color of silty clay |
| KU1 |  | 13.5 – 14.0 | Yellowish brown and light grey color of silty clay |
| KU1 |  | 14.0 – 14.5 | Yellowish brown and light grey color of silty clay |
| KU1 |  | 14.5 – 15.0 | Yellowish brown and light grey color of silty clay |

Table A1. Lithology and pictures of core samples from Borehole KU1 (continued).

| Sample No. | Core samples | Depth (m) | Sediment |
|------------|---|------------------|---|
| KU1 |  | 15.00 – 15.50 | Yellowish brown and light grey color of silty clay |
| KU1 |  | 15.75 – 16.00 | Yellowish brown and light grey color of silty clay |
| KU1 |  | 16.00 – 16.50 | Yellowish brown and light grey color of silty clay |
| KU1 |  | 16.75 – 17.00 | Yellowish brown and light grey color of silty clay |
| KU1 |  | 17.00 – 17.50 | Yellowish brown and light grey color of silty clay |
| KU1 |  | 17.75 – 18.00 | Yellowish brown and light grey color of silty clay |

Table A1. Lithology and pictures of core samples from Borehole KU1 (continued).


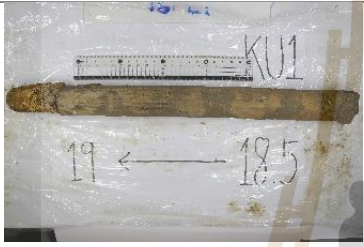
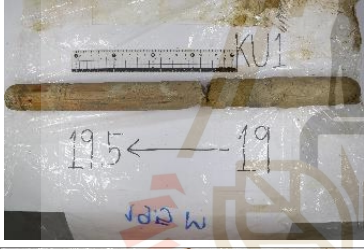

| Sample No. | Core samples | Depth (m) | Sediment |
|------------|---|------------------|--|
| KU1 |  | 18.00 – 18.50 | Yellowish brown and light grey color of silty clay, react with HCl |
| KU1 |  | 18.50 – 19.00 | Yellowish brown and light grey color of silty clay, react with HCl |
| KU1 |  | 19.00 – 19.50 | Yellowish brown and light grey color of silty clay, react with HCl |
| KU1 |  | 19.50 – 20.00 | Light yellowish white and light grey silty clay |

Table A2. Lithology and pictures of core samples from Borehole KU2.

| Sample No. | Core samples | Depth (m) | Sediment |
|------------|---|-----------|---|
| KU2 |  | 0.0 - 0.5 | Dark grey, well sorted clay with light brown silt |
| KU2 |  | 0.5 - 1.0 | Dark grey, well sorted clay with light brown silt |
| KU2 |  | 1.0 - 1.5 | Dark grey, well sorted clay with light brown silt |
| KU2 |  | 1.5 - 2.0 | Calcareous dark grey, well sorted clay |
| KU2 |  | 2.0 - 2.5 | Calcareous dark grey, well sorted clay |
| KU2 |  | 2.5 - 3.0 | Calcareous dark grey, well sorted clay |

Table A2. Lithology and pictures of core samples from Borehole KU2 (continued).

| Sample No. | Core samples | Depth (m) | Sediment |
|------------|---|-----------|--|
| KU2 |  | 3.0 – 3.5 | Calcareous dark grey, well sorted clay |
| KU2 |  | 3.5 – 4.0 | Calcareous dark grey, well sorted clay |
| KU2 |  | 4.0 – 4.5 | Calcareous dark grey, well sorted clay |
| KU2 |  | 4.5 – 5.0 | Calcareous dark grey, well sorted clay |
| KU2 |  | 5.0 – 5.5 | Calcareous dark grey, well sorted clay |
| KU2 |  | 5.5 – 6.0 | Calcareous dark grey, well sorted clay |

Table A2. Lithology and pictures of core samples from Borehole KU2 (continued).

| Sample No. | Core samples | Depth (m) | Sediment |
|------------|---|-----------|--|
| KU2 |  | 6.0 – 6.5 | Calcareous dark grey, well sorted clay |
| KU2 |  | 6.5 – 7.0 | Calcareous dark grey, well sorted clay |
| KU2 |  | 7.0 – 7.5 | Calcareous dark grey, well sorted clay |
| KU2 |  | 7.5 – 8.0 | Calcareous dark grey, well sorted clay |
| KU2 |  | 8.0 – 8.5 | Calcareous dark grey, well sorted clay |
| KU2 |  | 8.5 – 9.0 | Calcareous dark grey, well sorted clay |

Table A2. Lithology and pictures of core samples from Borehole KU2 (continued).

| Sample No. | Core samples | Depth (m) | Sediment |
|------------|---|-------------|--|
| KU2 |  | 9.0 – 9.5 | Calcareous dark grey, well sorted clay |
| KU2 |  | 9.5 – 10.0 | Calcareous dark grey, well sorted clay |
| KU2 |  | 10.0 – 10.5 | Calcareous dark grey, well sorted silty clay |
| KU2 |  | 10.5 – 11.0 | Calcareous dark grey, well sorted silty clay |
| KU2 |  | 11.0 – 11.5 | Calcareous dark grey, well sorted silty clay |
| KU2 |  | 11.5 – 12.0 | Calcareous dark grey, well sorted silty clay |

Table A2. Lithology and pictures of core samples from Borehole KU2 (continued).





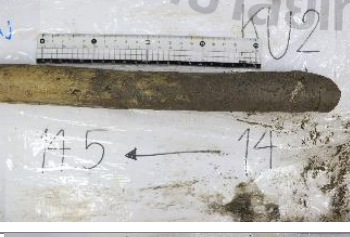

| Sample No. | Core samples | Depth (m) | Sediment |
|------------|---|----------------|--|
| KU2 |  | 12.0 – 12.5 | Calcareous dark grey, well sorted silty clay |
| KU2 |  | 12.5 – 13.0 | Calcareous dark grey, well sorted silty clay |
| KU2 |  | 13.0 – 13.5 | Calcareous dark grey, well sorted silty clay |
| KU2 |  | 13.5 – 14.0 | Calcareous dark grey, well sorted silty clay |
| KU2 |  | 14.0 – 14.5 | Light grey, well sorted clay with brown color of silt |
| KU2 |  | 14.5 – 15.0 | Light grey, well sorted clay with brown color of silt |

Table A3. Lithology and pictures of core samples from Borehole KU3.



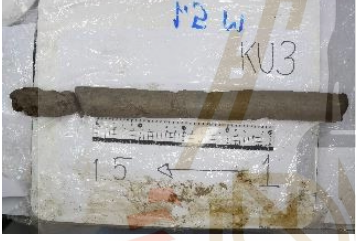


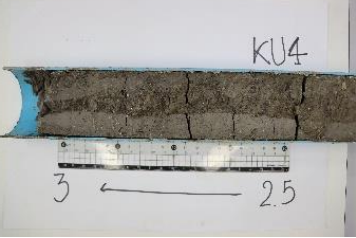
| Sample No. | Core samples | Depth (m) | Sediment |
|------------|---|--------------|--|
| KU3 |  | 0.0 - 0.5 | Light grey, well sorted silty clay with oxidation on the sediment surface |
| KU3 |  | 0.5 - 1.0 | Calcareous light grey, well sorted silty clay with oxidation on the sediment |
| KU3 |  | 1.0 - 1.5 | Calcareous dark grey, well sorted clay |
| KU3 |  | 1.5 - 2.0 | Calcareous dark grey, well sorted clay |
| KU3 |  | 2.0 - 2.5 | Calcareous dark grey, well sorted clay |
| KU3 |  | 2.5 - 3.0 | Calcareous dark grey, well sorted clay |

Table A3. Lithology and pictures of core samples from Borehole KU3 (continued).


| Sample No. | Core samples | Depth (m) | Sediment |
|------------|---|-----------|--|
| KU3 |  | 3.0 – 3.5 | Calcareous dark grey, well sorted clay |
| KU3 |  | 3.5 – 4.0 | Calcareous dark grey, well sorted clay |
| KU3 |  | 4.0 – 4.5 | Calcareous dark grey, well sorted clay |
| KU3 |  | 4.5 – 5.0 | Calcareous dark grey, well sorted clay |
| KU3 |  | 5.0 – 5.5 | Dark grey, well sorted clay |
| KU3 |  | 5.5 – 6.0 | Calcareous dark grey, well sorted clay |

Table A3. Lithology and pictures of core samples from Borehole KU3 (continued).


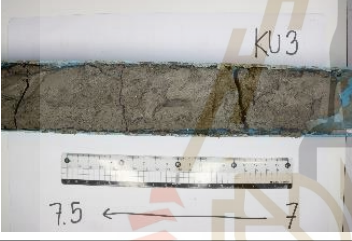
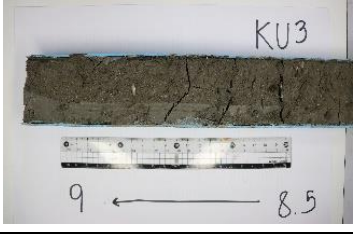
| Sample No. | Core samples | Depth (m) | Sediment |
|------------|---|-----------|--|
| KU3 |  | 6.0 – 6.5 | Calcareous dark grey, well sorted clay |
| KU3 |  | 6.5 – 7.0 | Calcareous dark grey, well sorted clay |
| KU3 |  | 7.0 – 7.5 | Calcareous dark grey, well sorted clay |
| KU3 |  | 7.5 – 8.0 | Calcareous dark grey, well sorted clay |
| KU3 |  | 8.0 – 8.5 | Calcareous dark grey, well sorted clay |
| KU3 |  | 8.5 – 9.0 | Calcareous dark grey, well sorted clay |

Table A3. Lithology and pictures of core samples from Borehole KU3 (continued).

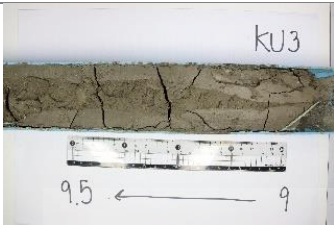
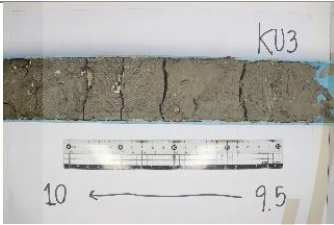
| Sample No. | Core samples | Depth (m) | Sediment |
|------------|---|------------|--|
| KU3 |  | 9.0 – 9.5 | Calcareous dark grey, well sorted clay |
| KU3 |  | 9.5 – 10.0 | Calcareous dark grey, well sorted clay |

Table A4. Lithology and pictures of core samples from Borehole KU4.


| Sample No. | Core samples | Depth (m) | Sediment |
|------------|---|-----------|---|
| KU4 |  | 0.0 - 0.5 | Calcareous sediment with light grey, well sorted silty clay, shell fragment can be observed |
| KU4 |  | 0.5 - 1.0 | Calcareous sediment with light grey, well sorted silty clay, shell fragment can be observed |
| KU4 |  | 1.0 - 1.5 | Calcareous sediment with dark grey, well sorted silty clay, shell fragment can be observed |
| KU4 |  | 1.5 - 2.0 | Calcareous sediment with dark grey, well sorted silty clay, shell fragment can be observed |
| KU4 |  | 2.0 - 2.5 | Calcareous sediment with grey color, well sorted silty clay, shell fragment can be observed |
| KU4 |  | 2.5 - 3.0 | Dark grey silty clay, no reaction with HCl |

Table A4. Lithology and pictures of core samples from Borehole KU4 (continued).

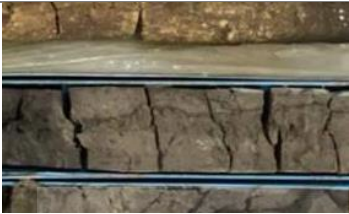





| Sample No. | Core samples | Depth (m) | Sediment |
|------------|---|-----------|--|
| KU4 |  | 3.0 – 3.5 | Calcareous sediment of light grey, well sorted silty clay |
| KU4 |  | 3.5 – 4.0 | Calcareous sediment of yellowish brown and white color of well sorted silty clay |
| KU4 |  | 4.0 – 4.5 | Calcareous sediment of yellowish brown and white color of well sorted silty clay |
| KU4 |  | 4.5 – 5.0 | Calcareous sediment of yellowish brown and white color of well sorted silty clay |
| KU4 |  | 5.0 – 5.5 | Calcareous sediment of light brown and white color of clayey silt with CaCO ₃ fragments |
| KU4 |  | 5.5 – 6.0 | Calcareous sediment of light brown and white color of clayey silt with CaCO ₃ fragments |

Table A4. Lithology and pictures of core samples from Borehole KU4 (continued).







| Sample No. | Core samples | Depth (m) | Sediment |
|------------|---|-----------|---|
| KU4 |  | 6.0 – 6.5 | Light grey, well sorted clay with yellowish brown silt |
| KU4 |  | 6.5 – 7.0 | Light grey, well sorted clay with yellowish brown silt |
| KU4 |  | 7.0 – 7.5 | Calcareous sediment of light grey, well sorted clay with yellowish brown silt |
| KU4 |  | 7.5 – 8.0 | Grey clay and white silt sediment with brown color of oxidation on the sediment surface |
| KU4 |  | 8.0 – 8.5 | Light grey clayey silt |
| KU4 |  | 8.5 – 9.0 | Grey clay and white silt sediment |

Table A4. Lithology and pictures of core samples from Borehole KU4 (continued).



| Sample No. | Core samples | Depth (m) | Sediment |
|------------|---|-------------|---|
| KU4 |  | 9.0 – 9.5 | Light grey, well sorted clay with yellowish brown silt |
| KU4 |  | 9.5 – 10.0 | Light grey, well sorted clay with yellowish brown silt |
| KU4 |  | 10.0 – 10.5 | Light grey, well sorted clayey silt |
| KU4 |  | 10.5 – 11.0 | Light grey clay with yellowish brown silt |
| KU4 |  | 11.0 – 11.5 | Calcareous light grey clay with yellowish brown silt |
| KU4 |  | 11.5 – 12.0 | Light grey clay with yellowish brown silt, with CaCO ₃ fragments |

Table A4. Lithology and pictures of core samples from Borehole KU4 (continued).



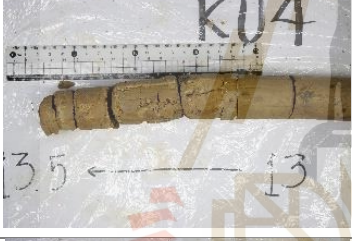



| Sample No. | Core samples | Depth (m) | Sediment |
|------------|---|----------------|---|
| KU4 |  | 12.0 – 12.5 | Dark grey, well sorted clay with yellowish brown silt |
| KU4 |  | 12.5 – 13.0 | Light grey silty clay with brown color of oxidation on the sediment surface |
| KU4 |  | 13.0 – 13.5 | Calcareous sediment of light grey, well sorted silty clay |
| KU4 |  | 13.5 – 14.0 | Calcareous sediment of light grey, well sorted silty clay |
| KU4 |  | 14.0 – 14.5 | Calcareous sediment of light grey, well sorted silty clay |
| KU4 |  | 14.5 – 15.0 | Grey clay with calcareous yellowish-brown silt |

Table A4. Lithology and pictures of core samples from Borehole KU4 (continued).


| Sample No. | Core samples | Depth (m) | Sediment |
|------------|---|----------------|--|
| KU4 |  | 15.0 – 15.5 | Grey clay with calcareous yellowish-brown silt |
| KU4 |  | 15.5 – 16.0 | Grey clay with calcareous yellowish-brown silt |
| KU4 |  | 16.0 – 16.5 | Grey clay with calcareous yellowish-brown silt |
| KU4 |  | 16.5 – 17.0 | Grey clay with calcareous yellowish-brown silt |
| KU4 |  | 17.0 – 17.5 | Grey clay with calcareous yellowish-brown silt |
| KU4 |  | 17.5 – 18.0 | Light brown and white color of clayey silt, with CaCO ₃ fragments |

Table A4. Lithology and pictures of core samples from Borehole KU4 (continued).





| Sample No. | Core samples | Depth (m) | Sediment |
|------------|---|----------------|---|
| KU4 |  | 18.0 – 18.5 | Light brown and white color of clayey silt |
| KU4 |  | 18.5 – 19.0 | Light grey silty clay with brown color of silt |
| KU4 |  | 19.0 – 19.5 | Calcareous light grey silty clay with brown color of silt |
| KU4 |  | 19.5 – 20.0 | Light brown and light grey color of silty clay |

Table A5. Lithology and pictures of core samples from Borehole KU5.




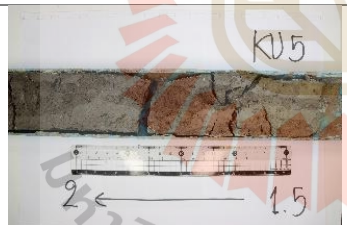

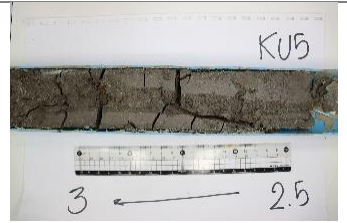
| Sample No. | Core samples | Depth (m) | Sediment |
|------------|---|-----------|---|
| KU5 |  | 0.0 - 0.5 | Dark grey, well sorted clay with yellowish brown silt |
| KU5 |  | 0.5 - 1.0 | Light grey silty clay with brown color of oxidation on the sediment surface |
| KU5 |  | 1.0 - 1.5 | Dark grey, well sorted clay |
| KU5 |  | 1.5 - 2.0 | Dark grey clay with brown color of oxidation on the sediment surface |
| KU5 |  | 2.0 - 2.5 | Dark grey clay with brown color of oxidation on the sediment surface |
| KU5 |  | 2.5 - 3.0 | Dark grey clay with brown color of oxidation on the sediment surface |

Table A5. Lithology and pictures of core samples from Borehole KU5 (continued).

| Sample No. | Core samples | Depth (m) | Sediment |
|------------|---|-----------|--|
| KU5 |  | 3.0 – 3.5 | Dark grey clay with brown color of oxidation on the sediment surface |
| KU5 |  | 3.5 – 4.0 | Dark grey clay with brown color of oxidation on the sediment surface |
| KU5 |  | 4.0 – 4.5 | Dark grey clay with brown color of oxidation on the sediment surface |
| KU5 |  | 4.5 – 5.0 | Dark grey clay with brown color of oxidation on the sediment surface |
| KU5 |  | 5.0 – 5.5 | Calcareous fragment rich, dark grey silty clay |
| KU5 |  | 5.5 – 6.0 | Calcareous fragment rich, dark grey silty clay |

Table A5. Lithology and pictures of core samples from Borehole KU5 (continued).

| Sample No. | Core samples | Depth (m) | Sediment |
|------------|---|-----------|--|
| KU5 |  | 6.0 – 6.5 | Calcareous fragment, dark grey silty clay |
| KU5 |  | 6.5 – 7.0 | Dark grey clay with brown color of oxidation on the sediment surface |
| KU5 |  | 7.0 – 7.5 | Dark grey, well sorted clay |
| KU5 |  | 7.5 – 8.0 | Dark grey, well sorted clay |
| KU5 |  | 8.0 – 8.5 | Dark grey, well sorted clay |
| KU5 |  | 8.5 – 9.0 | Dark grey, well sorted clay |

Table A5. Lithology and pictures of core samples from Borehole KU5 (continued).

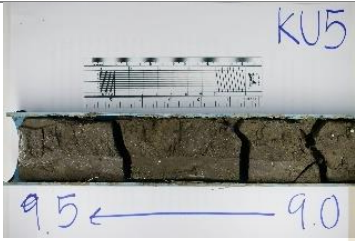

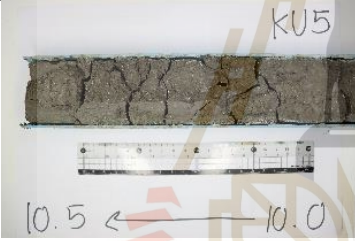



| Sample No. | Core samples | Depth (m) | Sediment |
|------------|---|-------------|--|
| KU5 |  | 9.0 – 9.5 | Calcareous fragment rich, dark grey silty clay |
| KU5 |  | 9.5 – 10.0 | Calcareous fragment, dark grey silty clay |
| KU5 |  | 10.0 – 10.5 | Calcareous fragment, dark grey silty clay |
| KU5 |  | 10.5 – 11.0 | Calcareous fragment, dark grey silty clay |
| KU5 |  | 11.0 – 11.5 | Calcareous fragment, dark grey silty clay |
| KU5 |  | 11.5 – 12.0 | Dark grey, well sorted clay |

Table A5. Lithology and pictures of core samples from Borehole KU5 (continued).

| Sample No. | Core samples | Depth (m) | Sediment |
|------------|---|----------------|--|
| KU5 |  | 12.0 – 12.5 | Dark grey, well sorted clay |
| KU5 |  | 12.5 – 13.0 | Calcareous fragment rich, dark grey silty clay |
| KU5 |  | 13.0 – 13.5 | Calcareous fragment, dark grey silty clay |
| KU5 |  | 13.5 – 14.0 | Calcareous fragment, dark grey silty clay |
| KU5 |  | 14.0 – 14.5 | Calcareous sediment with light grey silt to fine grain sand, no shell fragment can be observed |
| KU5 |  | 14.5 – 15.0 | Dark grey silty clay |

Table A5. Lithology and pictures of core samples from Borehole KU5 (continued).

| Sample No. | Core samples | Depth (m) | Sediment |
|------------|---|------------------|--|
| KU5 |  | 15.00 – 15.50 | Calcareous fragment light grey silt to fine grain sand |
| KU5 |  | 15.75 – 16.00 | Calcareous fragment light grey silt to fine grain sand |
| KU5 |  | 16.00 – 16.50 | Calcareous sediment with yellowish white and light grey clay and silt |
| KU5 |  | 16.75 – 17.00 | Calcareous fragment light grey silty clay with zone of oxidation on the surface |
| KU5 |  | 17.00 – 17.50 | Yellowish white and light grey clay and silt |
| KU5 |  | 17.75 – 18.00 | Calcareous light yellowish white silty clay, yellowish red color with no reaction of HCl |

Table A5. Lithology and pictures of core samples from Borehole KU5 (continued).







| Sample No. | Core samples | Depth (m) | Sediment |
|------------|---|------------------|--|
| KU5 |  | 18.00 – 18.50 | Light yellowish white silty clay |
| KU5 |  | 18.75 – 19.00 | Calcareous light yellowish white silty clay, yellowish red color with no reaction of HCl |
| KU5 |  | 19.00 – 19.50 | Calcareous fragment rich, light yellowish white and light grey silty clay |
| KU5 |  | 19.75 – 20.00 | Light yellowish white and light grey silty clay |
| KU5 |  | 20.00 – 20.50 | Light yellowish white silty clay |
| KU5 |  | 20.75 – 21.00 | Light yellowish white and light grey silty clay |

Table A5. Lithology and pictures of core samples from Borehole KU5 (continued).



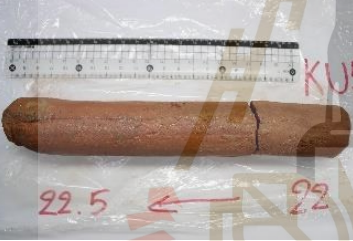



| Sample No. | Core samples | Depth (m) | Sediment |
|------------|---|------------------|---|
| KU5 |  | 21.00 – 21.50 | Red and yellowish-brown silty clay |
| KU5 |  | 21.75 – 22.00 | Yellowish-brown, red and white silt, clay and fine grain sand |
| KU5 |  | 22.00 – 22.50 | Yellowish-brown, red and white silt and clay |
| KU5 |  | 22.75 – 23.00 | Yellowish-brown, red and white silt, clay and fine grain sand |
| KU5 |  | 23.00 – 23.50 | Yellowish-brown, red and white silt, clay and fine grain sand |
| KU5 |  | 23.75 – 24.00 | Greyish brown, red and white silt, clay and fine grain sand |

Table A5. Lithology and pictures of core samples from Borehole KU5 (continued).







| Sample No. | Core samples | Depth (m) | Sediment |
|------------|---|------------------|---|
| KU5 |  | 24.00 – 24.50 | Light color of fine to medium grain sand with quartz and mica |
| KU5 |  | 24.75 – 25.00 | Light color of fine to medium grain sand with quartz and mica |
| KU5 |  | 25.00 – 25.50 | Light color of medium to coarse grain sand with pebble |
| KU5 |  | 25.75 – 26.00 | Light color of medium to coarse grain sand with pebble |
| KU5 |  | 26.00 – 26.50 | Calcareous fragment, light grey coarse grain sand |
| KU5 |  | 26.75 – 27.00 | Light grey coarse grain sand |

Table A5. Lithology and pictures of core samples from Borehole KU5 (continued).



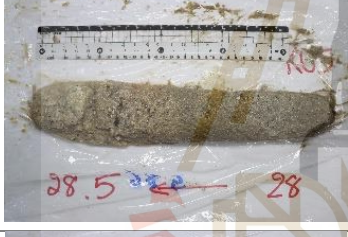






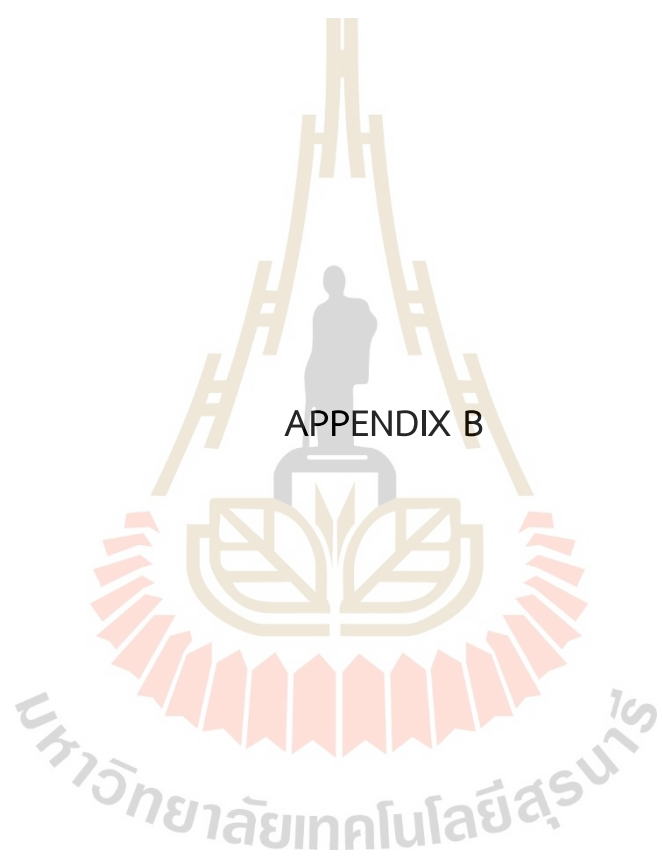
| Sample No. | Core samples | Depth (m) | Sediment |
|------------|---|------------------|---|
| KU5 |  | 27.00 – 27.50 | Light color silt and fine to medium grain sand |
| KU5 |  | 27.75 – 28.00 | Light color silt and fine, medium to coarse grain sand |
| KU5 |  | 28.00 – 28.50 | Calcareous fragment rich, light color silt and fine to medium grain sand |
| KU5 |  | 28.75 – 29.00 | Light grey with yellowish brown silt and fine to medium grain sand with mica |
| KU5 |  | 29.00 – 29.50 | Calcareous fragment, light grey with yellowish brown silt and fine to medium grain sand with mica |
| KU5 |  | 29.75 – 30.00 | Light grey with yellowish brown silt and fine to medium grain sand with mica |

Table A5. Lithology and pictures of core samples from Borehole KU5 (continued).

| Sample No. | Core samples | Depth (m) | Sediment |
|------------|---|------------------|---|
| KU5 |  | 30.00 – 30.50 | Yellowish brown clay and silt |
| KU5 |  | 30.75 – 31.00 | Yellowish brown clay and silt |
| KU5 |  | 31.00 – 31.50 | Yellowish brown clay and silt |
| KU5 |  | 31.75 – 32.00 | Calcareous fragment light yellowish brown color clay and silt |
| KU5 |  | 32.00 – 32.50 | Yellowish white color silt and fine grain sand |
| KU5 |  | 32.75 – 33.00 | Yellowish white color silt and fine grain sand |

Table A5. Lithology and pictures of core samples from Borehole KU5 (continued).

| Sample No. | Core samples | Depth (m) | Sediment |
|------------|---|------------------|---|
| KU5 |  | 33.00 – 33.50 | Calcareous fragment dark grey clayey silt |
| KU5 |  | 33.75 – 34.00 | Yellowish brown clay with red silty clay |
| KU5 |  | 34.00 – 34.50 | Calcareous fragment greenish grey silty clay |



APPENDIX B

(Coupled TwoTheta/Theta)

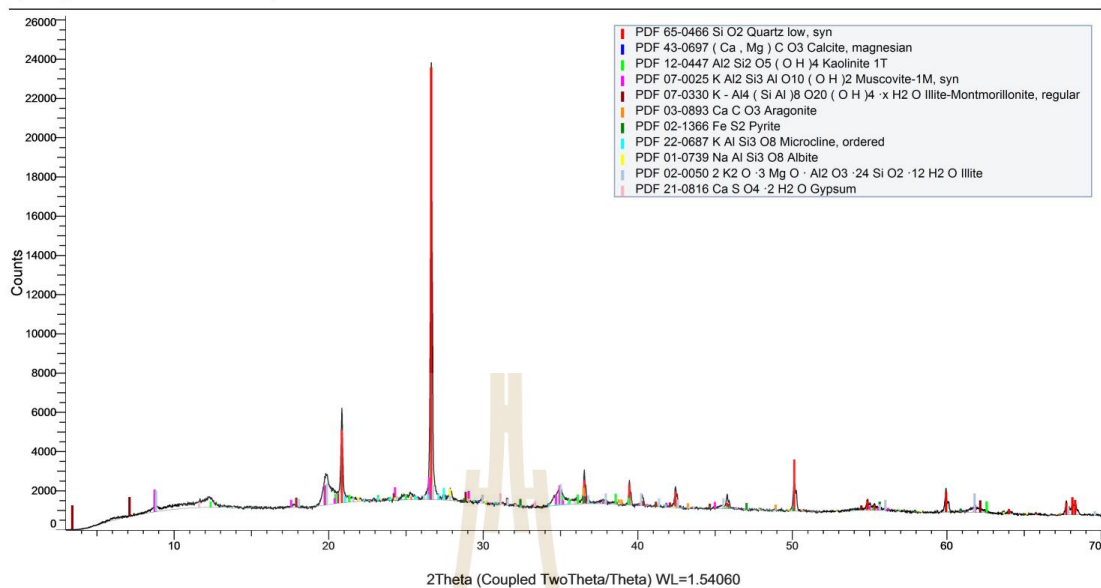


Figure B1. X-ray Diffractogram of sediment at 2.25-meter depth (Borehole KU1)

(Coupled TwoTheta/Theta)

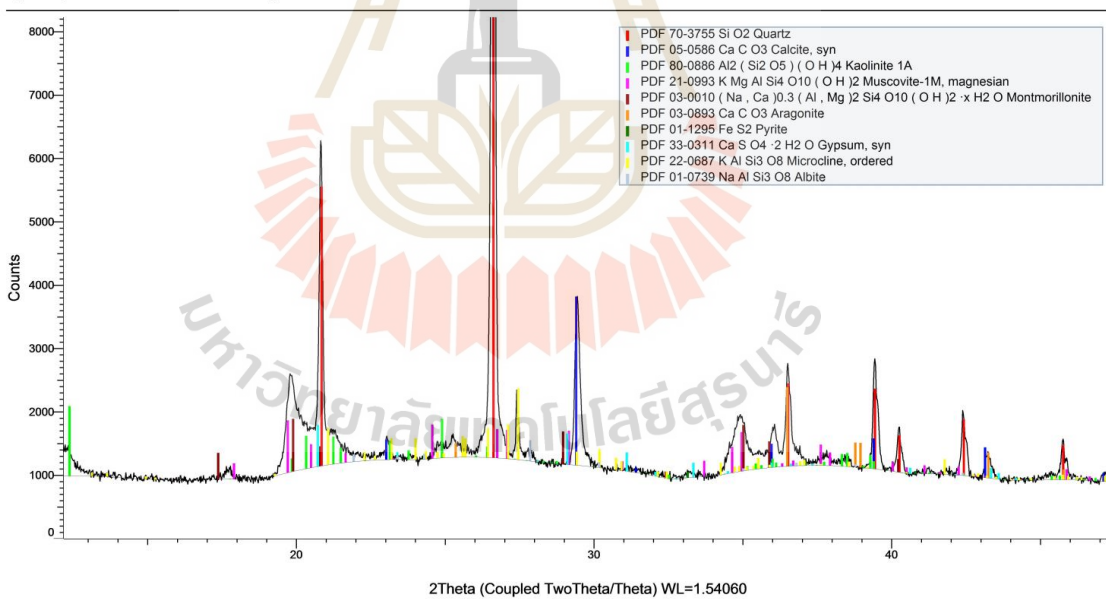


Figure B2. X-ray Diffractogram of sediment at 18.75-meter depth (Borehole KU1)

(Coupled TwoTheta/Theta)

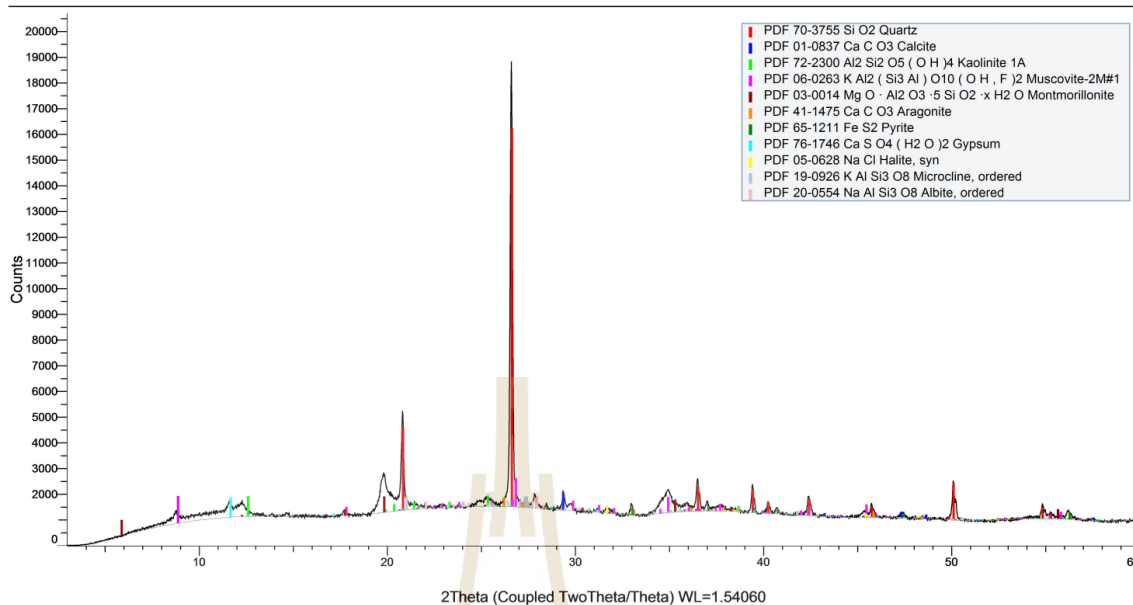


Figure B3. X-ray Diffractogram of sediment at 8.25-meter depth (Borehole KU2)

(Coupled TwoTheta/Theta)

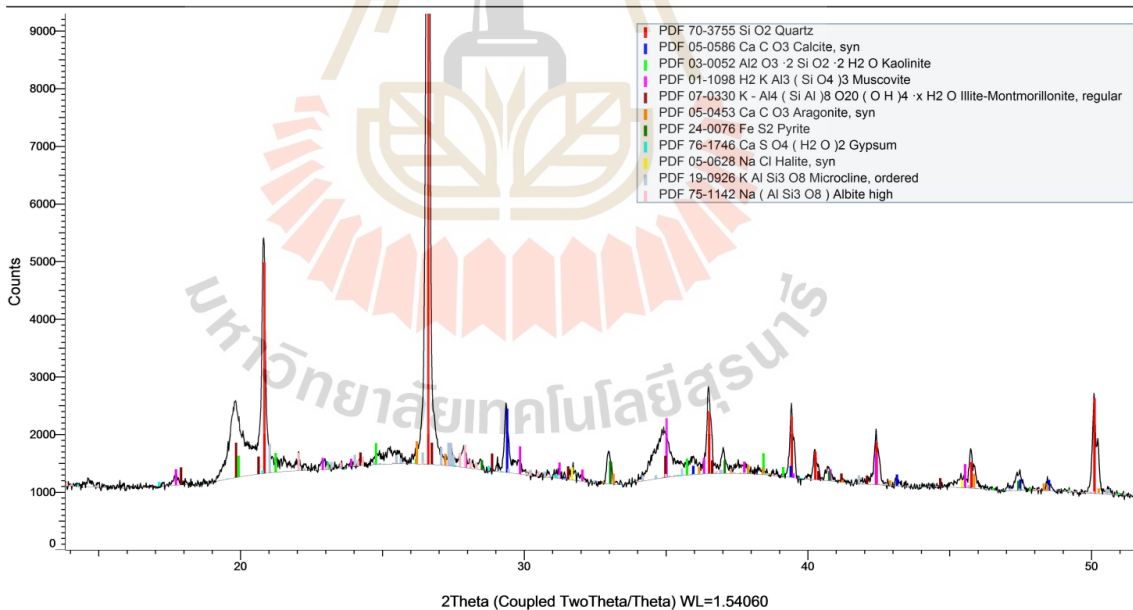


Figure B4. X-ray Diffractogram of sediment at 6.25-meter depth (Borehole KU3)

(Coupled TwoTheta/Theta)

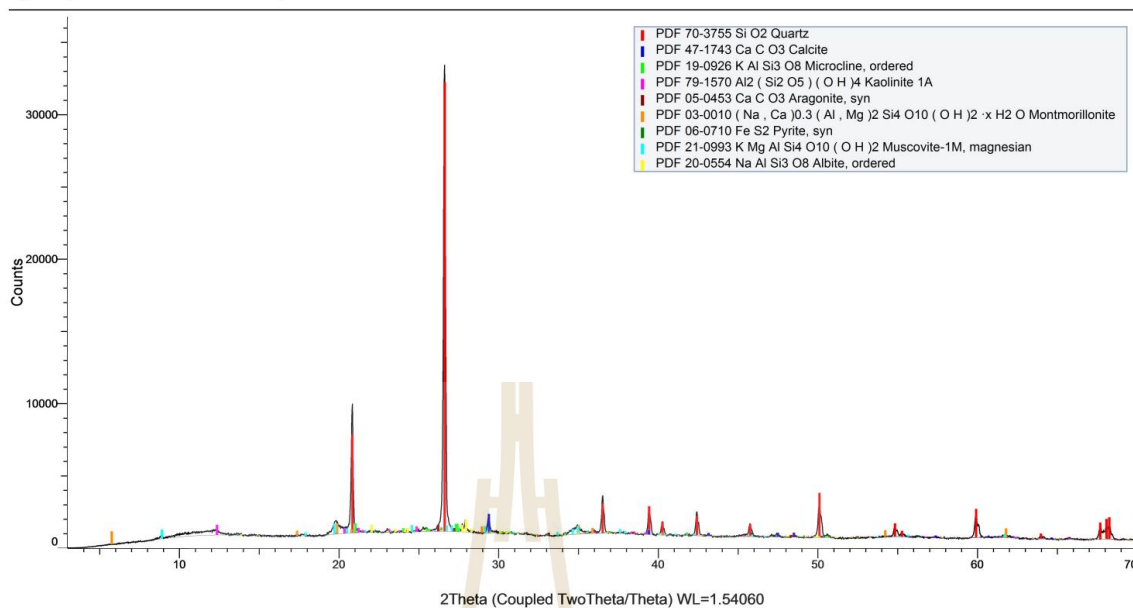


Figure B5. X-ray Diffractogram of sediment at 1.00-meter depth (Borehole KU4)

(Coupled TwoTheta/Theta)

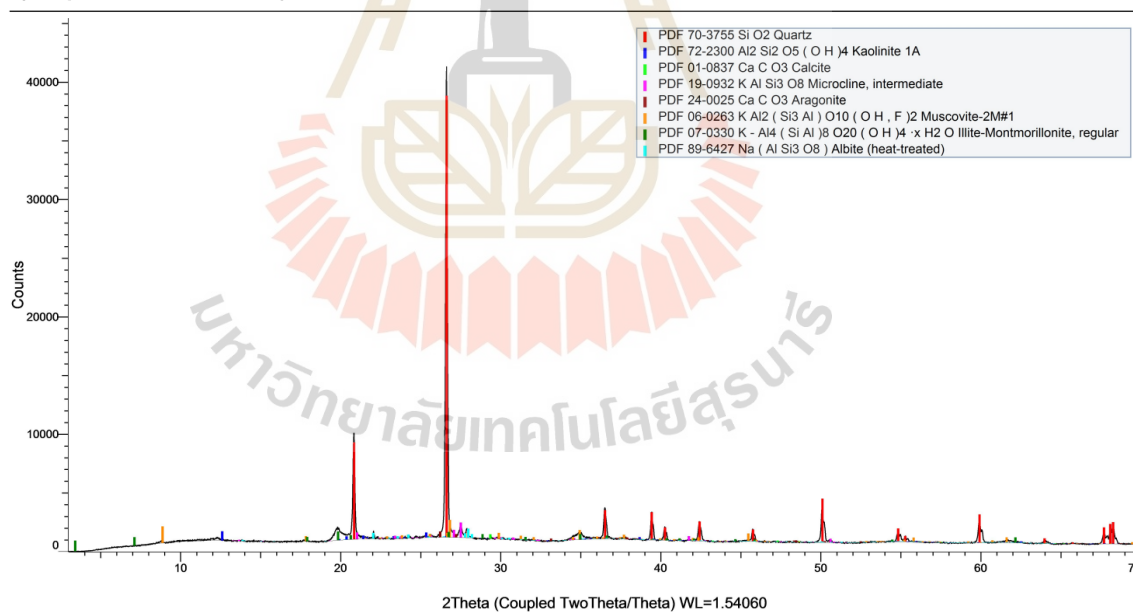


Figure B6. X-ray Diffractogram of sediment at 19.75-meter depth (Borehole KU4)

(Coupled TwoTheta/Theta)

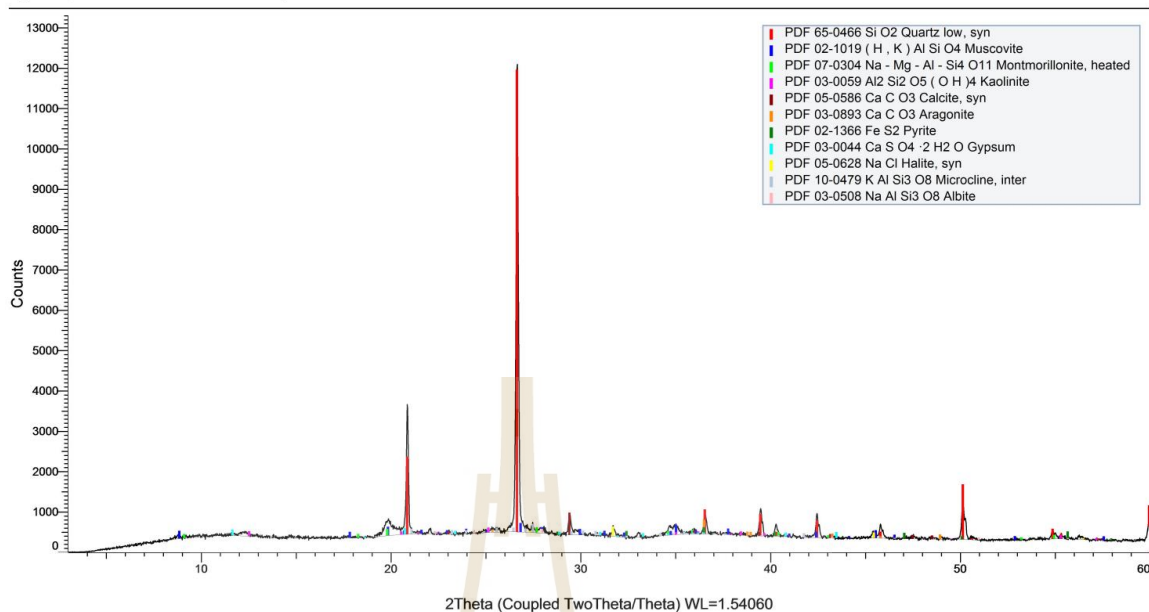


Figure B7. X-ray Diffractogram of sediment at 13.00-meter depth (Borehole KU5)

(Coupled TwoTheta/Theta)

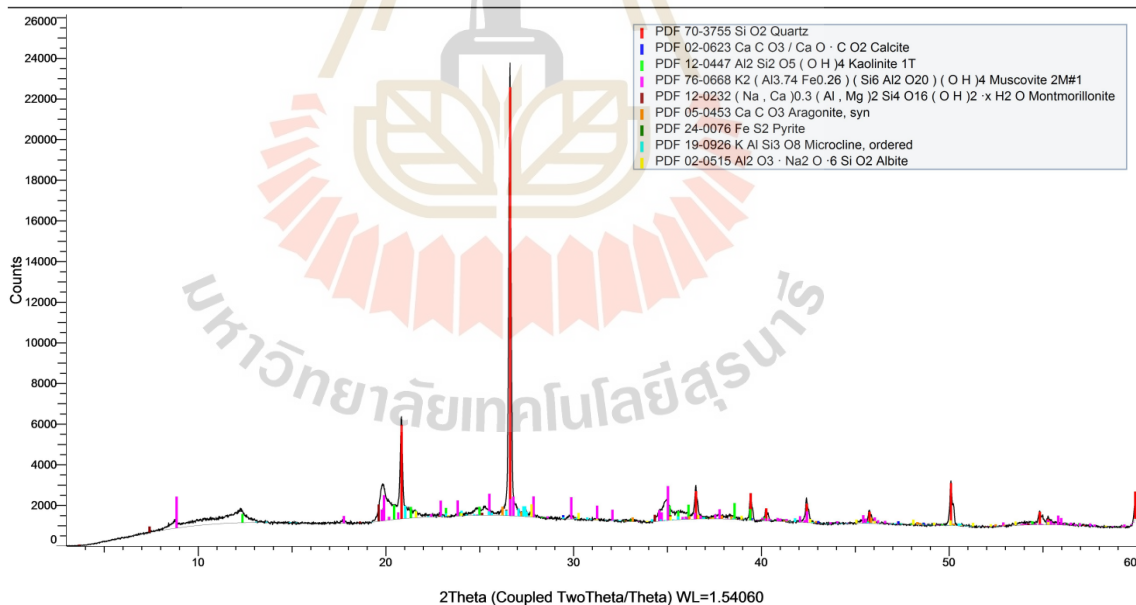


Figure B8. X-ray Diffractogram of sediment at 21.25-meter depth (Borehole KU5)

(Coupled TwoTheta/Theta)

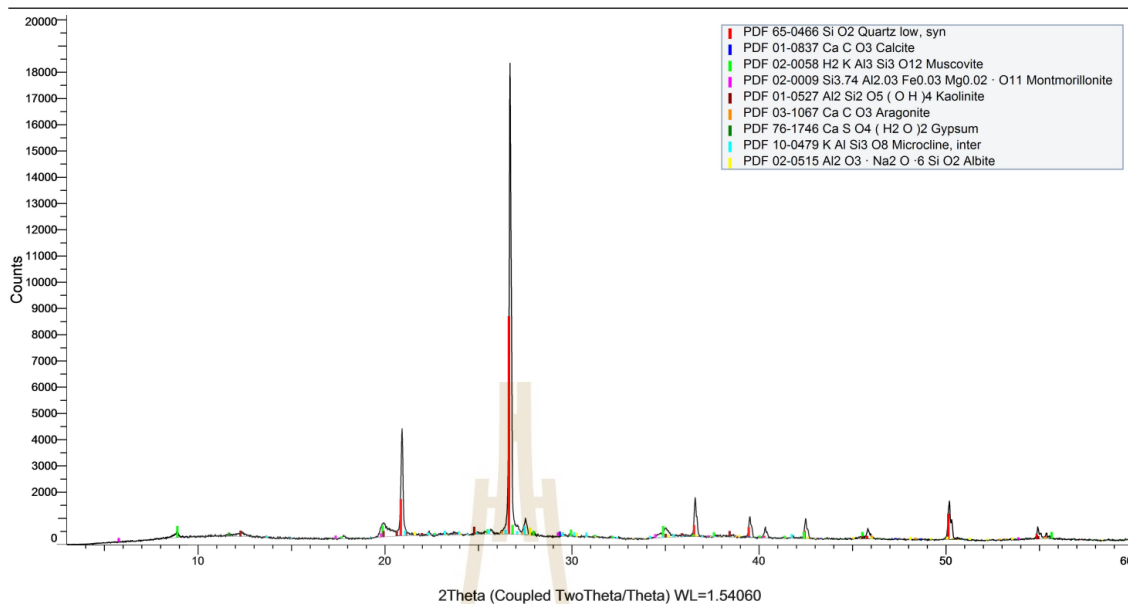


Figure B9. X-ray Diffractogram of sediment at 24.25-meter depth (Borehole KU5)

(Coupled TwoTheta/Theta)

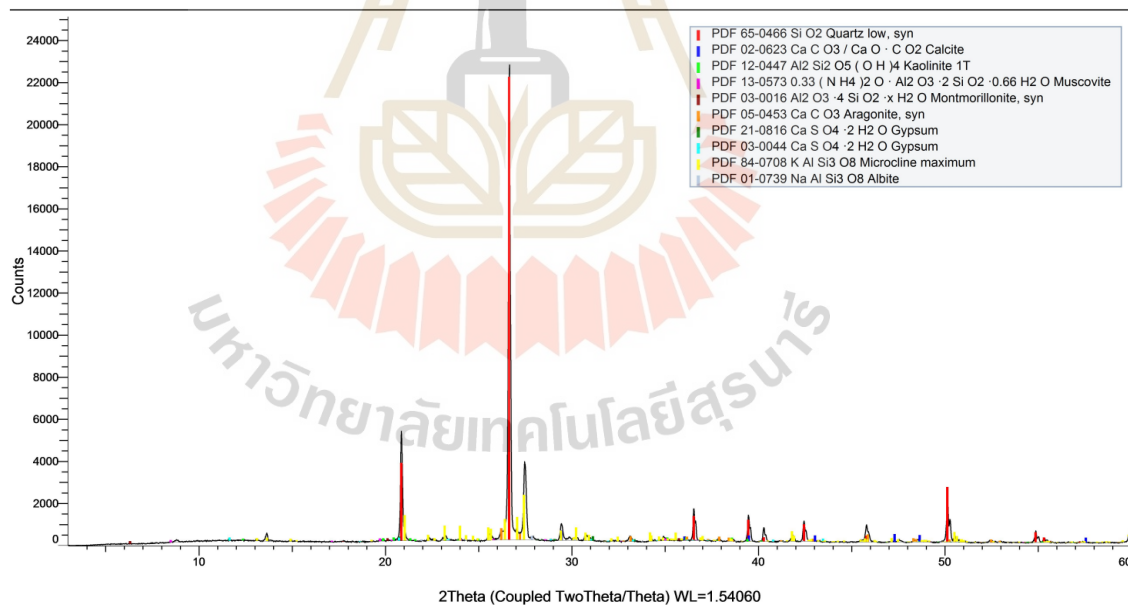


Figure B10. X-ray Diffractogram of sediment at 28.25-meter depth (Borehole KU5)

BIOGRAPHY

Miss Lalita Weerachai was born on November 3, 1999 in Udon Thani Province, Thailand. She received her Bachelor's Degree in Geological Engineering Geological from Suranaree University of Technology in 2022. For her post-graduate, she continued to study with a Master's degree in Civil, Transportation and Geo-resources Engineering Program, Institute of Engineering, Suranaree University of Technology. During graduation, 2022-2023, she has been a teaching assistant at School of Geotechnology, and a research assistant at Georesources Research Unit, Institute of Engineering, Suranaree University of Technology.

